Collapses of linearly decaying three-dimensional perturbations in homogeneous and weakly stratified boundary layers

Joseph Otieno Oloo

Submitted in partial fulfilment of the requirements for the degree of Doctor of Philosophy

Keele University
School of Computing and Mathematics

December 2020

"This thesis is dedicated to my loving mother (Caren Mboya Oloo)."

I certify that this thesis submitted for the degree of Doctor of Philosophy is the result of my own research, except where otherwise acknowledged, and that this thesis has not been submitted for a higher degree to any other university or institution.

Acknowledgements

First of all, many thanks are due to almighty God, whose mercy, blessings, and guidance have given me good health, enthusiasm, resilience, and insight to complete this work.

This study has been made possible by financial support from the Commonwealth Scholarship Commission(CSC) in the United Kingdom, grant number KECA-2016-30. I greatly acknowledge the financial support from the CSC for the award of a Ph.D. Scholarship without which this work would not have happened. It is also my great pleasure to accord special thanks to my employer The Catholic University of Eastern Africa for granting me the study leave to pursue a Ph.D. in the United Kingdom.

This work would not be possible without the dedicated guidance, persistent help, and patience from my lead Ph.D. supervisor, Prof. Victor Shrira, to him I am deeply grateful. During our discussions Prof. Shrira through his meticulous approach to scientific matters made me to appreciate how apparent setbacks can be turned into investigative opportunities. In addition to productive frequent meetings and discussions regarding this thesis, he offered beneficial professional career advice and leadership that will definitely shape my future work and collaborations with future potential researchers. Moreover, Prof. Shrira encouraged and supported me to participate in many international conferences from which I benefited a lot. During my participation at the international conferences, I learned a lot through constructive criticism and engagement in my research that made me mature as a mathematician, and for that, I am most grateful.

I would also like to acknowledge and convey my unreserved gratitude to my co-supervisor(s) Prof. Jonathan Healey and Dr. Sergei Annenkov for their creative and helpful advice. I would like to thank my thesis examiners, Dr. Sergei Timoshin and Dr. Shailesh Naire, for being true role models and mentors, and for taking their time to read my thesis and make helpful suggestions that improve the presentation of this work. My sincere thanks also goes to the viva panel chair Dr. Danila Prikazchikov for facilitating a conducive environment during the discussions. Most of the things I have learned about advanced mathematical techniques including just to mention a few: advanced asymptotic methods, hydrodynamic stability theory, numerical solution of Partial Differential Equations (PDEs) by Matlab and Python computational

soft wares, and not forget to mention Mathematica for symbolic computation have been inspired by Prof. Victor Shrira, Prof. Jonathan Healey, Dr. Sergei Annenkov, Dr. Dan Lucas, and Mr. Andrew Looms. In addition, I would like to thank Dr. Dan Lucas for numerous discussions and insight on pseudo-spectral methods, and Andrew Looms for scientific writing using Latex typesetting, you have told me many things I need to hear before knowing I needed to hear them. I am deeply grateful to Lisa Cartlidge and Andrea Boardman from the FNS PGR office and School of Mathematics office respectively for their consistent help in providing necessary information and documents from time to time. I am thankful to all the faculty members, with whom I interacted, from across all departments of Keele University. I would also like to thank my friends and colleagues who offered encouraging words and helped enormously in individual ways over the four years of my studies.

Finally, a heartfelt thanks to my family. Words cannot express how grateful I am to my mother (Caren Mboya Oloo), brothers (Jacob Oloo and Naman Tindi Oloo), and sister (Noel Achieng Oloo) for all the sacrifices that you have made on my behalf. I dedicate this thesis to my family without whose love, endless support, and encouragement this work would have remained unwritten.

Abstract

The physical mechanisms of why an orderly laminar flow suddenly becomes turbulent are still poorly understood, despite more than a century of incessant efforts. The thesis puts forward a radically new approach to understanding of the fundamental challenge of bypass laminar-turbulent transition. In contrast to the overwhelming majority of other transition studies concerned primarily with linear instabilities, here the focus is on finite amplitude three-dimensional (3d) longwave perturbations of boundary layer which are weakly decaying in the linear approximation.

The principal novelty is in simultaneous account of viscous decay, three-dimensionality and nonlinearity. To describe analytically the dynamics of such perturbations Witham type pseudo-differential nonlinear evolution equations have been derived and examined. The equations are derived asymptotically in the distinguished limit: nonlinearity, dispersion and viscous decay (shown to be described by the Rayleigh friction type term) are assumed to be in balance. The two models describe the 3d perturbations in generic semi-infinite uniform boundary layers for unidirectional flows in homogeneous and weakly stratified fluids (the equation for the homogeneous case is the essentially two-dimensional Benjamin-Ono equation modified by the account of the Rayleigh friction term), while the third one examines the effect of confined boundary layer in homogeneous fluids.

The key feature of the derived models is that they support collapse, i.e. a specific blow up with formation of a point singularity in finite time. Self-similar solutions describing behaviour of the solution in the neighbourhood of singularity have been derived for all three models. The phase space of these models is simply organised: there are two attractors corresponding to the unperturbed linearly stable boundary layer and the singularity. The boundary in the space of the initial conditions separating the regimes of collapse and decay has been examined analytically and numerically. For the situations where the Rayleigh friction is negligible, the systems are Hamiltonian and an analytical criterion of vanishing of the Hamiltonian specifies the boundary between the regimes. For other situations the boundary is found by direct numerical simulations of the evolution equations.

The overall conclusion is that neither the Rayleigh friction, nor stratification or effect of a second boundary prevent collapse from happening, nor they change the perturbation amplitude time dependence in the vicinity of the singularity, however, these factors do affect the evolution and can strongly increase the amplitude threshold of collapse, often beyond the range of validity of weakly nonlinear models. Thus, within the framework of the derived weakly nonlinear models a broad class of initial conditions tends to form a singularity, in the process of evolution the emerging patterns strongly resemble the 3d coherent structures observed in the wind tunnel boundary layers.

Contents

List of Figures

Notations

x, y, z	the streamwise, spanwise and cross-boundary Cartesian coordinates
u, v, w	the x, y, z velocity components
$\tilde{u}$, $\tilde{v}$, $\tilde{w}$	non-dimensional velocity components
$\hat{u}$, $\hat{v}$, $\hat{w}$	re-scaled velocity components in the viscous sub-layer
$\hat{\hat{u}}$, $\hat{\hat{v}}$, $\hat{\hat{w}}$	Fourier transform of the re-scaled velocity components in the viscous sub-layer
$U(z)$	the mean flow directed streamwise (z the cross-boundary coordinate)
$\tilde{x}$, $\tilde{y}$, $\tilde{z}$	non-dimensional streamwise, spanwise and cross-boundary coordinates
$U' \equiv \partial_z U$	mean flow shear
V_0	characteristic velocity of the mean flow
ρ, ρ_0, $\bar{\rho}$	the fluid density, reference density and perturbation density
p, p'	pressure and perturbation of pressure
g	the gravitational acceleration
t, τ	fast and slow time variables
$\tilde{t}$	dimensionless fast time variable
ν	molecular viscosity
K	coefficient of density diffusivity
Re	the Reynolds number
d	thickness of the boundary layer
D	total thickness of the fluid layer
L	the characteristic streamwise lengthscale of the perturbations

$U(0)$	the mean flow at the boundary
U_0	the magnitude of the mean flow at the boundary in case of constant stress condition at the boundary
U_∞	the free stream velocity for the no-slip boundary layers
δ	characteristic thickness of the viscous sub-layer
ε	small parameter of nonlinearity/dispersion
γ, $\widetilde{\gamma}$	non-dimensional parameter of dissipation in the Rayleigh friction term
$Z_1 = \varepsilon z$	slow cross-boundary variable
ξ	dimensionless vertical length scale variable for the viscous sub-layer, $\xi = z/\delta$
Ri	the Richardson number
H	Hamiltonian
Sc	the Schmidt number
c	the speed of long-waves
A	amplitude of the three-dimensional long-wave perturbation
$\boldsymbol{k}$	wavenumber vector
ω	frequency
N_0	typical value of the buoyancy frequency at the boundary
σ_x, σ_y	streamwise and spanwise half-widths
α	the ratio of spanwise half-width σ_y to that of streamwise half-width σ_x

M	mass flux
$\boldsymbol{P}$	momentum
P_x, P_y	streamwise and spanwise components of momentum
$\mathcal{F}$, $\mathcal{F}^{-1}$	Fourier and inverse Fourier transform operators
∇	three-dimensional gradient operator, $\nabla = (\partial_x, \partial_y, \partial_z)$
$\nabla_\perp$	two-dimensional gradient operator, $\nabla_\perp = (\partial_x, \partial_y)$
∇^2	three-dimensional Laplace operator, $\nabla^2 = \partial_{xx}^2 + \partial_{yy}^2 + \partial_{zz}^2$
Δ	two-dimensional Laplace operator, $\Delta = \partial_{xx}^2 + \partial_{yy}^2$
D_t	material derivative, $D_t = \partial_t + U\partial_x$
$\hat{K}$	dispersion operator for homogeneous boundary layer evolution equation
$\hat{G}$	dispersion operator for confined homogeneous boundary layer evolution equation
$\hat{G}_1$, $\hat{G}_2$	dispersion operators for weakly stratified boundary layer evolution equation

Chapter 1

Introduction

1.1 Background: An overview of studies of boundary layers (BLs) in homogeneous and stratified flows in the context of laminar-turbulent transition

1.1.1 3d patterns in laminar-turbulent transition in boundary layers

1.1.1.1 Linear models

The problem of laminar-turbulent flow transition in the boundary layers is a classical problem that has been a subject of intense research efforts for more than a century. In attempt to unravel the features observed during transition a variety of approaches have been tried, including theoretical, numerical and experimental. Despite the huge corpus of literature and efforts dedicated to the problem of transition

our comprehension of the problem is still very far from being complete. In attempt to understand or explain the physical features observed during transition correctly or to predict the onset of transition accurately a sound knowledge of the individual physical parameters is needed. The overwhelming majority of studies concerned with boundary layer transition so far have been centred on linear stability analysis aimed at finding small amplitude perturbations which grow exponentially. For the plane parallel flows this has been carried out largely using Orr-Sommerfield equation. A comprehensive review of linear stability analysis of shear flows is available in a variety of textbooks and reviews [e.g.Schmid and Henningson [2001] , Drazin and Reid [2004], Wu [2019], Schmid [2007], Criminale et al. [2018]]. In recent years attention has shifted to the so called nonlinear extension of non-modal theory, i.e., consists of finding the disturbance to the flow state of a given amplitude that experiences the largest energy growth at a certain time later [e.g. Kerswell [2018]]. However, we do not take the linear theory of stability, it is irrelevant for our study, and, therefore, we do not discuss it here.

1.1.1.2 The aim and the main idea of the work

The primary aim of the thesis is to put forward a new approach. In contrast to the overwhelming majority of studies concerned with linearly unstable perturbations, the focus of this work is on the three dimensional (3d) linearly decaying perturbations. We develop a weakly nonlinear theory of three dimensional linearly decaying perturbations in boundary layers. By means of systematic asymptotic expansions we derive new Whitham type pseudo-differential evolution equations taking into account viscous dissipation, weak stratification and confinement of boundary layers. We analyse these new evolution equations analytically and numerically. We find that the main feature of the evolution of 3d perturbations is that those which satisfy a certain criterion tend to collapse, i.e. form a point singularity of infinite amplitude in finite time. We show that collapses occur in all cases and the main effect of accounting for finite Reynolds numbers and weak stratification is not in preventing collapses but in raising the amplitude threshold of blow-ups. We examine these collapses as a plausible physical mechanism of bypass laminar-turbulent transition and generation

of 3d coherent patterns, whereby the usual existence/absence of linear instability is immaterial and the transition is purely governed by a nonlinear mechanism resulting into finite time singularity or 'blow-up'. The underpinning mechanism of collapses is self-focusing well studied in nonlinear optics (e.g. Zakharov and Kuznetsov [2012]).

1.1.1.3 Alternative models of blow-up in boundary layers

There are other mechanism of bypass laminar-turbulent transition in the boundary layers that have been thoroughly studied theoretically, numerically and experimentally. Apart from our model which we will discuss in detail later, we mention four other models describing the mechanisms resulting in finite time blow-up and considered in the context laminar-turbulent transition. These models were developed more than two decades ago by Craik [1971], Hall and Smith [1991] and Stewart and Smith [1992]. The models of Smith and his co-workers, Philip Hall and his co-workers consider interactive boundary layer (IBL) theory for large Reynolds number.

The pioneering work of boundary layer transition involving resonant triad interaction or nonlinear instability was put forward in a weakly nonlinear analytical model by Craik [1971]. Craik [1971] considered triad resonant interactions between Tollmien-Schlichting (TS) waves and a pair of oblique subharmonic waves with the same streamwise celerity as the TS wave and the wavelengths twice that of the streamwise TS wave. Resonant triads of this type share the same critical layer, which plays the key role in this mechanism. In particular, Craik [1971] showed that the amplitudes of interacting harmonics become infinite in finite time. Although the collapses which are central to our work also lead to infinite amplitudes in finite time, there are three important differences: (i) in contrast to Craik's model where singularities occur only in time domain the collapses result in point singularities both in space and time; (ii) the harmonic perturbations considered by Craik are strongly dispersive, which means that the wavelengths of perturbations are comparable to the boundary layer thickness, while in the models we consider below the perturbations are long compared to the boundary layer thickness; (iii) in the Craik's model the shared critical layer

is crucial, while in our model of collapse, in what we are presenting now, it plays no role whatsoever.

Experimental results of Kachanov and his co-workers [Kachanov et al. [1977]; Kachanov and Levchenko [1984]], Saric and co-workers (Saric et al. [1981]); Thomas and Saric [1981]) added a lot of weight to the Craik's idea; the formation of Craik's triads and associated growth of subharmonics were indeed observed in unsteady boundary layers just prior to the transition.

Hall and Smith [1991] studied strongly nonlinear vortex-wave interactions (VWI) in the boundary layer transition at high Reynolds numbers. Their model is based on interactions between strongly nonlinear longitudinal vortices and the TS waves, hence the mean flow profile is completely different from its original undisturbed state. Stewart and Smith [1992] considered laminar-turbulent transition of boundary layer flows through a mechanism of vortex-wave interaction (VWI). This model is under the umbrella of mechanisms known as self-sustaining processes and transition to turbulence. In these models of Stewart and Smith [1992], Hall and Smith [1991], quasi-two dimensional T-S waves of high frequency and slow amplitude modulations are considered. The nonlinear viscous sublayer generates a streamwise vortex which in turn modifies the T-S waves. In our model, the motions we are concerned with, are long perturbations which are not the TS waves, the dynamics in the viscous sub-layer is ensured to be linear and has negligible contribution into the evolution of perturbations.

On generalising the Craik [1971] model of explosive resonant triads by including asymmetric coupled triads, Metcalfe [2013] developed a theoretical weakly nonlinear 3d model for moderate Reynolds numbers. It was found that for coupled triads the blow-up amplitude thresholds could be quite low for subcritical Reynolds numbers, which suggests a possibility of a role for this mechanism in bypass transition. In contrast to the triads studied by Smith and Stewart [1987] the interaction coefficients of the coupled triads were shown to be complex, it is this property of interaction coefficients which enables the amplitude of interacting harmonics to blow up. The purely imaginary coefficients of resonant-triads in Smith and Stewart [1987] is explained by

the different parameter range of validity, the Smith and Stewart [1987] model has been derived in the limit of very high Reynolds numbers.

1.1.1.4 Brief description of Kachanov (1989, 1990 and 1992) wind tunnel experimental observations in transitional boundary layers

The discovery of a particular class of coherent structures (CS) in boundary layers later shown to be solitary wave solutions of the Benjamin-Ono equations (BO solitons) is linked to the pioneer experiments carried by Borodulin and Kachanov [1989] in the wind tunnel. Borodulin and Kachanov [1989] found that the spikes they observed at the early stage of boundary layer exhibit properties of a soliton. This phemenon was investigated in more detail (Borodulin and Kachanov [1990] and Borodulin and Kachanov [1992]); for a comprehensive description of the CS soliton properties of both the initial and late stages of transition see sections §6.3 and §6.4 of the review by Kachanov [1994]. The specific properties of coherent structures (3d patterns) as observed at later stages of their development are also discussed in Borodulin and Kachanov [1990] and Borodulin and Kachanov [1992], and in section §6.4 of Kachanov [1994] (or a sample of snapshot of a typical 3d pattern see figure 2.1 of Chapter 2). In the process of laminar-turbulent transition in boundary layers a number of features emerge both at the early and late stages of the transition. During the early stages of the transition when the basic flow is still two-dimensional, these structures (spikes observed in experiments) were found to be essentially two-dimensional and well described by asymptotic theory of one-dimensional Benjamin-Ono equation(BO equation) as was first noted by Ryzhov [1990]. Kachanov et al. [1993] carried out a direct quantitative comparison of his experimental observations with the theoretical model of the BO equation in Ryzhov [1990] and found a good agreement. More importantly, during the early stages of the transition, the spikes appear to be planar and very robust (see Kachanov et al. [1993]). The solitons propagate downstream maintaining their form without dispersing, which is in contrast with behaviour of linear wave packets. These solitons were found to decay very slowly, which clearly indicates that nonlinearity plays a fundamental role in their evolution (Doorley and Smith [1992], Smith [1992]). At the intermediate/late stages of boundary layer transition

three-dimensional coherent structures emerge [see e.g., experiments in Borodulin and Kachanov [1990], theory and experiments in Kachanov et al. [1993], and a review paper in Kachanov [1994]]. Kachanov suggests that these features are deterministic and well ordered, not stochastic/random, therefore, could well modelled by a deterministic asymptotic theory. The main features of spike behaviour at later stages of its three-dimensional development are comprehensively discussed in (Borodulin and Kachanov [1990]). In the review paper of Kachanov [1994], it is noted that the theoretical model developed in Kachanov et al. [1993] can not yet describe the three-dimensional pattern described in the experiments (Borodulin and Kachanov [1990]). Kachanov remarked that all attempts to develop a three-dimensional asymptotic theoretical model to describe late stage 3d coherent structures were unsuccessful, the only promising 3d model was that of Shrira (1989) which had faithfully captured some qualitative features of the CS; the axisymmetric solitary wave solution of the Shrira equation obtained by Abramyan et al. [1992] showed a strong resemblance of the observed CS. Our study aims at this gap.

We intend to extend the model of Shrira (1989, 1998, 2005) to a more common no-slip boundary. Our intention is not to perform direct quantitative comparison with the Kachanov observations of the three-dimensional CS recorded at an intermediate stage of the transition, since these experimental works were carried out in non-parallel boundary layers. The model we consider at the first phase of this work is confined to the plane parallel flows, which does not allow for a quantitative comparison with the observations in inhomogeneous boundary layers.

1.1.1.5 Modelling of 3d coherent patterns

Asymptotic nonlinear model of the one-dimensional Benjamin-Ono equation was proposed by Ryzhov [1990] to explain the the 2d patterns observed at the early stages of transition. A qualitative agreement of properties of the Benjamin-Ono (BO) soliton solution with those of experimentally observed spikes was found, in particular, the spectrum of these Benjamin-Ono solutions was found to be close to that observed experimentally [Kachanov [1987] & Kachanov et al. [1985]]. Kachanov et al.

[1993] compared quantitatively the properties of the observed spikes with those of the Benjamin-Ono solitons and found a good agreement. However, at later stages the coherent structures (CS) become essentially three-dimensional (Kachanov [1994]). In his review of (1994) Kachanov noted that the attempts to generalise nonlinear asymptotic theory to 3d solitons propagating in the boundary layer were unsuccessful. This work, in particular, is aimed at this gap.

To our knowledge the first model suitable for describing 3d coherent structures (CS) is an anisotropic two-dimensional generalisation of the Benjamin-Ono equation (2d-BO) which was originally derived as a model of vorticity waves in the upper ocean (Shrira [1989]). The dependence on the third (cross-boundary) coordinate to leading order splits off and is given by an explicit solution of the corresponding boundary value problem (long-wave limit Rayleigh equation). In qualitative agreement with the wind tunnel observations (Kachanov [1994]) the 2d-BO planar wave solutions (both streamwise and oblique) were found to be unstable with respect to transverse perturbations (Pelinovsky and Stepanyants [1994], Gaidashev and Zhdanov [2004]). Abramyan et al. [1992] found numerically 3d stationary solitary wave solution of the 2d-BO that resembling 3d CS observed in wind tunnel by Borodulin and Kachanov [1990] and Borodulin and Kachanov [1992]. However, this 3d stationary solitary wave solution also proved to be unstable. A major step towards understanding the 3d CS in boundary layers was made by D'yachenko and Kuznetsov [1995] who showed the possibility of collapses within the framework of the 2d-BO equation. The collapsing solutions of the 2d-BO equation also resemble 3d CS observed in the tunnels. Pelinovsky and Shrira [1995] found explicit collapse transformation describing evolution of transverse instability of the initially planar solitary wave. The asymptotic procedure employed by Shrira [1989] for the derivation of the 2d-BO equation diverged in the critical layer, where the spanwise velocity component of the perturbation and the first order correction to the streamwise component of the perturbation velocity become singular. In (Voronovich et al. [1998]) a generalisation of the 2d-BO equation was derived which extends the evolution equation to the situations where fluid outside the boundary is arbitrarily stratified and the boundary layer is confined between

two parallel boundaries. The perturbation evolution and emergence of 3d CS within the framework of this new very rich equation have not been examined.

In Shrira et al. [2005] a closely related problem of transition in the free surface wind-induced accelerating boundary layer was examined, where both experimental and theoretical aspects of the transition were investigated. It was found that for the wind induced boundary layer shear flow there are no linear instabilities and the transition occurring in the observations is an example of bypass transition. The observations in the wind-wave facility in Shrira et al. [2005] have shown that the perturbations that emerge out of the primordial noise have the horizontal scales long compared to the boundary layer thickness, then they are growing very gradually becoming more nonlinear, then suddenly, a strongly localized instability occurs. This instability leads to the immediate breakdown of the laminar boundary layer and formation of strongly localized 3d turbulent spots (Shrira et al. [2005]). The most important aspect of this transition mechanism is that it does not require any universal critical Reynolds number for the transition as compared to the classical scenario of linear instability. To summarize the experimental findings, three salient features emerged: Firstly, the observed perturbations have small but finite amplitude, and they are long compared to the boundary layer thickness. The streamwise component of velocity perturbation far exceeds that of the transverse and vertical velocity scales. During the process of evolution the perturbation grows, manifests signs of nonlinear steepening and then suddenly collapses to form turbulent spots. The collapse is strongly localized. Following these observations, a plausible theoretical model of laminar-turbulent transition was put forward. The model differs from the 2d-BO equation by account of explicit dissipation in the boundary layer and due to weakly non-parallel effects which seems to explain qualitatively the salient features observed in the experiment, i.e the dynamics of 3d perturbations, their instability and strongly localised collapse. The main missing gap of the Shrira et al. [2005] model was its validity for the more common no-slip boundary condition, here we aim at addressing this issue.

1.1.1.6 3d coherent patterns in this work

In this work we extend the earlier works (Shrira [1989], Voronovich et al. [1998] and Shrira et al. [2005]) and apply systematic asymptotic methods to derive novel two-dimensional nonlinear evolution equations accounting for a stronger dissipation, weak stratification and confinement of the boundary layer. These new equations are analysed analytically and numerically.

In all cases the asymptotic derivation begins with a linear boundary value problem in the form of long wave limit of the Rayleigh equation to the leading order. The next order additive corrections to its leading order solution yield weak dispersion of two different kinds, nonlinearity, viscosity and stratification; all being in balance. The interplay of all these factors results in non-trivial two-dimensional (2d) Whitham type nonlinear pseudo-differential evolution equations which enable us to model dynamics of a broad class of boundary layers. To get insight into the dynamics governed by the derived evolution equations we apply both the analytical approaches developed for studies of collapses in other physical contexts (Zakharov and Kuznetsov [2012]) along with direct numerical simulation based upon pseudo-spectral method with fourth order Runge-Kutta time-stepping [e.g. Orszag [1969], Fornberg [1998], Kopriva [2009]].

1.1.2 Collapses in plasmas, nonlinear optics and boundary layers

1.1.2.1 The notion of collapse. Wave collapses in plasmas and hydrodynamics

The notion of collapse was introduced nearly half a century ago in the context of nonlinear wave systems by Zakharov to describe the behaviour of Langmuir waves in plasmas (see Zakharov et al. [1972], Kuznetsov [1996]). The idea of collapses as a generic scenario of singularity formation in finite time proposed by Zakharov has been widely applied in various physical contexts involving nonlinear dispersive waves.

To our knowledge all analytical results and the overwhelming majority of numerical studies of collapses are confined to Hamiltonian systems.

The specific type of blow-up singularity that arises in nonlinear wave systems is largely dependent on the physical model. Historically, the first and most studied is the case of self-focusing of light governed by the nonlinear Schrödinger (NLS) equation; the light intensity tends to infinity as the focus is approached (Bergé [1998]).

In physics the term "wave collapses" is used for describing the formation of particular type of point singularities in the solutions of evolution equations governing the dynamics of nonlinear waveforms. The nonlinearity of the evolution equation is the necessary, but not sufficient element for the occurrence of collapses. The collapsing solutions can occur only for certain classes of initial data and exist only during a finite time interval, until the instant at which they lose their initial smoothness and become singular. Wave collapses are of special interest in physics because in conservative systems they provide one of the most effective mechanism for transfer of energy into small scales and localising it in small spots(see e.g.,Kuznetsov [1996], Zakharov and Kuznetsov [2012]). Knowing *a priori* about the existence of collapse in a system under consideration is therefore very important. It also enables us to predict how the specific features of the singularity depend on the initial conditions. For the Hamiltonian systems, the sufficient condition of collapse is that the Hamiltonian unbounded from below is negative ($H < 0$), which means that the nonlinear localizing effects dominate over the wave dispersion. For the non-Hamiltonian systems, with which we are primarily concerned with in this work, at present there is no theory enabling one a priori predict the outcome of the evolution for any given initial conditions.

In various fields of applied mathematics and physics there are a number of nonlinear wave models that exhibit collapses. We briefly overview the most relevant ones.

1.1.2.2 Collapse in the 'Nonlinear Schrödinger Equation' (NLS)

The Vlasov-Petrishchev-Talanov (V-P-T) criterion of wave collapse within the framework of two- and three-dimensional nonlinear Schrödinger equation(NLS), found in

1971, is the first example of wave collapse which precedes the term collapse itself. This was the first rigorous result for nonlinear systems with dispersion, which showed the possibility of formation of a wave-field singularity in finite time, despite the presence of the linear dispersion of waves, the effect precluding the formation of point singularities in the linear optics.

The nonlinear Schrödinger equation written in terms of dimensionless variable ψ has the form

$$i\psi_t + \Delta\psi + |\psi|^2\psi = 0, \tag{1.1}$$

where the subscript t denotes a partial derivative with respect to time, while Δ is the two- or three-dimensional Laplacian operator. In nonlinear optics, the 2d and 3d NLS equations describe the stationary self-focusing of light in a medium with the Kerr nonlinearity [e.g. Kuznetsov [2003]]. Here we consider only the the 2d case. Here the wave function ψ is the envelope of the field of a quasi-monochromatic electromagnetic wave, the time t has the meaning of the coordinate along the direction of light beam propagation, while the second term describes diffraction of the beam in the transverse direction.

On multiplying the NLS equation by r^2, where $r = |\boldsymbol{r}|, \quad \boldsymbol{r} = (x, y)$ and integrating it with respect to spatial variables, after some algebra, it is possible to get the following exact relationship for the second derivative with respect to time of the quantity $\langle r^2 \rangle = N^{-1} \int r^2 |\psi|^2 \mathrm{d}\boldsymbol{r}$,

$$\frac{d^2}{dt^2} \int r^2 |\psi|^2 \mathrm{d}\boldsymbol{r} = 8H, \tag{1.2}$$

where

$$N = \int |\psi|^2 \mathrm{d}\boldsymbol{r},$$

is an integral of motion, often called the total number of the quasi-particles, and H is the Hamiltonian, another integral of motion given by

$$H = \int |\nabla\psi|^2 \mathrm{d}\boldsymbol{r} - \frac{1}{2} \int |\psi|^4 \mathrm{d}\boldsymbol{r} \equiv I_1 - I_2. \tag{1.3}$$

The Hamiltonian H is an integral of motion which is a sum of two constituents I_1 and I_2 corresponding to the dispersion and nonlinearity contributions respectively. The

relationship (1.2) is often called the virial theorem since the quantity $N\langle r^2\rangle$ can be interpreted as the angular momentum [e.g. Kuznetsov [1996]]. In classical mechanics, the simplest way of deriving the virial theorem, i.e the relationship between the average kinetic energy and potential energy, is to calculate the second time derivative of the total angular momentum of the whole system. Since the Hamiltonian H is a conserved quantity, integration of equation (1.2) two times yields the relationship

$$\int r^2|\psi|^2 \mathrm{d}\boldsymbol{r} = 4Ht^2 + C_1 t + C_2, \tag{1.4}$$

where C_1 and C_2 are arbitrary constants of integration. The V-P-T criterion follows immediately from (1.4). The quantity $\langle r^2\rangle$ interpreted as the mean square size of the field distribution is positive by definition. However, it is easy to see that in case of negative Hamiltonian ($H < 0$) and arbitrary constants C_1 and C_2 the mean square size $\langle r^2\rangle$ crosses zero in finite time, which indicates that the solution exists only up to this moment. Since N is conserved ($N = \int |\psi|^2 \mathrm{d}\boldsymbol{r}$), the vanishing of $\langle r^2\rangle$ suggests that the field $|\psi|$ becomes infinite at this moment.

In addition to the V-P-T criterion of collapse which is specific for the NLS equation, there also exists an important much more general sufficient criterion for collapse which requires the Hamiltonian H to be negative and unbounded from below. We elaborate this point below. Assuming that there are solitary wave type steady solutions $\psi_s(\boldsymbol{x})$ in the appropriately shifted frame, consider a scaling transformation

$$\psi_s(\boldsymbol{x}) = \tilde{\alpha}^{-\tilde{D}/2}\psi_s(\boldsymbol{x}/\tilde{\alpha}).$$

This transformation preserves the number of particles N. The Hamiltonian can be presented as a sum of dispersive and nonlinear contributions, I_1 and I_2, i.e.

$$H = I_1 + I_2.$$

Examining dependence of the Hamiltonian H as function of the scaling parameter $\tilde{\alpha}$, more specifically examining the boundness/unboundness of H from below as $\tilde{\alpha} \to 0$,

we easily get explicit expression for $H(\tilde{\alpha})$,

$$H(\tilde{\alpha}) = \frac{1}{2}\left(\frac{I_1}{\tilde{\alpha}^2} - \frac{I_2}{\tilde{\alpha}^{\tilde{D}}}\right). \tag{1.5}$$

The unboundness of $H(\tilde{\alpha})$ from below indicates the possibility of collapse. This possibility depends on the dimension of space $\tilde{D}$; for the NLS the collapses are possible when the dimension $\tilde{D} \geq 2$. There is a general observation that with increase in $\tilde{D}$ the role of nonlinearity increases.

When $\tilde{D} = 1$, the NLS Hamiltonian H is bounded from below, it realises its minimum which corresponds to a stable planar soliton. In the two-dimensional situations, $I_1 = I_2$, hence, $H = 0$ for the entire soliton family. For $\tilde{D} = 3$, $H(\tilde{\alpha})$ has a maximum instead of a minimum (saddle point) which suggests the instability of the soliton. It is easy to see that for $\tilde{D} = 3$ in equation (1.5), $H(\tilde{\alpha})$ turns out to be unbounded function as the characteristic scale of the collapsing domain $\tilde{\alpha} \to 0$, which is one of the collapse criteria [Kuznetsov and Musher [1986]]. Therefore, for the unboundedness of Hamiltonian from below ($H < 0$), the characteristic size $\tilde{\alpha}$ of the collapsing domain behaves as $\tilde{\alpha} \sim (t_0 - t)^{1/2}$ where t_0 is the finite time singularity and $\frac{1}{2}$ is the exponent of the collapse. It is important to note that 2d NLS equation is regarded as the *critical* NLS case: the dispersion integral I_1 and nonlinear integral I_2 terms in the Hamiltonian behaves similarly under the scaling transformation with characteristic scale $\tilde{\alpha}$ of the collapsing domain.

1.1.2.3 Collapse in boundary layers governed by the 2d-BO model (Shrira's model)

Strong/critical collapse behaviour occurs not only for the NLS equation chosen here as an example of collapse. In the context of boundary layers it has been shown by D'yachenko and Kuznetsov [1995] that the two-dimensional Benjamin-Ono equation (2d-BO) describing the nonlinear evolution of longwave 3d perturbations can be cast

in the Hamiltonian form

$$u_t = \frac{\partial}{\partial x}\hat{k}u - 6uu_x = \frac{\partial}{\partial x}\frac{\delta H}{\delta u}, \tag{1.6}$$

with the Hamiltonian

$$H = \frac{1}{2}\int u\hat{k}u\mathrm{d}\mathbf{r} - \int u^3\mathrm{d}\mathbf{r} = \frac{1}{2}I_1 - I_2. \tag{1.7}$$

In the context of the current discussion, the 2d-BO belongs to the class of 'critical models'. Equation (1.6) is the anisotropic two-dimensional generalisation of Benjamin-Ono equation derived by Shrira [1989] in the context of upper ocean with shear localised in the upper thin boundary layer and infinite bottom layer. Here $\hat{k}$ is the integral operator whose Fourier transform is the modulus $|\mathbf{k}| = \sqrt{k_x^2 + k_y^2}$. The 2d-BO is an asymptotic model describing the motions of longwave perturbations in boundary layers at large Reynolds numbers $\mathrm{Re}^{-1/2} \leq \varepsilon \leq \mathrm{Re}^{-1/4}$. Equation (1.6) conserves four integrals of motion: mass, two components momentum and the Hamiltonian. Under the scaling transformation similar to that used for the NLS equation,

$$\psi \to \tilde{\alpha}^{-\tilde{D}/2}\psi(\mathbf{r}/\tilde{\alpha}),$$

where $\tilde{D} = 1, 2$ leads to the following dependencies of the Hamiltonian H on the scaling parameter $\tilde{\alpha}$ (the characteristic scale of the collapsing domain),

$$H(a) = \frac{1}{2}\frac{I_1}{\tilde{\alpha}} - \frac{I_2}{\tilde{\alpha}^{\tilde{D}/2}}. \tag{1.8}$$

Therefore it follows clearly that 2d-BO model as $\tilde{\alpha} \to 0$ becomes critical when $\tilde{D} = 2$. For the case when $\tilde{D} = 1$, the equation reduces to the classical Benjamin-Ono equation for which it is well known that the Hamiltonian is bounded from below and the soliton realises its minimum corresponding to the Benjamin-Ono soliton. The solitary wave solution of Benjamin-Ono equation for travelling waves $u = u_s(x - Vt)$ is well known to be of the Lorentz pulse form,

$$u_s = \frac{V}{1 + V^2x^2}, \qquad V > 0. \tag{1.9}$$

It has been shown that the plane BO soliton is unstable with respect to transverse perturbations[see D'yachenko and Kuznetsov [1995], Pelinovsky and Stepanyants [1994]]. In the longwave limit the instability growth rate of the BO plane soliton is (D'yachenko and Kuznetsov [1994], Pelinovsky and Stepanyants [1994]), Gaidashev and Zhdanov [2004],

$$\bar{\gamma}^2 = \frac{k_y^2 V^2}{2} > 0.$$

For the 2d-BO the Hamiltonian is unbounded for the states with negative energy. D'yachenko and Kuznetsov [1995] showed that indeed in the 2d-BO model collapse occurs for $H < 0$ and the collapsing solution tends to axially symmetric distribution as $t \to t_0$, where t_0 is the time of singularity.

1.2 Open questions

Despite more than a century of intensive research involving numerous theoretical and experimental studies of boundary layer transition in shear flows, a number of basic questions still remain open which we attempt to address in this thesis.

1. At present there is no consistent weakly nonlinear model able to describe nonlinear dynamics of 3d longwave perturbations in boundary layers with a more common 'no-slip' condition at the boundary. There is no model for 3d longwave perturbations accounting for finite Reynolds numbers.

2. How does account of dissipation affect boundary layer collapses? It is not known whether dissipation in the boundary layer can prevent collapses from occurring. If collapses can occur, how does the dissipation affect the character of singularity and the manifold of initial conditions resulting in collapse? At present all theoretical results on collapses were obtained for Hamiltonian systems.

3. In what respects the nonlinear dynamics of 3d longwave perturbations in boundary layers confined between two planes differs from that in the semi-infinite boundary layers? The effects of boundary layer confinement have not been studied.

4. At present there is no consistent weakly nonlinear model for 3d longwave perturbations in weakly stratified boundary layers. Nothing is known about their nonlinear dynamics. How does account of stratification affect collapses?

1.3 Structure of the thesis

The overview of the studies and open questions concerned with nonlinear dynamics of 3d longwave perturbations in boundary layers with the focus on collapses presented in this Chapter 1 is followed by three chapters devoted to various aspects of boundary layer dynamics, Conclusions and Discussion.

In Chapter 2 we revisit the derivation of the weakly nonlinear model for 3d longwave perturbations in homogeneous boundary layers extending the derivation to lower Reynolds numbers and the no-slip boundary layers. We show that the derived pseudo-differential generalisation of the 2d-BO equation is equally valid for the no-slip and constant stress boundary conditions. We investigate the properties of the new nonlinear evolution equation with and without the Rayleigh friction term describing the dissipation. We examine occurrence of collapses and, in particular, how the explicit account of dissipation affects collapses. We show that the account of dissipation doesn't change the type of the singularity, but raises the amplitude threshold.

In Chapter 3 we examine the effect of the boundary layer confinement for the case of homogeneous boundary layer. We investigate collapse in confined boundary layer within the framework of the '2d Intermediate long-wave equation' (2d-ILW). The 2d-ILW was originally derived by Voronovich et al. [1998], yet only its solitary stationary solution were found. We show that collapses still can occur in the boundary layers confined between two parallel planes and find the character of the singularity. We investigate how the manifold of the initial conditions ending up in collapse depends on the distance between the planes.

Chapter 4 extends the analysis to weakly stratified boundary layers for which we derive a novel nonlinear evolution equation. The model is a generalisation of the 2d-BO equation with the Rayleigh friction term, it has two dispersion terms. We examine under what conditions collapses can occur and the character of the singularity.

The Conclusions summarising the main results of the work are given in Chapter 5. A discussion of the findings, the new questions the work generates and an outline of further studies are given in the Chapter 5. In the Appendix A, B and we provide details of the derivations of the nonlinear evolution equation from the Navier-stokes equation.

Chapter 2

Collapses of linearly decaying three-dimensional perturbations in homogeneous boundary layers

2.1 Introduction

High Reynolds number boundary layers are ubiquitous in nature and engineering contexts. The remarkable progress in understanding of boundary layer instabilities and laminar-turbulent transition accumulated over one hundred years has been summarised in many books and reviews (e.g. Drazin and Reid [2004],Schmid and Henningson [2001], Schmid [2007], Kerswell [2018], Criminale et al. [2018], Wu [2019], Kachanov [1994]). To say that the issue is well studied would be an understatement. However, the question about the physical mechanisms of the laminar-turbulent transition continues to be debated. One of the least understood aspects of the transition is the emergence of three-dimensional localized coherent patterns often observed in wind tunnel experiments and their role in the transition. An example of such patterns taken from from (Kachanov 1994) is reproduced here. This study is aimed at

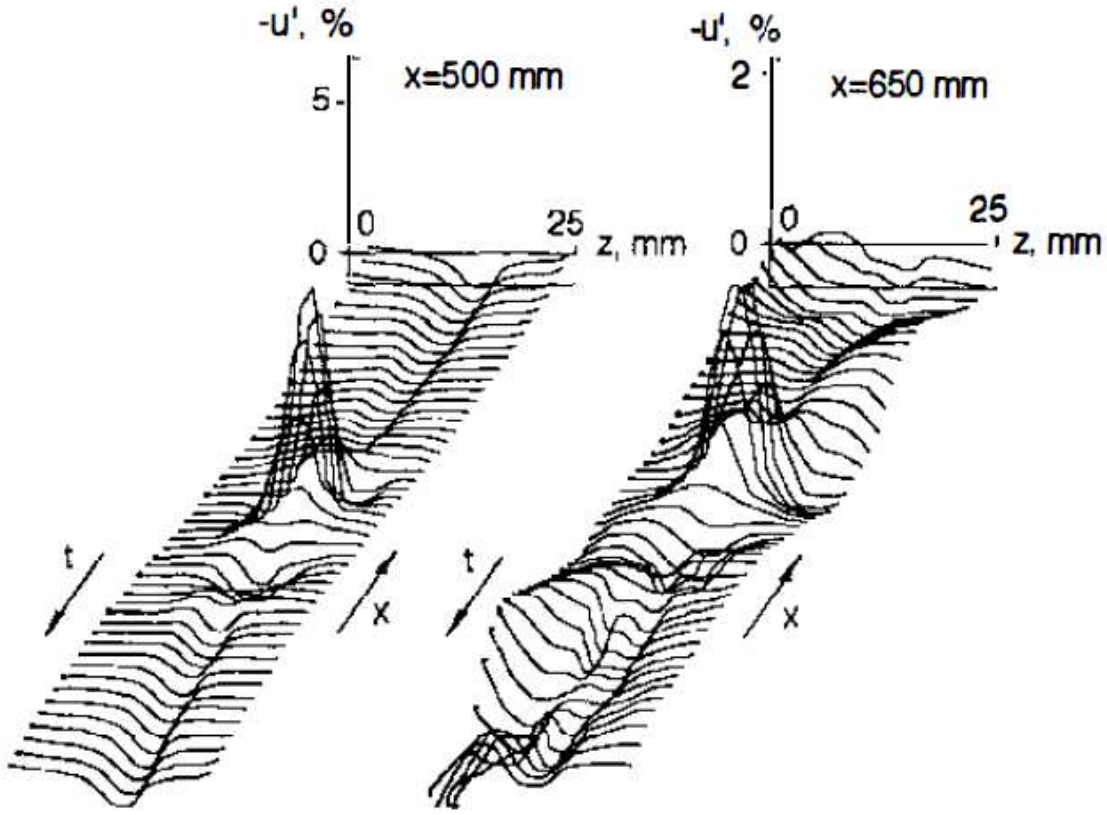

FIGURE 2.1: Localised coherent structures in boundary layer observed in wind tunnel experiments by Kachanov (1994). Two instantaneous span-wise cross-sections at two downstream positions x_1 and x_2 of the streamwise velocity of a localised disturbance at a distance $y = y_s$ from the boundary. Where $x_1 = 500$mm, $x_2 = 650$mm and $y_s = 1.0$mm.

describing a scenario of evolution of three-dimensional localised coherent patterns in generic boundary layers and modelling of their subsequent blow up within the framework of a weakly nonlinear asymptotic model.

Although the ideas underpinning this work are not entirely new and their origins could be traced as far as nearly fifty years back, to the best of our knowledge, in the context of transition in boundary layers they have not been consistently developed and presented; here we aim at this gap. The line of thought we pursue and briefly review below represents a departure from the conventional theoretical approaches to laminar-turbulent transition in the following main aspects.

First, our approach is not constrained by considering the linearly unstable modes.

Linear instabilities play no role in our consideration. Here we are primarily interested in nonlinear instabilities of linearly decaying modes which lead to a finite time 'explosive' growth of perturbations, more specifically, we are interested in blow ups resulting (within the framework of weakly nonlinear models) in point singularities both in space and time. Such scenarios of evolution common in nonlinear optics and plasmas are referred to as 'collapses' (e.g. Zakharov and Kuznetsov [2012]). In the context of high Reynolds number boundary layers we argue that the collapses, if they occur, would develop much faster than the possible linear instabilities. Of course, such a comparison is not entirely like-for-like, in contrast to linear instabilities the collapses have an amplitude threshold and the rate of the perturbation amplitude growth depends on amplitude and varies with time.

The perturbations we consider are often referred to as 'vorticity waves', since, indeed, in many respects they behave as waves with restoring force provided by the non-uniformity of background vorticity of the mean flow. We will use this term throughout the chapter. In linear setting a boundary layer shear flow supports specific long-wave modes which behave as a weakly dispersive weakly decaying wave (e.g. Shrira and Sazonov [2001]). Not only the terminology, but a significant part of the conceptual and mathematical framework of nonlinear wave theory used in other branches of applied mathematics and physics is applicable here.

To elucidate the specificity of boundary layer collapses which are the focus of the study, we first mention a few other mechanisms of blow up in boundary layers. Strongly nonlinear wave-vortex interactions between longitudinal vortices and the quasi-two dimensional Tollmien-Schlichting(TS) waves at high Reynolds numbers are viewed as a possible mechanism of the boundary layer transition (Hall and Smith [1991], Stewart and Smith [1992]). Such interactions do lead to blow up, but in contrast to the model we consider here, require pre-existing strongly nonlinear longitudinal vortices and, thus, are outside the realm of weakly nonlinear theory.

A totally different class of blow ups in boundary layers is exemplified by explosive resonant triad interactions of oblique perturbations first discovered by Craik [1971]. This line of research was further elaborated in Usher et al. [1975], Craik [1988],

Craik [2001], Metcalfe [2013]. In contrast to nonlinear wave-vortex interactions, in this scenario there is no need in preexisting longitudinal vortices. Similarly to the scenario we consider, the Tollmien-Schlichting instability is of little significance. The main qualitative difference between the Craik-type blow up and the collapses we focus upon is that the former is described in terms of evolving Fourier harmonics, the singularity is in time, but not in space, while in the collapse scenario the evolution is considered in the $\boldsymbol{x}$-space and results in a point singularity in both space and time. The Craik-type explosive resonant interactions occur for strongly dispersive, hence, relatively short, perturbations, while here we focus upon perturbations long compared to the boundary layer thickness. Yet another important difference between the explosive resonant interactions and the collapses we focus upon in this work is in the role played by the dynamics in the critical layer: for the explosive resonant interactions the processes in the critical layer play the crucial role, in contrast, the critical layer dynamics has no role in the scenarios of collapses we consider. The study by Reutov [1995] aimed at describing 3d patterns in the boundary layer at very large Reynolds numbers puts forward a model based on the two-dimensional Benjamin-Ono equation coupled with nonlinear critical layer exhibiting instabilities. Since in the chosen regime the critical layer dynamics is essentially nonlinear it is difficult to advance analytically, but under some extra assumptions Reutov (1995) was able find explosive triads. This places this work somewhere in between the Craik inspired studies of explosive interactions where the role of the critical layer is central, but the dynamics in the critical layer is still linear and the approach with linear viscous critical layer pursued here.

In contrast to the overwhelming majority of studies of boundary-layer instabilities strongly influenced by an extended interpretation of the Squire's theorem, here we are considering nonlinear evolution of essentially three-dimensional (3d) non-monochromatic perturbations of comparable streamwise and spanwise scales. Along with the already mentioned weak dispersion due to long-wave character of the perturbations, the essential three-dimensionality and nonlinearity are the key elements of the new conceptual picture. The main physical mechanism leading to collapses

- the self-focussing, was known in nonlinear optics and plasmas since the mid sixties (see e.g. review Zakharov and Kuznetsov [2012]), however its appropriation and adaptation in the context of boundary layers proved to be not straightforward.

To our knowledge the consideration of essentially 3d longwave perturbations in the boundary layers was originated by Shrira [1989] in the context of upper ocean. To describe weakly nonlinear evolution of such perturbations in the horizontally uniform boundary layer adjacent to the ocean surface the two-dimensional generalisation of the Benjamin-Ono (2d-BO) equation was derived. The key assumptions in the asymptotic derivation are the smallness of nonlinearity characterised by a nonlinearity parameter ε ($\varepsilon \ll 1$) and the balancing weakness of dispersion due to $O(\varepsilon)$ smallness of the characteristic wave number compared to the inverse of the boundary layer thickness. A perturbation of comparable streamwise and spanwise scales represents a broadband packet of vorticity waves. In the absence of instability such a packet is dispersing and slowly decaying. The 'Dissipative 2d-Benjamin-Ono' evolution equation we derive and examine in this work represents a "distinguished limit": it simultaneously balances weak nonlinearity, weak dispersion and dissipation described by the Rayleigh friction type term. The dependence of the perturbations on the cross-boundary coordinate z splits-off and is determined, to leading order in ε, by the corresponding linear boundary value problem. For a range of higher Reynolds numbers we specify below the dissipative effects become negligible and the evolution equation reduces to the well studied two-dimensional Benjamin-Ono (2d-BO) equation. In the non-dissipative limit the equation, i.e. 2d-BO, was found to possess axially symmetric steady solitary wave solutions obtained numerically Abramyan et al. [1992]. Although this equation was originally derived for the free surface flows under the 'rigid-lid' approximation, it was intuitively clear that the derivation could be extended for generic boundary layers with the more common 'no-slip' boundary condition. Kachanov (1994) noted that the growing three-dimensional coherent patterns observed in wind tunnels during the laminar-turbulent transition strongly resemble these solutions. Pelinovsky and Stepanyants [1994] analytically examined transverse instabilities of the cnoidal plane wave solutions of the 2d-BO equation and showed that all plane wave solutions, including the solitary waves, are

unstable with respect to long-wave transverse perturbations, while Gaidashev and Zhdanov [2004] further extended the stability analysis with respect to transverse perturbations. In the crucial development D'yachenko and Kuznetsov [1995] showed that within the framework of the 2d-BO equation collapses of initially localized two-dimensional perturbations can occur. Throughout the chapter we employ the notion of collapse widely used in physics to refer to a blow-up resulting in a point singularity (e.g. Zakharov and Kuznetsov [2012]). Pelinovsky and Shrira [1995] derived explicit description of the collapse in the 2d-BO equation employing Whitham's adiabatic approach. The asymptotic model resulting in the 2d-BO equation was extended in Voronovich et al. [1998] by considering a confined boundary layer and by taking into account density stratification outside the boundary layer. In this context the same asymptotic scheme yields a novel family of the evolution equations for confined boundary layers, this family turns into the essentially two-dimensional "intermediate long-wave equation" in the absence of stratification and the 2d-BO equation in the limit of unconfined boundary layer and zero stratification. The collapses in the confined boundary layers within the framework of the two-dimensional intermediate long-wave equation were examined in (Oloo and Shrira [2020]), this work will be reproduced in the next chapter of this thesis with minor modifications.

In the original derivation of the 2d-BO equation carried out in Shrira [1989] for the ideal fluid the asymptotic expansion proved to be nonuniform: the higher order terms diverge in the critical layer. At a hand waving level it was argued that the account of viscosity eliminates the singularities. In Shrira et al. [2005] a generalisation of the 2d-BO equation was derived to model laminar-turbulent transition in the accelerating Falkner-Skan boundary layer; on its basis numerical simulations of the perturbation evolution were carried out and experimental observations of the laminar-turbulent transition in the wind-driven steady boundary layer were presented and discussed.

The mosaic of the listed results doesn't easily add up into a coherent picture. The crucial missing bit is the lack of proof of the uniformity of the asymptotic expansion for the boundary layers with no-slip boundary. Here we outline a way an expansion uniform everywhere could be derived, but do not pursue this route further, instead,

we confine our consideration to the quasi-planar perturbations. For the latter the singularities disappear in the required order of asymptotic expansion. The second major outstanding issue is the role of viscous effects in the occurrence of collapses. The account of large but finite Reynolds number effects in a long-wave evolution equation is straightforward (Zhuk and Ryzhov [1982],Ryzhov [1990]), but so far it has not been done for 3d perturbations with no-slip boundary conditions. At present it is not clear in what range of Reynolds' numbers the boundary layer collapses occur and under what conditions. Without clarifying this point it is not possible to discuss the possible place of collapses in the laminar turbulent transition. This study aims at addressing these key gaps. The main question we want to address is whether the account of strong dissipation changes qualitatively the nonlinear dynamics of long-wave 3d perturbations in homogeneous boundary layer. The specific open questions we aim at clarifying are:

1. Can the evolution of 3d localised finite amplitude longwave perturbations in homogeneous boundary layers be captured by a single nonlinear evolution equation with nonlinearity, dispersion and dissipation in balance.

2. Within the framework of the 2d-BO what are the boundaries delineating the manifolds of the initial conditions ending up in collapse?

3. Are collapses possible when the dissipation is explicitly taken into account? What is the role of viscous effects in the occurrence of collapses? How does finite Reynolds number affect the manifolds of the initial conditions ending up in collapse and the character of the singularity?

The layout of the chapter addressing these questions is as follows. In section §2.2 we formulate the problem for a generic horizontally uniform boundary layer, introduce the small parameters, scaling, and asymptotic expansion for the bulk of the boundary layer. In §2.3 we derive the evolution equation in the distinguished limit: we balance nonlinearity, dispersion and dissipation. Under the adopted scaling the longwave perturbations of boundary layer can be fully characterised by a single

scalar function - the amplitude $A(x, y, \tau)$ of the streamwise and spanwise coordinates x, y and "slow time" τ. We show that its evolution is governed by the equation

$$A_\tau + AA_x - \hat{K}[A_x] + \widetilde{\gamma}\, A = 0, \tag{2.1}$$

where the coefficient $\widetilde{\gamma}$ in the dissipative term $\widetilde{\gamma}\, A$ is proportional to the ratio of the basic flow vorticity curvature at the boundary and the Reynolds number, the dispersion operator $\hat{K}$ is two-dimensional,

$$\hat{K}[\varphi(\boldsymbol{k})] = \frac{1}{4\pi^2}\int_{-\infty}^{+\infty}\int_{-\infty}^{+\infty} |\boldsymbol{k}|\varphi(\boldsymbol{r}_1)e^{(i\boldsymbol{k}(\boldsymbol{r}-\boldsymbol{r}_1))}\mathrm{d}\boldsymbol{k}\mathrm{d}\boldsymbol{r}_1,$$

and $\boldsymbol{k} = (k_x, k_y)$, $k = |\boldsymbol{k}|$ .The dependence of the perturbations on the cross-boundary coordinate z splits-off: it is determined by the corresponding linear boundary value problem – the Orr-Sommerfeld equation with the standard boundary conditions, to leading order in ε it is solved explicitly.

The divergence of the asymptotic scheme in the critical layer could be dealt with in two different ways: (i) a detailed asymptotic analysis of the dynamics in the critical layer can be carried out, which requires a dedicated study, or , (ii) the difficulty can be circumvented by confining the consideration to the quasi-planar perturbations. Here we choose and stick to the second option. Although here the validity of the asymptotic scheme has been proven only for quasi-planar perturbations, the evolution equations we derive are examined for arbitrary perturbations. In §2.4 we consider collapses within the framework of the derived evolution equation in the range of Reynolds numbers where the dissipative term in the evolution equation can be neglected and the equation reduces to the well studied 2d-BO equation. In this regime there exist a simple analytical criterion specifying the initial perturbations which inevitably collapse. By analysing this criterion we find the amplitude threshold for a few simple initial distributions and get an idea of the overall picture. By numerical simulations of the evolution equation we verify that indeed all perturbations of the chosen shape with the amplitudes exceeding the threshold collapse, while the perturbations with the amplitudes below the threshold decay. In between these two worlds

is also a subclass of the decaying regime characterised by transient growth. In §2.5 we explore the evolution of lumps focussing on the effect of the dissipative term. For this range of Reynolds numbers there is no analytical theory and whether collapses could exist and if, yes, under what conditions was unknown. By examining numerically the dissipative 2d-BO equation we show that the account of the dissipative term strongly affects the lump evolution. The dissipative term does not prevent the collapse, but it might raise the threshold quite considerably, often beyond the domain of validity of our weakly nonlinear model. In the concluding §2.6 we summarize our findings.

2.2 The Model, Assumptions, Scaling and Asymptotic Scheme

2.2.1 Model Formulation

We consider evolution of three-dimensional localised finite-amplitude perturbations of a steady boundary layer shear flow $\boldsymbol{U}$ adjacent to an infinite flat boundary. The motion is governed by the Navier-Stokes equations for incompressible fluid of constant density ρ. In the Cartesian frame with the fluid in the half space $z > 0$ and with x and y directed streamwise and spanwise, respectively, the equations take the form

$$D_t u + wU' + p_x/\rho = -(\boldsymbol{u}\cdot\nabla)u + \nu/\rho\nabla^2 u \tag{2.2a}$$

$$D_t v + p_y/\rho = -(\boldsymbol{u}\cdot\nabla)v + \nu/\rho\nabla^2 v \tag{2.2b}$$

$$D_t w + p_z/\rho = -(\boldsymbol{u}\cdot\nabla)w + \nu/\rho\nabla^2 w \tag{2.2c}$$

$$\nabla\cdot\boldsymbol{u} = 0. \tag{2.2d}$$

where $\boldsymbol{U} = (U(z), 0, 0)$ is the basic boundary layer flow, $\boldsymbol{u} = (\boldsymbol{q}, w) = (u, v, w)$ and p are, respectively, the velocity and pressure perturbations, ν is fluid viscosity, $D_t = \partial_t + U\partial_x$ is the material derivative. The prime denotes the derivatives with respect to z. We impose no particular restrictions on $\boldsymbol{U}(z)$ apart from the assumption that the

flow is plane parallel (in this work we exclude consideration of non-parallel effects and three-dimensional boundary layers). In contrast to the original derivations in (Shrira [1989], Voronovich et al. [1998]), we do not require the profile $U(z)$ to have no inflection points.

The boundary conditions for the perturbations $\boldsymbol{u}$ at $z = 0$ are of two main types:

1. The "constant stress" conditions typical of environmental free surface-type flows,
$$w(z=0) = 0, \quad \frac{\partial u}{\partial z}\Big|_{z=0} = \frac{\partial v}{\partial z}\Big|_{z=0} = 0. \tag{2.3}$$
2. The more common "no-slip" conditions imply
$$\boldsymbol{u}(z=0) = 0. \tag{2.4}$$

The boundary condition at infinity is that of vanishing perturbation velocity, it is the same for both types of the boundary layers

$$\boldsymbol{u} \to 0, \quad \text{as} \quad z \to \infty. \tag{2.5}$$

We complete the formulation of our initial problem by specifying the perturbation velocity field at the initial moment, $\boldsymbol{u}(\boldsymbol{x}, 0)$. We are primarily interested in localised initial perturbations

$$\boldsymbol{u}(\boldsymbol{x}, 0) \to 0, \quad \text{as} \quad x, y \to \infty. \tag{2.6}$$

The Navier-Stokes equations (2.2) with the initial and boundary conditions (2.4, 2.5) or (2.3, 2.5) differing only the boundary condition at the surface $z = 0$ constitute the mathematical formulation of the problem.

The conventions for the "no-slip" and free-surface type "constant stress" boundaries differ. Usually, for the constant stress case the maximum of $U(z)$ is at the surface $z = 0$ with $U(z)$ vanishing as $z \to \infty$, while for the no-slip case, U is vanishing at $z = 0$ and tends to a finite "free stream velocity" U_∞ as $z \to \infty$. Mathematically these conventions are equally legitimate, one can switch from one to another by a

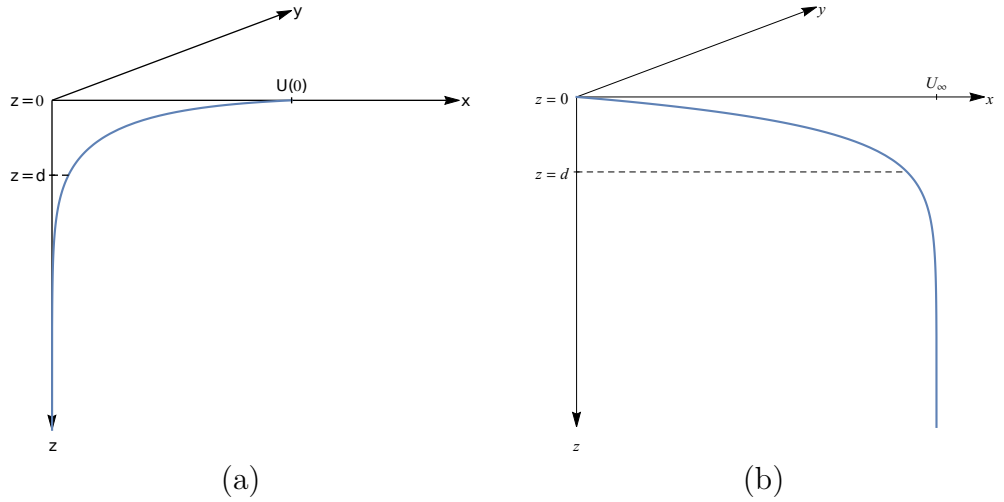

FIGURE 2.2: Sketch of geometry of a generic boundary layer profile with the shear localised in a thin layer of thickness d. (a) A typical free surface boundary layer with the maximum of velocity is attained at the surface $U_{max} = U(0)$. (b) Sketch of a boundary layer with a no-slip boundary. $U(\infty)$ is the free stream velocity.

galilean transformation, for example, setting $U(0)$ zero for a free surface type flow sketched in figure (2.2a) makes it undistinguishing from a typical no-slip boundary layer sketched in figure (2.2b). We assume the boundary layer profile $U(z)$ to be given, but do not specify it.

2.2.2 Scaling

We begin by specifying the scaling. The basic flow $U(z)$ has a characteristic velocity we denote as V_0. For the free-surface type boundary layers we choose it as the speed at the boundary $U(0)$, while for the no-slip case the natural choice for V_0 is the free-stream velocity, U_∞. For the time being we assume the characteristic streamwise and spanwise scales of perturbations to be comparable and denote as L, while as the cross-boundary scale we choose the boundary layer thickness d. Here we are considering long perturbations with $L \gg d$. We non-dimensionalise the dependent variables as follows:

$$\tilde{u} = \frac{u}{V_0}, \quad \tilde{v} = \frac{v}{V_0}, \quad \tilde{w} = \frac{w}{V_0}, \quad \tilde{x} = \frac{x}{L}, \quad \tilde{y} = \frac{y}{L}, \quad \tilde{z} = \frac{z}{d}, \quad \tilde{U} = \frac{U}{V_0},$$

$$\tilde{t} = \frac{V_0}{L} t, \qquad \tilde{p} = \frac{p}{\rho V_0^2}.$$

where quantities with tildes denote non-dimensional variables. To proceed, we first estimate the magnitudes of the perturbation from the basic governing equations ((2.2)). To this end we first write the incompressibility equation in non-dimensional form omitting the tildes. Then the magnitude of the vertical velocity perturbation $[\,w\,]$ expressed in terms of the magnitudes of the horizontal components $[\,\mathrm{q}\,]$,

$$[\,w\,] = \frac{d}{L}[\,q\,]. \tag{2.7}$$

The momentum equation (2.2a) yields the characteristic time scale,

$$[\,t\,] = \frac{L}{V_0}. \tag{2.8}$$

The viscosity is small but finite, it is supposed to affect, but not to dominate, the dynamics of perturbations of chosen scales inside the boundary layer at the timescale comparable to that of nonlinear effects.

After some algebra, upon eliminating pressure from the Navier-Stokes equations ((2.2)), we get a single nonlinear equation for vertical velocity perturbation w (see Appendix B for detail),

$$D_t^2\,\partial_{zz}^2\,w - U''\,D_t\,\partial_x w = \mathcal{N} + \left(\frac{d}{L}\,Re\right)^{-1} D_t \partial_{zzzz}^4 w, \tag{2.9}$$

where the horizontal gradient operators $\nabla_\perp = (\partial_x, \partial_y)$ and $\nabla_\perp^2 = \partial_{xx}^2 + \partial_{yy}^2$, while

$$\mathcal{N} = \frac{[\,q\,]}{V_0}\,D_t\,\partial_z\,\nabla_\perp[(\boldsymbol{u}\nabla)\boldsymbol{q}] - \left(\frac{d}{L}\right)^2 D_t^2\,\nabla_\perp^2 w - \left(\frac{d}{L}\right)^2 \frac{[\,q\,]}{V_0}\,D_t \nabla_\perp^2 (\boldsymbol{u}\nabla) w,$$

The Reynolds number Re should be sufficiently large,

$$Re^{-1} = \frac{\nu}{\rho V_0 d} \sim \frac{d}{L}\frac{[\,q\,]}{V_0}.$$

Note, that the equation is closed only in the linear approximation and just the leading-order viscous term is retained.

Thus, in the most general formulation of the problem, there are three independent non-dimensional parameters specifying respectively the smallness of nonlinearity ($[q]/V_0 = \varepsilon \ll 1$, dispersion ($d/L = \varepsilon_D \ll 1$) and dissipative effects ($Re^{-1} \ll 1$). Aiming to describe dynamics of three-dimensional perturbations in the boundary layer taking into account nonlinearity, dispersion and viscous effects in the distinguished limit we set

$$\varepsilon = \frac{[q]}{V_0} \ll 1, \qquad \varepsilon_D = \frac{d}{L} = O(\varepsilon), \qquad Re^{-1} \sim \frac{d}{L}\frac{[q]}{V_0} = O(\varepsilon^2). \tag{2.10}$$

This key assumption enables us to proceed with deriving the evolution equation (2.1) employing an asymptotic expansion in terms of a single small parameter and uniquely determines the scaling of dependent variables in the boundary layer. It is important to re-iterate at this point that the distinguished limit we consider here is applicable to a large variety of situations in boundary layer transition. In particular, we are aiming at critical Reynolds numbers of about $Re = 500 - 1000$. The characteristic velocity V_0 is $O(1)$, it depends on the specific type of the flow under consideration. The kinematic viscosity ν for air and water are, $1.5 \times 10^{-5} m^2 s^{-1}$ and $1.0 \times 10^{-6} m^2 s^{-1}$ respectively. In Kachanov wind tunnel experimental data the boundary layer thickness δ could vary from 0.7mm-38.0mm while the free stream velocity, U_∞ is $9.18 ms^{-1}$. The dimensionless boundary layer thickness $d = 1$.

2.2.3 Asymptotic expansion

To rationalise the specific choice of asymptotic expansion in powers of ε we will adopt, consider first the linearised inviscid reduction of the Navier-Sokes equations (2.2). It is straightforward to express pressure p, the streamwise and transverse perturbation velocities, u and v, in terms of vertical velocity w,

$$\partial_z D_t u = -[D_t \partial_z (wU') - \partial_x (D_t^2 w)] \tag{2.11a}$$

$$\partial_z D_t v = \partial_y (D_t w) \tag{2.11b}$$

$$\partial_z p = D_t w. \tag{2.11c}$$

Noting that under adopted assumption specifying the wavelength scale of the perturbations in terms of the nonlinearity, $\varepsilon_D = O(\varepsilon)$, we have

$$\partial_x \sim \partial_y \sim O(\varepsilon), \quad \partial_z \sim O(1).$$

Since in our scaling $U \sim O(1)$, it is easy to see that to leading order the material derivative $D_t = (U-c)\partial_x \sim O(\varepsilon)$, where c is yet unspecified phase velocity of long-wave perturbations. By virtue of our definition of ε ($\varepsilon = [u]/V_0$), $u \sim O(\varepsilon)$. Therefore, upon omitting the higher order terms, the relations ((2.11)), reduce to,

$$(U-c)\partial_x u = \underbrace{-wU'}_{O(\varepsilon^2)}, \quad \Longrightarrow \; w \sim O(\varepsilon^2) \tag{2.12a}$$

$$\partial_z[(U-c)v] = \underbrace{\partial_y(U-c)w}_{O(\varepsilon^3)}, \quad \Longrightarrow \; v \sim O(\varepsilon^3) \tag{2.12b}$$

$$\partial_z p = \underbrace{(U-c)\partial_x w}_{O(\varepsilon^3)}, \quad \Longrightarrow \; p \sim O(\varepsilon^3). \tag{2.12c}$$

Thus, assuming the streamwise perturbation velocity u to be $O(\varepsilon)$ and setting $\varepsilon_D = \frac{d}{L} = O(\varepsilon)$ uniquely dictates the scaling (2.12) of all other dependent variables inside the boundary layer. Taking into account the nonlinear and viscous terms neglected in this analysis, does not affect the found scaling. Therefore, we adopt the following asymptotic expansion,

$$u = U(z) + \varepsilon u_1 + \varepsilon^2 u_2 + \varepsilon^3 u_3 + ... \tag{2.13a}$$

$$w = \varepsilon^2 w_2 + \varepsilon^3 w_3 + \varepsilon^4 w_4 + ... \tag{2.13b}$$

$$v = \varepsilon^3 v_3 + \varepsilon^4 v_4 + ... \tag{2.13c}$$

$$p = \varepsilon^3 p_3 + \varepsilon^4 p_4 + ... \tag{2.13d}$$

where u_i, v_i, w_i, p_i are $O(1)$ functions of x, y, z, t.

The scaling (2.13) will be employed inside the boundary layer, outside the boundary layer and in the immediate vicinity of the boundary, in the viscous sublayer, the scaling is different and will be specified in the next section.

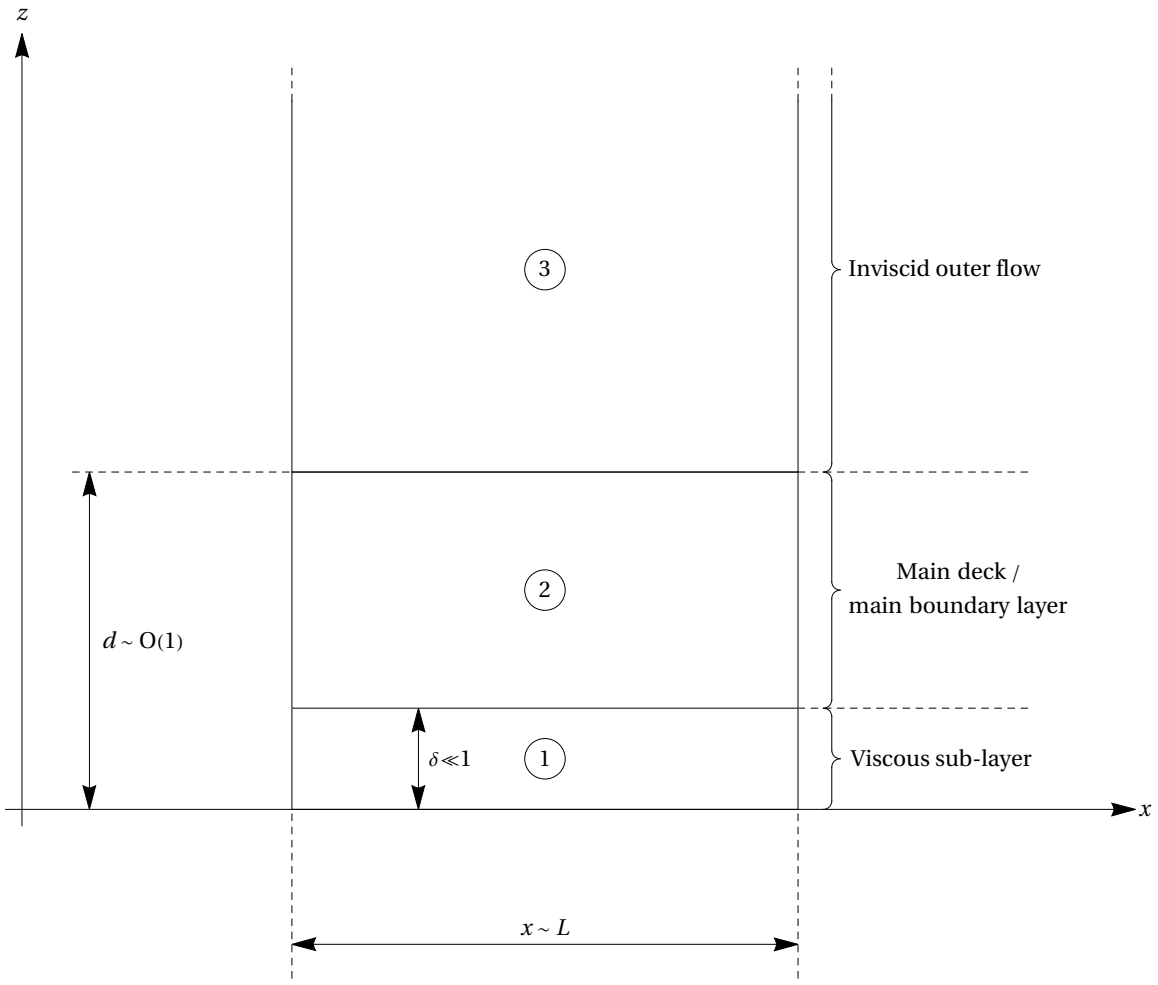

FIGURE 2.3: Sketch of triple deck structure illustrating three different regions of the boundary layer. The first region adjacent to the boundary is the viscous sub-layer where viscosity dominates, the second middle region is the main deck where viscosity, nonlinearity and dispersion are all balanced while the third semi-infinite region is the outer flow region where the flow is irrotational and its speed is equal to the mean flow.

2.3 Derivation of the nonlinear evolution equation

2.3.1 Preliminary consideration. Layout of the triple-deck scheme

In this section we derive the nonlinear evolution equation (2.1) for longwave three-dimensional perturbations employing a variation of 'triple deck' asymptotic approach (e.g. Van Dyke [1975], Sobey [2000], Timoshin [2016], Ruban [2017]). The

asymptotic scheme for large Reynolds numbers in the triple-deck context was independently invented by Stewartson [1969], Neiland [1969] and Messiter [1970] in their studies on trailing edge flow and supersonic separation. A few years later, Smith [1979] and Zhuk and Ryzhov [1980] extended the theory for hydrodynamic stability problems. As is common for this approach, we distinguish three domains in z, often called decks, with different balance between the terms in (2.9). The domains are sketched in figure 2.3. Following the convention the bulk of the boundary layer is referred to as the 'main deck' or 'middle deck', where we balance nonlinearity, dispersion and viscous effects and employ the asymptotic expansion (2.13). Immediately adjacent to the boundary lies much thinner viscous sub-layer or the 'first deck', where viscous terms are dominant, while the nonlinearity is negligible to leading order. The semi-infinite domain outside the boundary layer, where both viscous and nonlinear terms are negligible and the flow is potential, is often referred to as the 'outer flow' or the 'third deck'. We adopt this terminology introduced by Stewartson [1969]. In contrast to the triple deck convention we do not scale our variables in terms of powers of inverse Reynolds number, in our context we prefer to use the scaling in powers of ε. The derivation largely follows that in (Shrira [1989], and Voronovich et al. [1998]), with three key differences:

1. The case of no-slip boundary conditions is incorporated into consideration.
2. The viscous terms are included into the balance inside the main deck.
3. No assumption regarding the absence of inflection points in the mean flow $U(z)$ employed in (Shrira [1989], Voronovich et al. [1998]) is required.

We begin with analysis of the motion in the main deck.

2.3.2 Inside the boundary layer. The main deck

The scaling (2.13) based upon the distinguished limit which balances nonlinearity, weak dispersion and viscosity, provides the basis of our asymptotic analysis inside the main deck. On substituting the already adopted relations between the

small parameters $\varepsilon_D = \varepsilon$ and introducing re-scaled Reynolds number denoted as Re_*, $Re_* = Re\,\varepsilon^2$, into equation (2.9), we make the scaling of each term more explicit,

$$D_t^2\,\partial_{zz}^2\,w - U''\,D_t\,\partial_x w = \varepsilon\,D_t\,\partial_z\,N_L + \frac{\varepsilon}{Re}\,D_t\partial_{zzzz}^4 w - \varepsilon^2 D_t^2\,\nabla_\perp^2 w - \varepsilon^3\,D_t\nabla_\perp^2((\boldsymbol{u}\nabla)w), \tag{2.14}$$

where $Re^* = \varepsilon^2 Re$ is the re-scaled Reynolds number, $\nabla_\perp = (\partial_x,\,\partial_y)$,

$$N_L = [\partial_x(u\partial_x u + v\partial_y u + w\partial_z u) + \partial_y(u\partial_x v + v\partial_y v + w\partial_z v)],$$

$$= [\varepsilon\partial_x(\varepsilon^3 u\partial_x u + \varepsilon^5 v\partial_y u + \varepsilon^3 w\partial_z u) + \varepsilon\partial_y(\varepsilon^5 u\partial_x v + \varepsilon^7 v\partial_y v + \varepsilon^5 w\partial_z v)]$$

$$= \varepsilon^4[u\partial_x u + w\partial_z u] + \varepsilon^6[\partial_x(v\partial_y u) + \partial_y(u\partial_x v + w\partial_z v + \varepsilon^2 v\partial_y v)].$$

Although the streamwise and spanwise scales are assumed to be comparable, according to (2.13) the spanwise velocity is two orders of magnitude smaller, which enables us to split the nonlinear term N_L into two parts and neglect the $O(\varepsilon^6)$, $O(\varepsilon^7)$ and $O(\varepsilon^8)$ terms. The term $\varepsilon^3\,D_t\nabla_\perp^2((\boldsymbol{u}\nabla)w)$ in the right-hand-side of (2.14) will also be neglected in our further analysis. Upon these simplifications, recalling that $w = O(\varepsilon^2)$, we re-write equation (2.14) explicitly pulling out ε,

$$\underbrace{D_t^2\,\partial_{zz}^2\,w - U''\,D_t\,\partial_x w}_{\text{terms of } O(\varepsilon^4)} = \varepsilon^5\,D_t\,\partial_z\,\partial_x[u\partial_x u + w\partial_z u] + \frac{\varepsilon^5}{Re}\,D_t\partial_{zzzz}^4 w - \varepsilon^6 D_t^2\,\nabla_\perp^2 w. \tag{2.15}$$

Since $v = O(\varepsilon^3)$ and $u = O(\varepsilon^1)$, it is easy to see that by virtue of the continuity equation: $\partial_x u = -\partial_z w + O(\varepsilon^4)$. To solve equation (2.15) we adopt a moving coordinate frame and introduce fast and slow non-dimensional independent variables,

$$Z_1 = \varepsilon\tilde{z} = \frac{1}{L}z, \qquad \tau = \varepsilon\frac{V_0}{L}t, \qquad \tilde{x} = \frac{x - ct}{L}, \qquad \tilde{y} = \frac{y}{L}, \quad \tilde{z} = \frac{z}{d}, \qquad \tilde{c} = \frac{c}{V_0}, \tag{2.16}$$

where c is the speed of the long waves which will be specified later and the tildes denote non-dimensional quantities. Upon the introduction of the slow-spatial variable Z_1 and slow time τ, the material derivative D_t^2 and ∂_{zz}^2 in terms of the tilde variables

take the form,

$$D_t^2 = \frac{V_0^2}{L^2}[(\tilde{U}-\tilde{c})\partial_{\tilde{x}}+\varepsilon\partial_\tau]^2 = \frac{V_0^2}{L^2}\tilde{D}_t^2 \sim \varepsilon^2\tilde{D}_t^2, \qquad \partial_{zz}^2 = \frac{1}{d^2}(\partial_{\tilde{z}}+\varepsilon\partial_{Z_1})^2 = \frac{1}{d^2}\partial_{\tilde{z}\tilde{z}}^2 \sim \partial_{\tilde{z}\tilde{z}}^2,$$

From this moment we operate only with non-dimensional variables and omit tildes. The equation for the $z-$ component of velocity w (2.15) reduces to

$$D_t^2\partial_{zz}^2 w - U''D_t\partial_x w = \varepsilon D_t\partial_z\partial_x[u\partial_x u + w\partial_z u] + \frac{\varepsilon}{Re}D_t\partial_{zzzz}^4 w - \varepsilon^2 D_t^2\nabla_\perp^2 w, \quad (2.17)$$

where

$$D_t = (U-c)\partial_x + \varepsilon\partial_\tau, \qquad \partial_z = \partial_z + \varepsilon\partial_{Z_1}. \quad (2.18)$$

We assume the mean flow $U(z)$ to be entirely localised in the boundary layer and, correspondingly, to depend only on the fast scale z. The situations with U having also dependence on the slow scale are of interest and can be easily incorporated into the scheme, but are not considered here.

Here, for the time being, for both the free-surface-type flows with the constant stress boundary conditions and the flows with the no-slip conditions we impose only the no-flux condition at $z = 0$. We will deal with the true boundary conditions at the boundary in §2.3.4. We also require vanishing of velocity as $Z_1 \to \infty$. In addition, we introduce 'inner boundary conditions', by requiring matching at the outer boundary of the boundary layer, that is,

$$w(z=0) = 0; \qquad w(z\to\infty) = const = w(Z_1\to 0), \qquad w(Z_1\to\infty)\to 0. \quad (2.19)$$

We will seek an asymptotic solution to the boundary value problem (2.17), (2.18) and (2.19) employing power series in ε (2.13). On finding the solution to (2.17) for w at a desired order in ε, we find u, v and p with the corresponding accuracy from the basic equations, where we have set $\rho = 1$,

$$D_t u + wU' + p_x = -\varepsilon(\boldsymbol{u}\cdot\nabla)u + \frac{\varepsilon}{Re}u'' \tag{2.20a}$$

$$D_t v + p_y = -\varepsilon(\boldsymbol{u}\cdot\nabla)v + \frac{\varepsilon}{Re}v'' \tag{2.20b}$$

$$\partial_x u + \partial_y v + \partial_z w = 0. \tag{2.20c}$$

The solutions for u, v and p, accurate to the corresponding order in ε, are further used for the derivation of the next order terms for w; the cycle is repeated as many times as necessary.

At the first step, on substituting (2.13) into equation (2.17) and setting $\varepsilon = 0$, we see that in the leading order nonlinearity and viscous dissipation drop out. Taking into account (2.18) we obtain for the leading term in the expansion of w, which is w_2, the longwave limit of the Rayleigh equation,

$$(U-c)\partial_{xx}[(U-c)w_2'' - U''w_2] = 0, \tag{2.21}$$

where derivatives with respect to the fast variable z are denoted by primes. The key point of the scheme is, that, as it can be easily seen from (2.21), to leading order the x, y and z dependencies can be separated. Assuming the disturbance to be localized in the streamwise direction, the general solution to the Rayleigh equation (2.21) is convenient to present in the form,

$$w_2 = (f(x,y,Z_1) * \partial_x A(x,y,\tau))\cdot(U(z)-c), \tag{2.22}$$

where $*$ designates the convolution of two functions

$$\varphi * \psi = \int_{-\infty}^{+\infty}\int_{-\infty}^{+\infty}\varphi(\hat{x},\hat{y})\psi(x-\hat{x},y-\hat{y})\mathrm{d}\hat{x}\mathrm{d}\hat{y}.$$

Here, as it will be made obvious at the next step a few lines below, $A(x,y,\tau)$ is the amplitude of the x-component of velocity perturbation, while the arbitrary function $f(x,y,Z_1)$ in (2.22) is the general representation of a function of (x,y,Z_1) localized or periodic in (x,y). The fundamental properties of the convolution presentation (2.22) become more transparent on taking the Fourier transform of solution (2.22). The

standard way of representing a function of (x, y, Z_1, τ) is to decompose it into a set of spatial orthogonal functions with time-dependent amplitudes. We chose Fourier transform in (x, y) and a particular function f specifying each Fourier mode that depends on the slow cross-boundary spatial variable Z_1. The specific dependence on the slow spatial scale $f(Z_1)$ will be found below.

The adopted no-flux boundary condition $w_2(z = 0) = 0$ specifies the eigenvalue c,

$$c = U|_{z=0} = U(0). \tag{2.23}$$

The mode we are considering is a 'vorticity wave'. To leading order its speed is the the mean flow velocity at $z = 0$, i.e. $c_0 = U(0)$. Recall that for the typical free surface flows $U(0)$ attains its maximal value and equals zero for the flows with no-slip boundary, hence, $(c_0 = U(0) = 0)$. The speed of vorticity waves corresponding to either of these two types of boundary conditions is henceforth denoted by a constant U_0. In any case, it plays no role in further analysis since its only significance is in specifying the reference frame, it will be removed by the galilean transformation at the next step. The slow function $f(Z_1)$ will be specified later.

To proceed further, we first find the other components of perturbation wave field from equation (2.20) employing the asymptotic expansion (2.13). Substituting the leading order solution (2.22) for w_2 into (2.20) we get the other components of the perturbation field,

$$u_1 = -U'(f * A), \tag{2.24a}$$

$$v_2 = 0, \tag{2.24b}$$

$$p_2 = 0. \tag{2.24c}$$

Thus, we have found that $\partial_z p_2 = 0$. This implies that to leading order pressure does not depend on z, i.e. $p = \varepsilon^2 p_2(x, y, \tau)$. Here we briefly demonstrate why the horizontal variation of pressure equal to zero for the case of the no-slip boundary condition within the framework of linearised Euler equations. Let us consider x and y components of the linearised momentum equation which follow from from equations

(2.20a) and (2.20b). If we substitute $u = v = w = 0$ at $z = 0$ dictated by the no-slip condition on the boundary into the equations (2.20a) and (2.20b), it is easy to see that the $z-$independent pressure must vanish, since $p_x = p_y = 0$.

Note that (2.24a) clarifies the physical sense of amplitude A, it is indeed, up to a factor $-U'$, amplitude of the x-component of perturbation velocity. The above relations show that to leading order the motion is extremely simple: the particles of the vorticity wave motion oscillate, mainly, in the streamwise direction, while the cross-boundary and, especially, spanwise velocities and pressure perturbations are much smaller in the adopted long-wave approximation. This extraordinary feature is specific for long vorticity waves (see Voronovich et al. [1998]). Such a simplicity of the motion of interest in the leading order is the key element enabling for a remarkably simple description of nonlinear dynamics of perturbations which we will discuss below.

Substituting expressions (2.22) for w_2 and (2.24a) for u_1 into (2.17) we get an equation for w_3,

$$w_3'' - \frac{U''}{U-c} w_3 = -M \frac{U''}{U-c} + \frac{P}{Re} \frac{U''''}{U-c} - T \frac{[(U-c)^2]'}{U-c} + R \frac{[(U')^2 - (U-c)U'']'}{U-c}, \tag{2.25}$$

where,

$$M = (f * A_\tau), \quad P = (f * A), \quad T = (f_{Z_1} * A_x), \quad R = (f * A)(f * A_x),$$

the subscripts x and τ stand for the corresponding derivatives. Upon solving the inhomogeneous Rayleigh equation (2.25) employing solutions to the homogeneous equation found at the previous, the general solution to (2.25) can be written as,

$$w_3 = M - T(U-c) \int_z^\infty \mathrm{d}\xi + B(U-c) \int_z^\infty \frac{\mathrm{d}\xi}{(U-c)^2} + \frac{P}{Re} (U-c) \int_z^\infty \left[\frac{U'''}{(U-c)^2} \right] \mathrm{d}\xi - RU', \tag{2.26}$$

where, B is an arbitrary constant specifying the "amplitude" of the second solution to the homogeneous Rayleigh equation in the longwave limit (2.21). To eliminate singularity in the integrals in (2.26), we chose B in such a way that the equation for

w_3 takes the form,

$$w_3 = M - T\,(U-c)\int_z^\infty \left[1 - \frac{Y}{(U-c)^2}\right] \mathrm{d}\xi + \frac{P}{Re}\,(U-c)\int_z^\infty \left[\frac{U'''}{(U-c)^2}\right] \mathrm{d}\xi - RU', \tag{2.27}$$

where Y is an integration constant which is redefined differently for the no-slip and rigid lid boundaries. For the no-slip boundary $c = U(0) = 0$, Y is chosen as,

$$Y = \lim_{z\to\infty}(U)^2 = U^2|_{z=\infty} = U_\infty^2 = constant. \tag{2.28}$$

For the free-surface type boundary layers we choose the constant of integration Y as,

$$Y = \lim_{z\to 0}(U-c)^2 = c^2 = U^2|_{z=0} = U(0)^2 = constant. \tag{2.29}$$

In both cases the constants of integration are equal to the maximal velocity of the basic flow squared, it is therefore convenient to treat these constants as equal and denote them as U_{max}^2. We remind that under the adopted convention for the no-slip case $U(0) = 0$ and $U' > 0$, while for the free surface type boundary layers: $U(0) = U_{max}$ and $U' < 0$.

To evaluate the singular integrals in (2.27) we assume that near the boundary $z = 0$ we expand $U - c$ as $U'(0)z = U_0'z$. Upon applying the no-flux boundary condition at the boundary, $w|_{z=0,Z_1=0} = 0$, to equation (2.27), after some algebra, we get equation for the amplitude A containing so far unspecified function $f(Z_1)$ of the slow cross-boundary variable Z_1,

$$\begin{aligned}(f(0) * A_\tau) - U'(0)\,(f(0) * A)(f(0) * A_x) + \left(\frac{U_0^2}{U'(0)}\right)(f_{Z_1}(0) * A_x) \\ + \frac{1}{Re}\left(\frac{U'''(0)}{U'(0)}\right)(f(0) * A) = 0\end{aligned} \tag{2.30}$$

where $f(0) \equiv f(x, y, Z_1 = 0)$.

2.3.3 The outer flow

To specify the dependence of the solution (2.22) and (2.27) on the slow variable Z_1, first we need to proceed to the next order in ε in our main equation (2.17) for w_2. Employing the same asymptotic procedure and using (2.22) and (2.27) we express u, v, p in terms of amplitude A,

$$u_2 = -U_{max}^2(f_{Z_1} * \nabla_\perp^{-2} A_{xx})(U-c)^{-1} + (f_{Z_1} * A)U' \int_z^\infty [1 - U_{max}^2(U-c)^{-2}]\mathrm{d}\xi$$

$$+ \frac{1}{2}(f*A)^2 U'' - \frac{\bar{P}U'}{Re}\int_z^\infty \left(\frac{U'''}{(U-c)^2}\right)\mathrm{d}\xi - \frac{\bar{P}}{Re}\frac{U'''}{(U-c)} \tag{2.31}$$

$$v_3 = -U_{max}^2(f_{Z_1} * \nabla_\perp^{-2} A_{xy})(U-c)^{-1} \tag{2.32}$$

$$p_3 = U_{max}^2\,(f_{Z_1} * \nabla_\perp^{-2} A_{xx}) \tag{2.33}$$

where $\bar{P} = (f * \partial_x^{-1} A)$ and Y is given by expression (2.28).

We now consider the next order term for the cross-boundary velocity, w_4. After some algebra it can be brought to the form,

$$\partial_x[(U-c)w_4'' - U''w_4] = R_1, \tag{2.34}$$

where,

$$R_1 = -(f_{Z_1 Z_1} * A_{xx})(U-c)^2 - (f * \nabla_\perp^2 A_{xx})(U-c)^2 + F(x,y,\tau,z,Z_1),$$

The term $F(x,y,\tau,z,Z_1)$ is given by a bulky expression which tends to zero as $z \to \infty$ faster than $|z|^{-1}$. In contrast, for an arbitrary function of $f(x,y,Z_1)$ the first two terms on the right-hand side of equation (2.34) do not vanish as $z \to \infty$. As a result, the integration of (2.34) yields secular growth of w_4 as $z \to \infty$, which does not allow the matching condition $w(z \to \infty, Z_1) \to$ const to be satisfied. Therefore, we put these secular terms to zero, which gives us an equation determining the dependence of the unspecified yet function f on the slow variable Z_1,

$$(f_{Z_1 Z_1} * A_{xx}) + (f * \nabla_\perp^2 A_{xx}) = 0. \tag{2.35}$$

The equation is complemented by the boundary condition at infinity

$$w(Z_1 \to \infty) = 0. \tag{2.36}$$

To find $f(Z_1)$ we perform the Fourier transform with respect to x, y in the boundary problem (2.35) and (2.36). Making the Fourier transform of the convolution and omitting the amplitude A, we get the boundary value problem,

$$\partial^2_{Z_1 Z_1} \hat{f}(\boldsymbol{k}) - k^2 \hat{f}(\boldsymbol{k}) = 0, \tag{2.37}$$

with the boundary conditions,

$$\hat{f}(\boldsymbol{k})|_{Z_1 \to \infty} = 0, \quad \hat{f}(\boldsymbol{k})|_{Z_1 = 0} = 1. \tag{2.38}$$

Here $\hat{f}(\boldsymbol{k}, Z_1)$ is the Fourier transform of $f(x, y, Z_1)$

$$f(x, y, Z_1) = \frac{1}{4\pi^2} \int_{-\infty}^{+\infty} \int_{-\infty}^{+\infty} \hat{f}(k_x, k_y, Z_1) e^{(i(k_x x + k_y y))} \mathrm{d}k_x \mathrm{d}k_y, \tag{2.39}$$

and $k = |\boldsymbol{k}|$, $k^2 = k_x^2 + k_y^2$. The boundary condition $\hat{f}(\boldsymbol{k})|_{Z_1=0} = 1$ has been introduced for convenience to normalize the motion in the outer deck $\hat{f}(k_x, k_y, Z_1)$ near the boundary. As one could anticipate, the motion in the outer layer is potential and satisfies the Laplace equation (2.37). Hence, the boundary value problem (2.37), (2.38) is easily solvable. Its solution satisfying the boundary condition (2.38) has the form

$$\hat{f}(\boldsymbol{k}, Z_1) = e^{-kZ_1}. \tag{2.40}$$

Next we designate $\partial_{Z_1} \hat{f}(\boldsymbol{k}, 0) \equiv Q(k_x, k_y)$ and take into account that at the boundary $\hat{f}(0) = \delta(x)\delta(y)$. The solution to equation (2.37) yields the kernel of the integral operator $Q(\boldsymbol{k}) = -|\boldsymbol{k}| = -k$ in the long wave limit. Substituting these notations into (2.30), we obtain nonlinear evolution equation for the amplitude of three-dimensional long-wave boundary layer perturbations in the distinguished limit,

$$A_\tau - \alpha_1 A A_x - \beta_1 \hat{K}[A_x] + \gamma A = 0, \tag{2.41}$$

where $\alpha_1 = U'(0)$, $\beta_1 = \frac{U_0^2}{U'(0)}$, $\gamma = \frac{1}{Re}\frac{U'''(0)}{U'(0)}$, and the dispersion operators $\hat{K}$ in the integral form reads

$$\hat{K}[\varphi(\boldsymbol{k})] = \frac{1}{4\pi^2}\int_{-\infty}^{+\infty}\int_{-\infty}^{+\infty}|\boldsymbol{k}|\varphi(\boldsymbol{r}_1)e^{(i\boldsymbol{k}(\boldsymbol{r}-\boldsymbol{r}_1))}\mathrm{d}\boldsymbol{k}\mathrm{d}\boldsymbol{r}_1. \tag{2.42}$$

The evolution equation (2.41) differs from the 2d-BO only by the explicit account of viscous dissipation, which contributes into the evolution equation the Rayleigh friction type term γA. The coefficients α_1 and β_1 of (2.41) will be removed by rescaling in the next section to obtain the final evolution equation that will form the framework of our further study.

At this point it is appropriate to summarise the scalings and behaviour of all components of the perturbation field inside and outside of the boundary layer, i.e. in the main deck and the outer layer. Recall that inside the the bulk of the boundary layer according to (2.13), (2.24)

$$u \sim \varepsilon, \quad w \sim \varepsilon^2, \quad v \sim \varepsilon^3, \quad p \sim \varepsilon^3.$$

At the outer periphery of the boundary layer we have

$$u \sim \varepsilon^2, \quad w \sim \varepsilon^2, \quad v \sim \varepsilon^3, \quad p \sim \varepsilon^3.$$

Note that although the basic flow shear vanishes and $u \sim w$, the potential flow remains essentially 2d: $v \sim \varepsilon^3 \ll u, w$. The $O(\varepsilon^2)$ perturbations of velocity produce $O(\varepsilon^3)$ variations of pressure. In the outer layer the pressure perturbations and all components of velocity decay exponentially as e^{-kZ_1}.

To check whether this picture, although entirely self-consistent, is not an artefact of the adopted scaling assumptions we considered the simplest piece-wise inviscid model of boundary layer: a constant vorticity layer of thickness d confined between the boundary and potential flow. In the linear setting this model could be solved exactly without any *a priori* scaling hypotheses. Then assuming the perturbations to be longwave, i.e. setting $kd = \varepsilon$, upon expanding the exact solutions in powers of ε we recover the results obtained by means of the asymptotic expansion.

2.3.4 Viscous sub-layer

In this section we outline how a uniformly valid asymptotic expansion could be obtained.

2.3.4.1 Divergence of the asymptotic expansion and Tollmien's rescaling

Consider more closely behaviour of the main deck solutions u_2 and v_3 of (2.31) and (2.32) as $z \to 0$. Near the boundary as $z \to 0$, we apply Taylor series to expand $(U - c) \approx U'(0)\, z$ to obtain,

$$u_2 = -\frac{U_{max}^2}{U'(0)}(f_{Z_1} * \nabla_\perp^{-2} A_{xx})\frac{1}{z} + \frac{U_{max}^2}{U'(0)}(f_{Z_1} * A)\frac{1}{z} + \frac{1}{2}(f * A)^2 U''(0), \tag{2.43}$$

$$v_3 = -\frac{U_{max}^2}{U'(0)}(f_{Z_1} * \nabla_\perp^{-2} A_{xy})\frac{1}{z}, \tag{2.44}$$

Let us take a closer look at the divergence of the streamwise velocity u_2 of (2.43) and try to carry out some algebra to simplify the first two terms on the RHS with singularities at $z = 0$. To this end we transform them into Fourier space i.e,

$$-\frac{U_{max}^2}{U'(0)}\frac{k_x^2}{k_x^2 + k_y^2}(\hat{f}_{Z_1} \cdot \hat{A})\frac{1}{z} + \frac{U_{max}^2}{U'(0)}(\hat{f}_{Z_1} \cdot \hat{A})\frac{1}{z} = \frac{U_{max}^2}{U'(0)}\left[\frac{k_x^2 + k_y^2 - k_x^2}{k_x^2 + k_y^2}\right](\hat{f}_{Z_1} \cdot \hat{A})\frac{1}{z},$$

$$= \frac{U_{max}^2}{U'(0)}\left[\frac{k_y^2}{k_x^2 + k_y^2}\right](\hat{f}_{Z_1} \cdot \hat{A})\frac{1}{z}, \tag{2.45}$$

Substituting the simplified form of the singular terms of equation (2.45) and taking into account their inverse Fourier transform we obtain a more compact form of the expression u_2,

$$u_2 = \frac{U_{max}^2}{U'(0)}(f_{Z_1}(0) * \nabla_\perp^{-2} A_{yy})\frac{1}{z} + \frac{1}{2}(f * A)^2 U''(0), \tag{2.46}$$

It is easy to see that uniformity of the asymptotic expansion employed in the previous section breaks down as $z \to 0$. Indeed, according to (2.46) and (2.44) velocity components u_2 and v_3 diverge as $1/z$, unless spanwise dependence of amplitude vanishes,

$$u_2 \sim 1/z, \quad v_3 \sim 1/z. \tag{2.47}$$

The cause of this singularity is the critical layer that coincides with the fluid boundary in the long-wave limit. It is obvious that in the generic case the scaling (2.13) adopted for the main deck is invalid near the boundary. A quick fix is to confine our consideration to quasi-planar perturbations, i.e. assume $A_y \ll A_x$. Then the singular terms in the expressions for u_2 and v_3 given by (2.46) and (2.44) drop into the next order.

In principle, it is also possible to derive a uniformly valid asymptotic solution for generic perturbations as well. Here we just outline how to do this. To get uniformly valid asymptotic expansion we have to apply singular perturbation technique: to re-scale the variables appropriately and solve the Navier-Stokes equations in the region immediately adjacent to the boundary and then match the resulting inner solution with the outer solutions already obtained for the main deck. By choosing the scaling we choose different regimes with different balances and, correspondingly, different thicknesses of this region. For example, Reutov [1995] considered nonlinear critical layer where nonlinearity is dominant. In this scenario relevant for very high Reynolds numbers the dynamics of the critical layer is very complicated and does not allow straightforward analytic treatment. Here, we focus upon the opposite limit, the regime where viscosity is dominant, while nonlinearity in the critical layer is negligible. Our approach has its roots in the insight by Tollmien [see Tollmien et al. [1931]] that at the critical layer both the fourth order derivative term and the second order derivative term in the Orr-Sommerfeld equation are dominant, that is,

$$w^{iv} = ik_x \, Re(U - c)w''.$$

Assuming $k_x \sim O(1)$ Tollmien showed that after a re-scaling of the length scale and the Taylor series expansion of the mean flow $U(z)$ in the vicinity of the critical layer

using:

$$\chi = \frac{(z - z_c)}{\delta}, \qquad \delta = (ik_x \, Re \, U'(z_c))^{-1/3}, \quad U(z) - c \sim U'(z_c)(z - z_c), \text{ as } \quad z \to z_c,$$

the Orr-Sommerfeld equation reduces to

$$\frac{d^4 w}{d\chi^4} - \chi \frac{d^2 w}{d\chi^2} = 0.$$

Solution of this equation satisfying the arbitrary boundary conditions can be expressed in terms of the well known Airy functions and their integrals (see, Drazin and Reid [2004]). The known drawback of the Tollmien's solutions, as pointed out by Drazin [2002], is that the characteristic critical layer thickness $\delta \sim Re^{-1/3}$ proves large compared to the overall thickness of the boundary layer δ_{BL}, which contradicts the basic assumption $\delta \ll \delta_{BL}$. For example, for the Blasius boundary layer $\delta_{BL} \sim Re^{-1/2}$.

Here, we do not encounter this difficulty if we pursue the Tollmien idea, since we are concerned only with motions with $O(\varepsilon)$ small wavenumbers. In this section, following (Voronovich et al. [1998]), we exploit the fact that we consider only long perturbations with $O(\varepsilon)$ wavenumbers and include into the scaling of the critical layer thickness δ the ε smallness of wavenumbers ($\varepsilon \ll 1$):

$$\delta = (\varepsilon \, Re \, U_0')^{-1/3} \sim \varepsilon^{1/3} \quad (U_0' = U'|_{z=0}),$$

which ensures that δ is small compared to the $O(1)$ overall thickness of the boundary layer δ_{BL}. For further consideration it is crucially important that

$$1 \gg \delta \gg \varepsilon, \tag{2.48}$$

which means that the thickness of viscous critical layer we are considering far exceeds the thickness of nonlinear critical layer, while it is small compared to the boundary layer thickness.

2.3.4.2 Re-scaling. Inner variable

To proceed with the study of the perturbation dynamics inside the viscous critical layer we re-scale our variables as follows,

$$\xi = \frac{z}{\delta}; \qquad T = U_0'\tau; \qquad U - c = \delta\, U_0'\, \xi + o(\delta)$$

$$u = U_0'\hat{u}; \qquad v = \frac{\varepsilon}{\delta} U_0'\hat{v}; \qquad w = \delta\, U_0'\hat{w}, \qquad p = \varepsilon (U_0')^2 \hat{p}, \tag{2.49}$$

In terms of the new variables after some algebra, equations for w and the complementary Navier-Stokes equations for other components of velocity take the form,

$$\xi\,(U_0')^2\,\partial_x\,\partial^2_{\xi\xi}\,\hat{w} + \frac{\varepsilon}{\delta}\,(U_0')^2\,\partial_T\,\partial^2_{\xi\xi}\hat{w} = \frac{\varepsilon}{\delta}\,(U_0')^2\,\partial_\xi\,\partial_x\,[\hat{u}\,\partial_x\,\hat{u} + \hat{w}\,\partial_\xi\hat{u}] + \frac{(\varepsilon\, Re)^{-1}}{\delta^3}\,(U_0')\,\partial^4_{\xi\xi\xi\xi}\,\hat{w} \tag{2.50a}$$

$$(U_0')^2\,\xi\,\partial_x\,\hat{u} + \frac{\varepsilon}{\delta}\,(U_0')^2\,\partial_T\hat{u} + (U_0')^2\,\hat{w} + \frac{\varepsilon}{\delta}\,(U_0')^2\,\hat{p}_x = -\frac{\varepsilon}{\delta}\,(U_0')^2\,[\hat{u}\,\partial_x\,\hat{u} + \frac{\varepsilon}{\delta}\,\hat{v}\,\partial_y\,\hat{u} + \hat{w}\,\partial_\xi\,\hat{u}] + \frac{(\varepsilon\, Re)^{-1}}{\delta^3}\,U_0'\,\partial^2_{\xi\xi}\,\hat{u} \tag{2.50b}$$

$$\xi\,(U_0')^2\,\partial_x\,\hat{v} + (U_0')^2\,\frac{\varepsilon}{\delta}\,\partial_T\,\hat{v} + (U_0')^2\,\hat{p}_y = -(U_0')^2\,[\frac{\varepsilon}{\delta}\hat{u}\,\partial_x\,\hat{v} + (\frac{\varepsilon}{\delta})^2\,\hat{v}\,\partial_y\,\hat{v} + \frac{\varepsilon}{\delta}\hat{w}\,\partial_\xi\,\hat{v}] + \frac{(\varepsilon\, Re)^{-1}}{\delta^3}\,U_0'\,\partial^2_{\xi\xi}\,\hat{v} \tag{2.50c}$$

$$U_0'\,\hat{u}_x + \frac{\varepsilon}{\delta}\,U_0'\,\hat{v}_y + U_0'\,\hat{w}_\xi = 0 \tag{2.50d}$$

Eliminating U_0' and substituting $\delta = (\varepsilon\, U_0'\, Re)^{-1/3}$, while retaining only the leading order $O(1)$ terms and ϵ/δ correction terms, equation (2.50) can be written as,

$$(\partial^2_{\xi\xi} - \xi\partial_x)\hat{w}'' = \frac{\varepsilon}{\delta}\,(\,\partial_T\,\hat{w}'' - \partial_\xi\partial_x(\hat{u}\hat{u}_x + \hat{w}\hat{u}_\xi)) \tag{2.51a}$$

$$(\partial^2_{\xi\xi} - \xi\partial_x)\hat{u} = \hat{w} + \frac{\varepsilon}{\delta}(\partial_T\hat{u} + \hat{p}_x + \hat{u}\hat{u}_x + \hat{w}\hat{u}_\xi) \tag{2.51b}$$

$$(\partial^2_{\xi\xi} - \xi\partial_x)\hat{v} = \hat{p}_y + \frac{\varepsilon}{\delta}(\partial_T\hat{v} + \hat{u}\hat{v}_x + \hat{w}\hat{v}_\xi) \tag{2.51c}$$

$$\hat{u}_x + \hat{w}_\xi = -\frac{\varepsilon}{\delta}\,\hat{v}_y, \tag{2.51d}$$

where $\hat{w}'' = \partial^2_{\xi\xi}\hat{w}$.

The next step we do not pursue here is to find solution to (2.51) in the form of asymptotic power series in ε/δ rather than ε, subject to the appropriate boundary conditions. At the boundary the solutions should satisfy either constant stress conditions,

$$\hat{w}|_{\xi=0} = 0, \qquad \hat{u}'|_{\xi=0} = \hat{v}'|_{\xi=0} = 0, \tag{2.52}$$

or, the no-slip conditions

$$u|_{\xi=0} = v|_{\xi=0} = 0. \tag{2.53}$$

These solutions should not exhibit any singularities in the critical layer. They have to be matched with the main deck solution at $\xi \to \infty$. Hence, the resulting matched asymptotic expansion will be uniformly valid.

2.3.5 Conclusions

The main result of this section is the nonlinear evolution equation (2.41) for long three-dimensional perturbations in semi-infinite boundary layers with explicit account of viscous effects. The equation is universal in the sense that the specific profile of the boundary layer is immaterial. The rudimentary specificity of the boundary layer retained in the coefficients in (2.41) can be further reduced by re-scaling the variables

$$\tau_1 = \tau\,U'(0), \quad d = \frac{U_0}{U'(0)}, \quad x_1 = x/d, \quad A_1 = -\frac{1}{d}\,A, \tag{2.54}$$

and setting $d = 1$, which yields (with the subscripts dropped)

$$A_\tau + AA_x - \hat{K}[A_x] + \widetilde{\gamma}\,A = 0, \tag{2.55}$$

the dispersion operators $\hat{K}$ remains the same,

$$\hat{K}[\varphi(\boldsymbol{k})] = \frac{1}{4\pi^2}\int_{-\infty}^{+\infty}\int_{-\infty}^{+\infty}|\boldsymbol{k}|\varphi(\boldsymbol{r}_1)e^{(i\boldsymbol{k}(\boldsymbol{r}-\boldsymbol{r}_1))}d\boldsymbol{k}d\boldsymbol{r}_1, \tag{2.56}$$

where, $k = |\boldsymbol{k}|$. Although at the moment we have proved the uniform validity of the expansion only for $k_x \ll k_y$ we will examine the evolution equation for the arbitrary scales of k_x and k_y. The only remaining coefficient,

$$\widetilde{\gamma} = \frac{1}{\varepsilon^2 Re}\frac{U'''(0)}{(U'(0))^2},$$

showing the importance of the Rayleigh friction type term compared to the nonlinear one in the evolution equation. The magnitude of the friction term is proportional to the ratio of the curvature of vorticity at the boundary and the Reynolds number. In the adopted normalisation it is also proportional to ε^{-2}, i.e. the inverse square of the nonlinearity or dispersion parameter. We stress that both the Reynolds number and the curvature of vorticity at the boundary are equally important.

We re-iterate that the evolution equation (2.55) is equally valid both for the boundary layers with no-slip and constant stress conditions at the boundary.

The nonlinear evolution equation (2.55) provides the framework for studying collapses of three-dimensional perturbations and, in particular, the role of the Rayleigh friction in §2.4 and §2.5.

2.4 Collapses in the 2d Benjamin-Ono equation

In this section we examine collapses of three-dimensional localised perturbations, lumps, within the framework of equation (2.55) with $\widetilde{\gamma} = 0$. The reduction of (2.55) to the 2d-BO equation is justified for larger Reynolds numbers, $Re \gg \varepsilon^{-2}$ and for the situations with sufficiently small curvature of vorticity at the boundary $U'''(0)$. Note that for the Blasius boundary layers $U'''(0)$ vanishes (e.g. Schlichting and Gersten [2016]).

The layout of the section is as follows. We begin in 2.4.1 with an overview of relevant earlier works. In 2.4.2 we discuss some basic properties of the 2d-BO equation and introduce a notion of 'neutral curves' and 'neutral surfaces' for collapses- the separatices delineating the manifolds of initial conditions which in the course of evolution collapse from those which decay. In 2.4.3, on examining the sufficient criterion for collapse for a few simple initial distributions, we attempt at making a rough general picture of collapses in the 2d-BO equation. Numerical simulation of collapse of laterally stretched initial pulse and its comparison with the self-similar solution is the subject of 2.4.4.

2.4.1 Overview of earlier studies

The one dimensional Benjamin-Ono equation (hereinafter BO) is one of the few celebrated universal weakly nonlinear long-wave evolution equation which emerge in various physical contexts, it was originally derived in the context of long internal waves in deep stratified fluid with a thin layer with stronger stratification Benjamin [1967], Davis and Acrivos [1967] and Ono [1975]. The BO equation is integrable, possesses both multi-soliton and multi-periodic wave solution and conserves an infinite set of integrals of motion and other properties typical of integrable systems (e.g., Case [1978],Case [1979], Ablowitz and Segur [1981],Matsuno [1984]). Obviously, by neglecting transverse variability of the perturbations we see that the BO equation describes nonlinear evolution of one dimensional perturbations in generic boundary layers, which has been known for long time (e.g. Zhuk and Ryzhov [1982],Ryzhov [1990], Kachanov et al. [1993]).

In our context the following point is the most relevant: usually, a localised initial pulse of 'right' polarity generates a number n of the BO solitons provided the integral over the area of the perturbation exceeds n times the area of a single soliton which does not depend on the soliton amplitude, although, counter intuitively, emergence of solitons out of continuous spectrum might be also possible for the BO equation (Pelinovsky and Sulem [1998]). The BO solitons are very robust in the

one-dimensional setting. A weakly two-dimensional generalisation of the Benjamin-Ono equation was derived in Ablowitz and Segur [1980] for waves in isotropic media, leading to a Kadomtsev-Petviashvili type extension with a similar pattern of longwave transverse instability in case of positive dispersion (Kadomtsev and Petviashvili [1970], Kadomtsev [2001]). The anisotropic essentially-two-dimensional Benjamin-Ono equation(2d-BO) derived by Shrira [1989] is the subject of this section – the evolution equation (2.55) with $\widetilde{\gamma} = 0$.

First we overview the results of the studies of 2d-BO equation which are most relevant for the current work. An obvious class of its exact solutions - all steady and unsteady oblique plane wave solutions of the one-dimensional Benjamin-Ono. However, such solutions proved to be unstable to long transverse perturbations Pelinovsky and Stepanyants [1994]. In particular, for instability of plane solitary waves the maximal growth rates are $\sim \varepsilon^2 a^2$ (here ε is used to denote the smallness of the magnitude of amplitude, therefore it has no links with small parameters used in this thesis), while the range of unstable transverse wavenumbers is between zero and the $O(\varepsilon a)$ cut-off wavenumber, where a is the $O(1)$ solitary wave amplitude. A more detailed analysis of this instability was carried out in Gaidashev and Zhdanov [2004]. Abramyan et al. [1992] found that the 2d-BO equation possesses axially symmetric stationary solitary wave solutions. In that work the attention was focussed on the 'zero mode' or 'ground mode' solitary waves, which decay monotonically as $x^2 + y^2 \to \infty$, although solutions with oscillatory decay also exist. These stationary solutions proved to be unstable. D'yachenko and Kuznetsov [1995] were the first to show that the 2d-BO equation describes collapses: localised perturbations collapse provided the nonlinearity is stronger than dispersion. It has also been shown that the equation also possesses self-similar solutions which describe emergence of axially symmetric singularity in finite time. An explicit description of the collapse evolving as a result of transverse instability of plane solitary waves was derived employing Whitham's adiabatic approach in Pelinovsky and Shrira [1995].

The sufficient condition of collapse for any chosen initial condition is that the Hamiltonian should be negative (D'yachenko and Kuznetsov [1995], Zakharov and Kuznetsov [2012]). However, the integral condition of negativity of the Hamiltonian is

implicit, *a priori* it is not obvious what initial perturbations collapse and what decay. For a chosen shape of the perturbation there is a threshold in amplitude above which the perturbation collapses. In this section we will find dependence of the threshold on the parameters of the perturbation and outline the range of parameters where the threshold does not exceed the limitations imposed by the weakly nonlinear nature of the equation.

2.4.2 Basic properties and 'neutral curves'

The 2d-BO equation (2.1) when $\widetilde{\gamma} = 0$ can be written in the Hamiltonian form as follows (D'yachenko and Kuznetsov [1995]),

$$A_\tau = \partial_x \left[\hat{K} A - \frac{1}{2} A^2 \right] = \partial_x \frac{\delta H}{\delta A}, \tag{2.57}$$

where the Hamiltonian H is made of two constituent integrals I_1 and I_2, which describe respectively dispersion and nonlinearity,

$$H = \frac{1}{2} I_1 - \frac{1}{6} I_2, \quad I_1 = \int A \hat{K}[A] \, \mathrm{d}x\mathrm{d}y, \qquad I_2 = \int A^3 \, \mathrm{d}x\mathrm{d}y, \quad (\mathbf{dr} \equiv \mathrm{d}x\mathrm{d}y). \tag{2.58}$$

Besides the Hamiltonian, the 2d-BO equation (2.1) conserves three other integrals of motion: the streamwise and spanwise components of the 'momentum' $\boldsymbol{P}$ and the mass flux M,

$$P_x = \frac{1}{2} \int\int A^2 \, \mathrm{d}x\mathrm{d}y, \quad P_y = \frac{1}{2} \int\int A \phi_y \, \mathrm{d}x\mathrm{d}y, \quad (\phi_x \equiv A), \quad M = \int\int A \, \mathrm{d}x\mathrm{d}y. \tag{2.59}$$

The way these integrals depend on parameters of the perturbations enables us to infer the existence of collapses for certain initial conditions and to outline the manifolds of collapsing initial conditions for a few particular *a priori* chosen classes of initial conditions.

2.4.3 Domains of collapses in parameter space

Here, we apply the sufficient condition of collapse, $H < 0$, to find separatrices delineating the domains of collapse ('supercritical region') and domains of decay('subcritical region') in the parameter space. Stretching the analogy with the linear hydrodynamic stability studies we will refer to the curves or surfaces where the Hamiltonian vanishes as nonlinear neutral curves/surfaces. By means of direct numerical simulations of the 2d-BO equation (which we describe below) we verify that this criterion indeed predicts the emergence of collapse or decay of initial perturbations. Applying this criterion to a few simple asymmetric distributions enables us to get a good *a priori* idea how the fate (i.e. collapse or decay) of an initial perturbation depends on its parameters. To outline these dependencies we first examine a few simple asymmetric distributions: the Gaussian and Lorentzian pulses,

$$A_G(x,y) = a e^{-\left(\frac{x^2}{2\sigma_x^2}+\frac{y^2}{2\sigma_y^2}\right)}, \qquad A_L(x,y) = \frac{a}{1+4(x^2/\sigma_x^2+y^2/\sigma_y^2)}. \tag{2.60}$$

These initial perturbations are fully characterized by just three parameters: amplitude a and characteristic half-widths σ_x and σ_y, which we will refer to as the 'widths' for brevity.

It is easy to see that in the Hamiltonian H given by (2.58), both its constituent integrals, the dispersion one, I_1, and the nonlinear one, I_2, can be expressed in terms of the perturbation initial amplitude a and perturbation widths σ_x and σ_y. On re-scaling the variables,

$$\tilde{x} = \frac{x}{\sigma_x}, \qquad \tilde{y} = \frac{y}{\sigma_y}, \qquad A(\tilde{x},\tilde{y}) = a\,\mathcal{A}, \quad \left(\mathcal{A}_G = e^{-(\tilde{x}^2+\tilde{y}^2)/2}, \quad \mathcal{A}_L = \frac{1}{1+4(\tilde{x}^2+\tilde{y}^2)}\right)$$

we re-write our integrals as,

$$I_1 = \alpha\, a^2 \sigma_x \tilde{I}_1, \qquad \tilde{I}_1 = \int\int \mathcal{A}\,\hat{K}\,[\mathcal{A}]\,\mathrm{d}\tilde{x}\mathrm{d}\tilde{y}, \qquad I_2 = \alpha\, a^3 \sigma_x^2 \tilde{I}_2, \qquad \tilde{I}_2 = \int\int \mathcal{A}^3 \mathrm{d}\tilde{x}\mathrm{d}\tilde{y},$$

where $\tilde{I}_1$ depends implicitly on the ratio α through the kernel of the integral operator,

$\hat{K}$. In the Fourier space $\hat{K} = \left(\tilde{k}_x^2 + \frac{1}{\alpha^2}\tilde{k}_y^2\right)^{1/2}$, where, $\alpha = \sigma_y/\sigma_x$. The 'nonlinear integral' $\tilde{I}_2$ is a constant which is evaluated analytically or numerically; for the Gaussian initial conditions $\tilde{I}_2 = \frac{2}{3}\pi$. The 'dispersion integral' $\tilde{I}_1$ cannot be evaluated analytically and is dealt with numerically. It is easy to see that I_1 depends on σ_x linearly, while I_2 has quadratic dependence on σ_x. The parameter α is the ratio of spanwise half-width σ_y to that of streamwise half-width σ_x. From now on, we will drop the subscript and denote σ_x by σ and proceed to finding nonlinear neutral curves/surfaces in terms of amplitude a, width σ and aspect ratio α.

Recall that the Hamiltonian vanishes when $3\,I_1 - I_2 = 0$, which thus yields nonlinear 'neutral surfaces' separating the domains of collapse and decay in the $a - \sigma - \alpha$ space,

$$a^2\sigma(3\,\tilde{I}_1 - a\sigma\tilde{I}_2) = 0. \tag{2.61}$$

It proved to be convenient to present the results of such an analysis as cross-sections with fixed values of α. Then the relationship between the amplitude threshold a_{thr} and perturbation width σ prescribed by equation (2.61) for constant values of α is hyperbola. This amplitude threshold depends implicitly on the ratio α through integral $\tilde{I}_1$. A set of cross-sections for different values of asymmetry parameter α for the Gaussian and the Lorentzian initial conditions is shown in figure 2.4. The figure illustrates several salient features of the separatrices in the $a - \sigma$ plane. For every value of the asymmetry parameter α the cross-sections are hyperbola. The initial pulses with a, σ above the curve collapse. For larger σ the threshold decreases for any asymmetry. Since the main mechanism of the collapse is self-focussing asymmetry quite noticeably affects the threshold: as expected, the threshold decreases for the pulses stretched in the spanwise direction ($\alpha > 1$), it increases for the or the pulses stretched in the streamwise direction ($\alpha < 1$). For the evolution to be weakly nonlinear and to allow for a substantial growth, the initial amplitude should be sufficiently small. Quite arbitrarily we have chosen this threshold to be 0.1, pulses of amplitudes below this value could grow up to, say, 0.3 remaining weakly nonlinear. The neutral curves for the Gaussian and Lorentzian initial pulses are qualitatively very similar. However, quantitatively, the Gaussian pulses for moderate values of σ

have a noticeably smaller threshold. The comparison of the neutral curves for the Gaussian and Lorentzian initial pulses suggests that their behaviour is robust and at the qualitative level we can generalise and to expect to see the same salient features: a decrease of the amplitude threshold for collapse with the increase of both spatial scales, crucially, $a_{thr} \to 0$ as σ or α tend to infinity. Recall that for the plane wave soliton solutions of the 2d-BO equation of any amplitude $H = 0$ and, hence these solutions are at the boundary of the domain of collapsing initial conditions even for vanishingly small amplitudes. The transverse instabilities of plane solitons are known to be possible for any amplitude of the solitary waves (Pelinovsky and Stepanyants [1994]), Gaidashev and Zhdanov [2004]), although the instability growth rate is proportional to the soliton amplitude and, hence, tends to zero as the amplitude tends to zero. This instability is known to end up in collapse (Pelinovsky and Shrira [1995]).

To complement the overall picture of the manifolds of initial conditions resulting in collapse, we note that for the axially symmetric solitary wave solutions found in (Abramyan et al. [1992]) the Hamiltonian is always negative. The fact that in contrast to the Gaussian and Lorentzian pulses for these solitary waves there is no amplitude threshold does not contradict our overall qualitative picture that for collapse to happen for a small amplitude perturbation the spatial scale of the perturbation should be very large, since the width of the axially symmetric solitary waves tends to infinity as their amplitude tends to zero.

2.4.4 Collapse and self-similarity: example of simulation

2.4.4.1 Self-similar solution

Consider the spatial and temporal dependence of a collapsing perturbation in a certain vicinity of the blow-up singularity assumed to be occurring at $\boldsymbol{r} = \boldsymbol{r}_0\,\{x_0, y_0\}$. Introduce time to singularity $\check{\tau} = \tau_0 - \tau$ and distance to singularity $\check{x} = x - x_0$, $\check{y} = y - y_0$. There is a self-similar solution in the form

$$A(\boldsymbol{r}, \check{\tau}) = \check{\tau}^{-\frac{1}{2}} g(\check{\boldsymbol{\xi}}), \quad \check{\boldsymbol{\xi}} = \frac{\check{\boldsymbol{r}}}{\check{\tau}^{\frac{1}{2}}}. \tag{2.62}$$

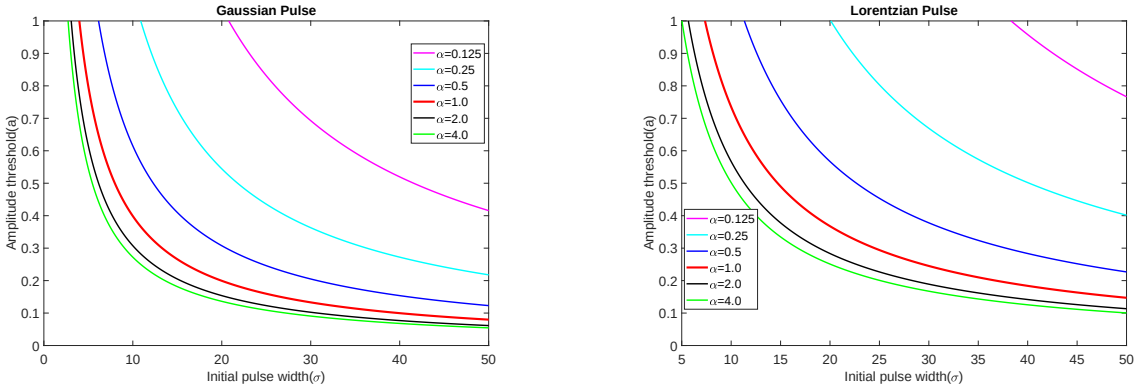

(a) (b)

FIGURE 2.4: Cross-sections of 'neutral surfaces' separating the domains of collapse and decay for different degree values of ($\alpha = 0.125,\ 0.25,\ 0.5,\ 1.0,\ 2.0,\ 4.0$) for: (a) the Gaussian and (b) the Lorentzian initial conditions. For any chosen α the initial pulses with a, σ in the domain above the corresponding curve collapse, those in in the domain below - decay. The threshold decreases for the pulses stretched in the spanwise direction ($\alpha > 1$), it increases for the pulses stretched in the streamwise direction ($\alpha < 1$).

where $g(\check{\boldsymbol{\xi}})$ is specified by the equation,

$$\frac{\check{\boldsymbol{\xi}} g}{2} + \frac{g^2}{2} + \hat{K}[\,g\,] = 0. \tag{2.63}$$

This is (up to a typo in the time dependence exponent in (D'yachenko and Kuznetsov [1995]) a known self-similar solution of the 2d-BO equation which predicts the $1/\sqrt{\tau_0 - \tau}$ singularity in time and the shrinking spatial distribution given by $g(\check{\boldsymbol{\xi}})$, its width shrinks as $\sqrt{\tau_0 - \tau}$. Our equation for g specifying the shape of the distribution has a simpler form than its counterpart in (D'yachenko and Kuznetsov [1995]), since we integrated our equation once.

2.4.4.2 Numerical simulation

To simulate numerically the 2d-BO equation for localized initial perturbations we use the pseudo-spectral method (e.g. Orszag [1969], Kopriva [2009]). The pseudo-spectral method with periodic boundary conditions uses efficient fast Fourier transform (FFT) routines in handling dependencies on x and y, while for the time evolution the classic fourth order Runge-Kutta method is employed.

In our context it was found to be optimal to use a rectangular box of length 512π and width 128π. This choice provides sufficient domain for the spatial decay of the localized perturbations we were simulating and also to allow the perturbation sufficient time to move in the streamwise direction during the evolution. To resolve the rapidly growing and increasingly localized amplitude distribution we used 4096×1024 grid points. It is convenient to present our evolution equation in the flux-conservation form,

$$A_\tau + F_x = 0$$

where the flux $F = -\hat{K}[A] + \frac{1}{2}A^2$. The integral operator $\hat{K}[A]$ was dealt with in the Fourier space, while nonlinear terms were considered in the physical space on collocation points with the 'two-third de-aliasing rule' (e.g.Orszag [1969]). The accuracy of the simulations was controlled by ensuring that the integrals of motion (2.59) remain constant with the error not exceeding $O(10^{-4})$.

Here, let us briefly demonstrate how we compute the amplitude $A(x, y, \tau)$ using two-dimensional de-aliased pseudo-spectral method. We start with a more general nonlinear evolution equation for three-dimensional perturbation accounting for both stratification due to $\widetilde{\beta}_2$ and dissipation, $\widetilde{\gamma}$, which is expressed as,

$$\frac{\partial A}{\partial \tau} = F(A)_x + \widetilde{\beta}_2 \hat{G}_2(A_x) - \widetilde{\gamma} A, \tag{2.64}$$

where,

$$F(A) = \hat{K}[A] - \frac{1}{2}A^2, \qquad \widetilde{\beta}_2 = \frac{N_0^2}{2\varepsilon^2 (U'(0))^2}, \qquad \widetilde{\gamma} = \frac{1}{\varepsilon^2 Re}\frac{U'''(0)}{(U'(0))^2},$$

while $\hat{K}$ and $\hat{G}$ are integral operators of dispersion. In the Fourier space,

$$\hat{K} = |\boldsymbol{k}| = k = (k_x^2 + k_y^2)^{1/2}$$

and $\hat{G}_2 = \frac{k_y^2}{k_x^2}$. If $\hat{A}(\boldsymbol{k}) = fft(A(\boldsymbol{x}))$ is the fast Fourier transform of A with $\boldsymbol{k} = (k_x, k_y)$ the evolution equation in spectral space is

$$\frac{\partial \hat{A}}{\partial \tau} = F_1(\hat{A}) + \widetilde{\beta}_2 i k_x \hat{G}_2(\hat{A}), \tag{2.65}$$

where $F_1(\hat{A}) = ik_x\Big((k\hat{A} - \frac{1}{2}fft\Big([ifft(\hat{A})]^2\Big)\Big) - \widetilde{\gamma}\hat{A}$. The fourth order time step classical Runge-Kutta ($RK4$) method which uses four approximations to the slope is employed to handle $F_1(\hat{A})$, while the Crank-Nicolson (C-N) method is applied in the expression for the dispersion term due to stratification. Thus,

$$\frac{\hat{A}^{n+1} - \hat{A}^n}{\Delta\tau} = \underbrace{\frac{1}{6}\Big(K_1 + 2K_2 + 2K_3 + K_4\Big)}_{RK4} + \underbrace{\frac{1}{2}i\widetilde{\beta}_2\frac{k^2}{k_x}\Big(\hat{A}^n + \hat{A}^{n+1}\Big)}_{C-N}, \tag{2.66}$$

where,

$$K_1 = F_1(\hat{A}^n), \qquad K_2 = F_1\left(\hat{A}^n + \frac{\Delta\tau}{2}K_1\right), \qquad K_3 = F_1\left(\hat{A}^n + \frac{\Delta\tau}{2}K_2\right),$$

$$K_4 = F_1(\hat{A}^n + \Delta\tau K_3).$$

Here the superscript is the time step index. It is easy to see that the RHS of equation (2.65) splits into two components: the $C-N$ term which is very straightforward to compute and the first term due to the classical fourth order Runge-Kutta $RK4$ method. With de-aliasing, a resolution of $N_x \times N_y$ corresponds in practice to the representation

$$A(x, y, \tau) = \sum_{k_x=-N_x/3}^{N_x/3-1}\sum_{k_y=-N_y/3}^{N_y/3-1}\hat{A}_{k_xk_y}(\tau)e^{i(\bar{\alpha}k_xx+k_yy)},$$

where, $\bar{\alpha} = L_y/L_x$, $\boldsymbol{k} = (\bar{\alpha}k_x, k_y)$, $\hat{A}_{00} = 0$ and a mask is employed so that $\hat{A}_{k_xk_y} = 0$ for wave-numbers outside a specified domain $\sum$. The calculations obtained here have $\bar{\alpha} = 1/4$ and $N_x = N_y$ so the specified domain for wave-numbers is a circle of radius $N_x/3$, i.e $\sum = \{(k_x, k_y) : k_x^2 + k_y^2 \leq (N_x/3)^2\}$ is used. The system is solved in a double periodic domain of $[0, L_x] \times [0, L_y]$, where L_x is the streamwise length while L_y is the transverse length of the computational box.

After some algebra we re-arrange equation (2.66) to obtain,

$$\left(1 - \frac{1}{2}i\Delta\tau\widetilde{\beta}_2\frac{k^2}{k_x}\right)\hat{A}^{n+1} = \left(1 + \frac{1}{2}i\Delta\tau\widetilde{\beta}_2\frac{k^2}{k_x}\right)\hat{A}^n + \frac{1}{6}\Delta\tau\Big(K_1 + 2K_2 + 2K_3 + K_4\Big),$$

To this end, it is easy to see that the expression for the amplitude in Fourier space at any time interval n valid on the collocation grid points is

$$\hat{A}^{n+1} = \frac{(1+\eta)\hat{A}^n + \frac{1}{6}\Delta\tau\Big(K_1 + 2K_2 + 2K_3 + K_4\Big)}{(1-\eta)}. \tag{2.67}$$

where

$$\widetilde{\beta}_2 = \frac{N_0^2}{2\varepsilon^2(U'(0))^2}, \qquad \eta = \frac{1}{2}i\Delta\tau\widetilde{\beta}_2\frac{k^2}{k_x},, \qquad \widetilde{\gamma} = \frac{1}{\varepsilon^2 Re}\frac{U'''(0)}{(U'(0))^2},$$

For our simulations we adopted a time step ($\Delta\tau$) that is regulated by the absolute value of the maximum amplitude at each instance. This is because the amplitude of the wave might grow very rapidly with time, therefore, for large values of the amplitudes the time steps become much smaller. More specifically, our time steps are given by,

$$\Delta\tau = \frac{Cdx}{||u||_\infty},$$

where C is the Courant-Fredricks-Lewy condition (CFL) for numerical stability, which can be varied depending on the context. For example. for the most of the simulations it has been chosen to be 1.0×10^{-3}, which is less than one for the purposes of numerical stability; $||u||_\infty$ is the maximum absolute value of the amplitude at each time step. The grid size $dx = dy = L_x/N_x = L_y/N_y \approx 0.19$, therefore our time steps is approximately of order 10^{-5} or less depending on the maximum of the amplitude at each time interval. It is easy to see that if the amplitude becomes order 1 the time step gets smaller hence the longer time for the simulations. For the homogeneous boundary layer which we examine in this current Chapter, we set the term due to stratification to be zero, i.e. $\widetilde{\beta}_2 = 0$.

2.4.4.3 Evolution scenarios

On obtaining in 2.4.3 the boundaries separating the domains of the initial conditions resulting in collapse or decay, we verified the findings by numerical simulations of the evolution of symmetric and asymmetric Gaussian pulse initial conditions (2.60). By choosing the initial perturbations slightly above and slightly below the

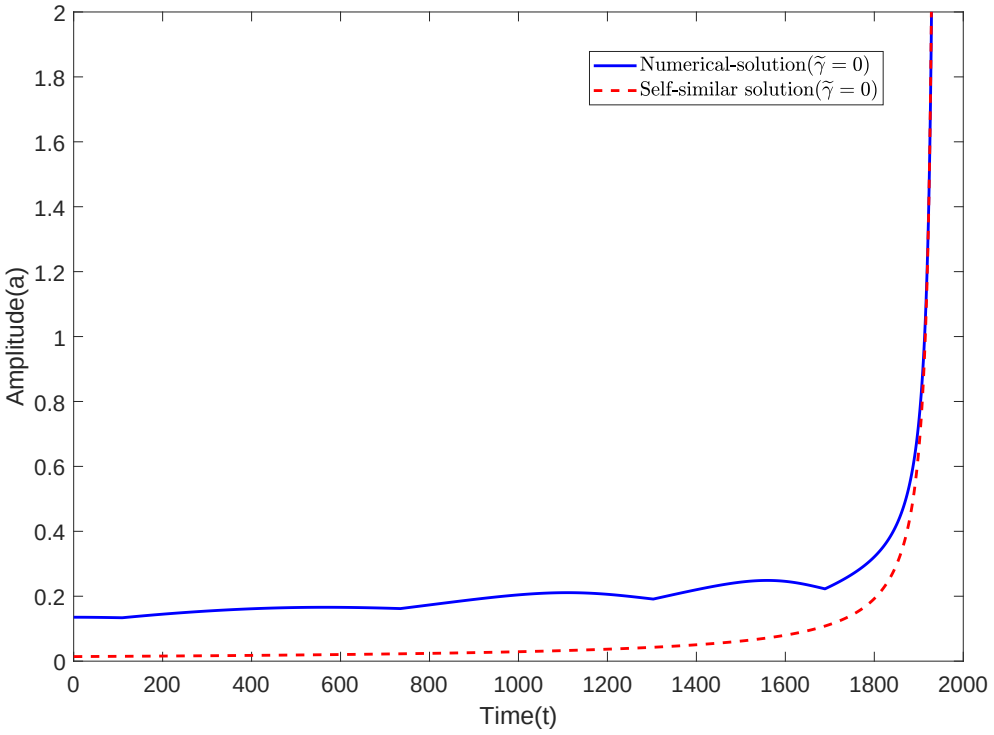

FIGURE 2.5: Example of time evolution of the amplitude of a collapsing laterally stretched pulse with $\alpha = 2$. Blue solid line: simulated evolution of the amplitude of a collapsing pulse with the asymmetric Gaussian initial condition ($a = 0.1353, \sigma_x = 25, \sigma_y = 50, \widetilde{\gamma} = 0$). Red dashed line: the self-similar solution (3.17)

hyperbola, we confirmed that, indeed, the initial perturbations with the amplitudes exceeding the threshold collapse, that is, such perturbations evolve into a coherent pattern which tends to a localized self-similar solution with a point singularity. The initial conditions with amplitude below the threshold decay, although, for the initial conditions close to the threshold surface, a temporary transient growth, sometimes substantial, can also occur. We do not illustrate it here.

We illustrate a typical collapse scenario by providing snapshots 2.6 based upon our simulations of the evolution of a collapsing pulse for a localized asymmetric initial conditions. The initial condition is a laterally stretched Gaussian pulse $\alpha = 2$ corresponding to $\sigma_x = 25$, $\sigma_y = 50$, $a = 0.1353$. Here, we highlight two features. Although the initial condition is a smooth well confined lump, the emerging pattern shown in figure [2.8] is not: at the pedestal, the pulse radiates at two distinguished directions; the resulting pattern resembles 'hair-pin' or 'lambda' vortices routinely

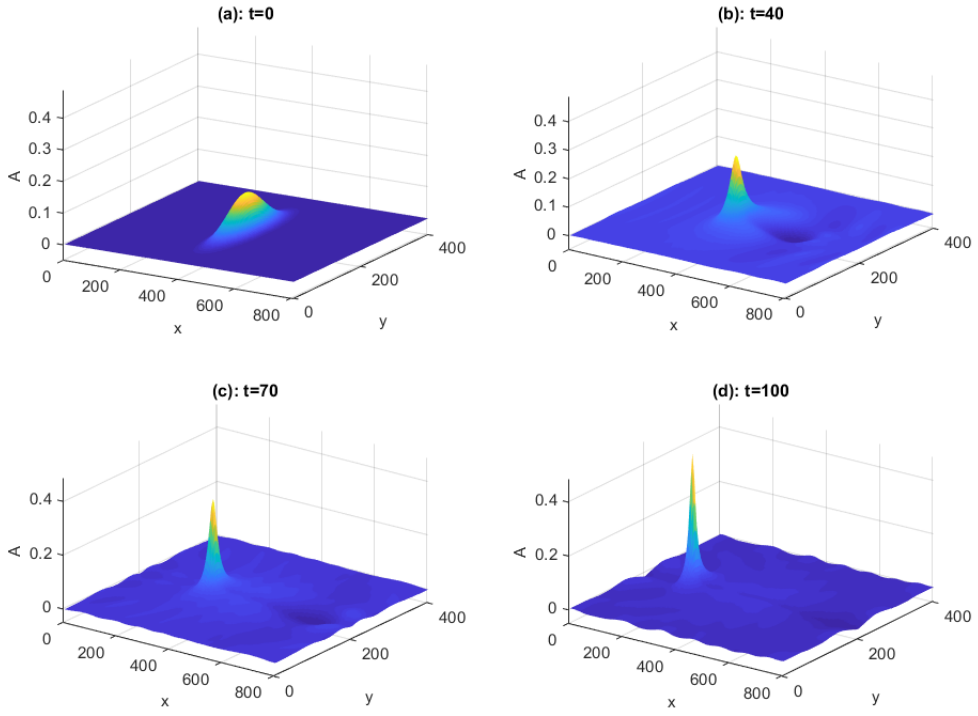

FIGURE 2.6: Snapshots showing the evolution of the amplitude $A(x, y, t)$ of a collapsing laterally stretched ($\alpha = 2$) pulse taken at the start of evolution($t = 0$) and finally at t=100 of the maximal amplitude at four-different moments. The simulation is for supercritical asymmetric Gaussian initial condition ($a = 0.1353, \sigma_x = 25, \sigma_y = 50, \widetilde{\gamma} = 0$).

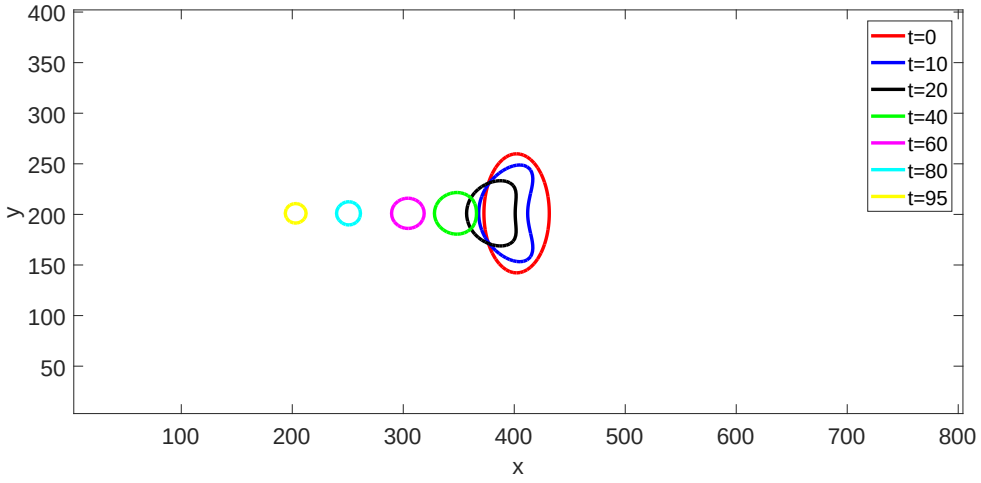

FIGURE 2.7: Single contours showing the evolution of the $A = 0.95A_{maximal}$ cross-sections of a collapsing laterally stretched pulse ($\alpha = 2$) taken at seven different moments of evolution. The initial condition is the supercritical laterally stretched Gaussian pulse with the parameters: $a = 0.1353, \sigma_x = 25, \sigma_y = 50, \widetilde{\gamma} = 0$.

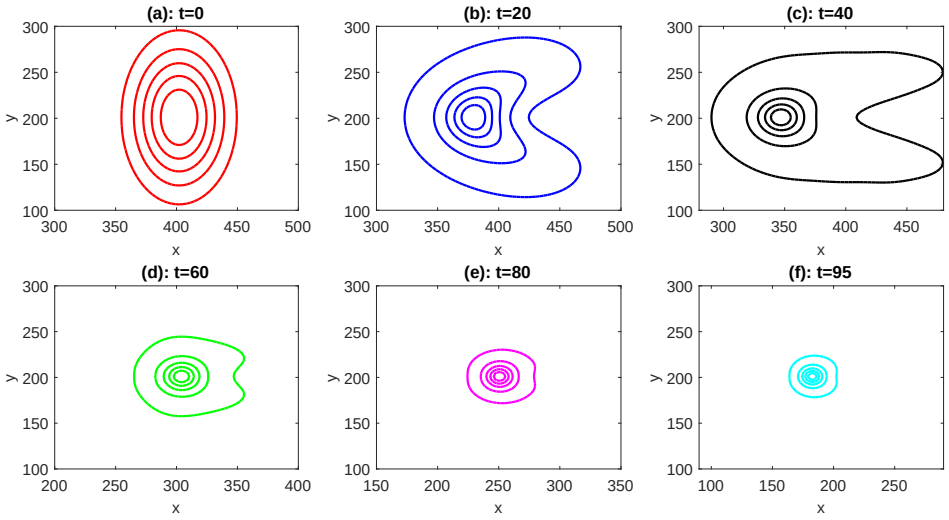

FIGURE 2.8: Evolution of the amplitude cross-sections of a collapsing laterally stretched pulse ($\alpha = 2$) taken at six-different moments showing hair-pin or lambda vortices. The initial conditions are the same as in figure 2.7.

observed in the wind tunnels (e.g. Kachanov [1994]). The top of the pulse evolves in an axially symmetric self-similar manner tending to a point singularity at the end.

The tendency of a collapsing pulse to become axially symmetric near its top is further illustrated by figure (2.7) and (2.8) showing vanishing of initial asymmetry at the level of 0.95 of the maximum for the same initially laterally stretched pulse. Figure (2.7) also demonstrates the tendency of an initially well localised pulse which radiates in two directions then accelerates in the streamwise direction before its eventual collapse. Figure (2.5) shows the simulated time dependence of a collapsing pulse amplitude for the same example along with the self-similar solution (2.62). Note that for a considerable part of the pulse evolution the amplitude grows slowly, the sharp growth occurs just immediately prior to the singularity. The figure also gives an idea how well the self-similar solution (2.62) captures the evolution.

2.5 Collapses in the evolution equation with the Rayleigh friction term ($\widetilde{\gamma} \neq 0$)

The aim of this section is a preliminary analysis of equation (2.55),

$$A_\tau + AA_x - \hat{K}[A_x] + \widetilde{\gamma}\, A = 0, \tag{2.68}$$

derived in 2.3. The only difference of this equation from the 2d-BO equation examined in the previous section is in the the Rayleigh friction term $\widetilde{\gamma}\, A$. Recall that the expression for the coefficient $\widetilde{\gamma}$

$$\widetilde{\gamma} = \frac{1}{\varepsilon^2 Re} \frac{U'''(0)}{(U'(0))^2},$$

that is magnitude is determined by the product of two factors: the first being the ratio of curvature of vorticity at the boundary and the Reynolds number, the second is the inverse of the nonlinearity parameter squared. For generic boundary layers we consider in this section $\widetilde{\gamma} \neq 0$. The evolution equation (2.41) has not been studied and there are no readily available analytical techniques. A nearly obvious but nevertheless crucial observation is that the same self-similar ansatz

$$A(\boldsymbol{r}, \check{\tau}) = \check{\tau}^{-\frac{1}{2}} g(\check{\boldsymbol{\xi}}), \quad \check{\boldsymbol{\xi}} = \frac{\check{\boldsymbol{r}}}{\check{\tau}^{\frac{1}{2}}}. \tag{2.69}$$

where $g(\check{\boldsymbol{\xi}})$ being specified by the equation,

$$\frac{\check{\boldsymbol{\xi}} g}{2} + \frac{g^2}{2} + \hat{K}[\, g\,] = 0.$$

provides a solution to equation (2.41) in a certain vicinity of the singularity. The relative contribution of the Rayleigh friction term decays as $\check{\tau}^1$. Recall that $\check{\tau} = 0$ at the moment of collapse.

Thus, in principle, the evolution (2.41) describes collapses. Figure 2.10 shows the time dependence of the amplitude of a collapsing lump with nonzero Rayleigh friction superimposed on the plot of the self-similar solution. As a reference, the figure also

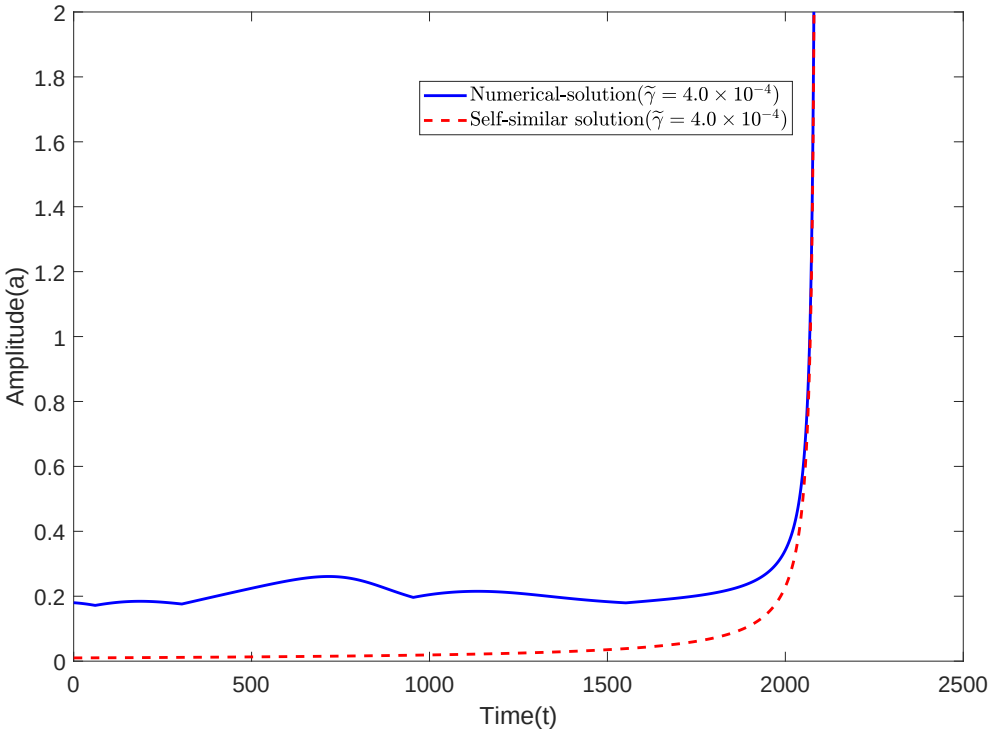

FIGURE 2.9: Example of time evolution of the amplitude of a collapsing laterally stretched pulse with $\alpha = 2$. Solid blue line: simulated evolution of the amplitude of a collapsing pulse with the asymmetric Gaussian initial condition ($a = 0.1800, \sigma_x = 25, \sigma_y = 50, \widetilde{\gamma} = 4.0 \times 10^{-4}$). Red solid line: the self-similar solution (3.17)

provides the time dependence of the amplitude of a collapsing lump with the same initial conditions for $\widetilde{\gamma} = 0$ and half the value of $\widetilde{\gamma}$ used for the solid blue curve we compared with the self-similar solution. In a quite substantial neigbourhood of the singularity the amplitude evolution is extremely well captured by the self-similar solution. Thus, we've established the character of the singularity by showing that is not affected by nonzero $\widetilde{\gamma}$.

The key outstanding question is what initial conditions result in collapse for each value of $\widetilde{\gamma}$. In contrast to the 2d-BO equation, for the evolution equation (2.41) there are no readily available mathematical tools to predict *a priori* the occurrence of collapse for a given initial condition. The aim of this section is by means of numerical simulations of equation (2.41) to get a rough idea of the effect the Rayleigh friction term on the domain of collapses in the space of parameters of initial perturbations.

The account of viscous effects in the evolution equation makes it non-conservative

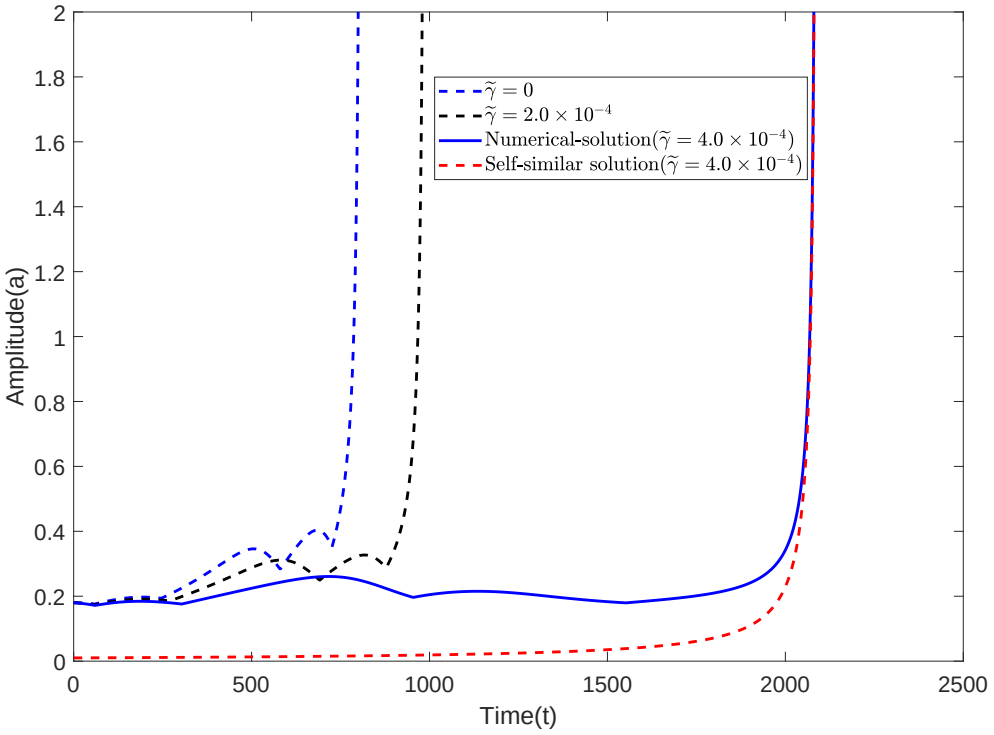

FIGURE 2.10: Example of time evolution of the amplitude of a collapsing laterally stretched pulse with $\alpha = 2$. Solid blue line: simulated evolution of the amplitude of a collapsing pulse with the asymmetric Gaussian initial condition ($a = 0.1800, \sigma_x = 25, \sigma_y = 50, \widetilde{\gamma} = 0$(blue dashed line), $\widetilde{\gamma} = 2.0 \times 10^{-4}$(black dotted line), $\widetilde{\gamma} = 4.0 \times 10^{-4}$. Red dashed line: the self-similar solution (3.17)

and destroys the integrals of motion (2.59), (2.58). However, it is easy to see that the mass flux $M = \int A dxdy$ and $x-$component of momentum $P_x = \int A^2 dxdy$ specified by (2.59) decay exponentially,

$$M(\tau) = M^0 e^{-\widetilde{\gamma}\tau}, \quad P_x(\tau) = P_x^0 e^{-2\widetilde{\gamma}\tau}. \tag{2.70}$$

For simulations we employ the same code based on the pseudo-spectral method as in 2.4. In order to control the accuracy of the simulations of equation (2.68) we ensure that at any moment in time the numerical values of the integrals M and P_x agree with (2.70) with an error not exceeding 10^{-4}.

For a range of $\widetilde{\gamma}$ we carried out a number of simulations for initially axisymmetric Gaussian perturbations of different amplitudes and widths. The results of the simulations are presented in figure 2.11, where dependence of the amplitude threshold a_{thr}

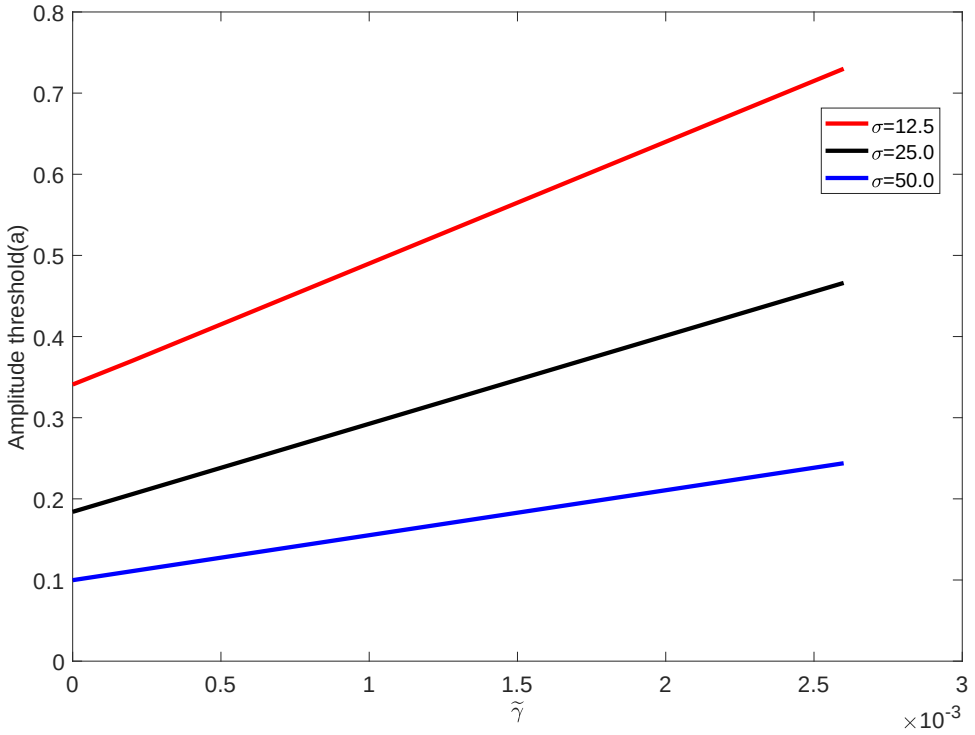

FIGURE 2.11: Example of stability curves for the amplitude threshold a_{thr} against small values of dissipation $\widetilde{\gamma}$ ranging from $O(10^{-4}) - O(10^{-3})$ for axisymmetric Gaussian initial condition of $\sigma = 12.5, \sigma = 25.0, \sigma = 50.0$.

on $\widetilde{\gamma}$ is plotted for several values of width σ. The most striking result is the observation that for the range of widths with $\sigma = 10^1 - 10^2$ only a surprisingly small values of $\widetilde{\gamma}$ ($\widetilde{\gamma} \sim 10^{-3}$) prove to be of interest in our context. In this range of $\widetilde{\gamma}$ the Rayleigh friction term causes an order one increase of the amplitude threshold a_{thr}, while for the values of $\widetilde{\gamma}$ as small as $\sim 10^{-2}$ the amplitude threshold goes out of the range of weak nonlinearity. In this sense, even a weak dissipation can prevent collapses by raising the threshold beyond the range of applicability of our weakly nonlinear model. The amplitude threshold for collapse to occur decreases with increase of σ. However, in contrast to the 2d-BO equation it does not tend to zero as $\sigma \to \infty$. The physical reason of the striking effect of small $\widetilde{\gamma}$ and "anomalous" behaviour of lumps at small amplitudes is the same: as figure 2.9 and its analogue for $\widetilde{\gamma} = 0$ (2.5) show, a collapsing lump goes through a substantial period of very weak growth during which even a weak decay can arrest the growth and thus prevent the collapse from happening. In the 2d-BO equation the overall picture of evolution was nearly "black-and-white":

the initial pulses either grew and collapsed or decayed, the manifold of "decaying" initial conditions exhibiting a transient growth was insignificant. In contrast to the 2d-BO case, the account of the Rayleigh friction significantly widens the manifold of the initial conditions exhibiting a transient growth and eventually decaying.

An insight into the physics of the observed phenomenology might be obtained by recalling that the physical mechanism of the collapses is the usual self-focussing and that the maximal growth rate for the transverse instability of plane solitary wave within the 2d-BO equation is $\sim \varepsilon^2 a^2$ (Pelinovsky and Stepanyants [1994]). For this instability to occur within the framework of (2.41) the necessary condition would be for the growth rate to exceed the decay rate $\widetilde{\gamma}$. This reasoning suggests existence of a threshold in amplitude below which even the instability, which is the necessary first stage of collapse, is not possible. For the amplitudes exceeding this threshold the transient growth scenarios might occur. The thresholds curves shown in figure (2.11) are above this transient growth domain threshold; they delineate the manifold of collapsing initial conditions.

2.6 Conclusions and discussion

Here we briefly summarise the results of the work of the current chapter and discuss the new questions it generates. The chapter presents an asymptotic model describing blow up of linearly decaying 3d long-wave perturbations in a generic semi-infinite boundary-layer flow. The model is a two-dimensional generalisation of the Benjamin-Ono equation with the Rayleigh-type dissipation. The Rayleigh-type dissipation is found to be proportional to the product of of the inverse nonlinearity parameter and the ratio of the curvature of the basic flow vorticity at the boundary and the Reynolds number. The model is derived in a unified way for both the 'no-slip' and 'constant-stress' boundary conditions in the distinguished limit with nonlinearity, dispersion and dissipation being in balance. We stress that in contrast to other studies of blow up in boundary layers the model is self-contained: the evolution equation describes dynamics of a single longwave mode which is weakly

decaying in linear setting. Under the adopted scaling the dynamics in the critical layer is dominated by viscosity, crucially, to leading order the critical layer does not affect the processes in the bulk of the boundary layer, at least for laterally stretched perturbations. The linear viscous character of the critical layer is ensured by the inequality $\varepsilon \ll \mathrm{R}e^{-\frac{1}{6}}$. The derivation largely follows earlier derivations (Shrira [1989], Voronovich et al. [1998]), with three important differences. First, the derivation has been extended to the boundary layers with the no-slip boundary conditions. Second, the range of possible Reynolds numbers was considerably extended towards lower values, down to $\mathrm{Re} \sim \varepsilon^{-2}$. Third, the restriction which excluded the flow profiles with inflection points employed in the earlier derivations was lifted. The rationale behind this restriction was to exclude the possibility of linear inflectional instability which in principle might interfere with the nonlinear dynamics we are studying. However, a closer look at the now available results on linear instabilities in boundary layers Healey [2017] enabled us to lift the restrictions. Although the profiles with inflection points points can be indeed unstable, these inflectional instabilities are long-wave instabilities with the maximal growth rates $O(\varepsilon^3)$ and, thus, the processes with the $O(\varepsilon^{-2})$ timescales resulting in collapses we focus upon develop much faster than the possible instabilities. This justifies our *a priori* disregard of the instabilities in the distinguished limit when the dispersion is balanced by nonlinearity. If the initial perturbations are much weaker they might go first through a stage of exponential growth until the balance is reached.

Along with the derivation of the model the work in this chapter also presents a preliminary analysis of nonlinear dynamics boundary layer perturbations within its framework. We show that an initial 'lump' of a given shape collapses, i.e. blows up forming a point singularity in finite time, provided its initial amplitude exceeds a certain threshold. The threshold is specific for each particular initial shape, vorticity curvature at the boundary and the Reynolds number. The initial perturbations exceeding the threshold collapse in a self-similar manner, the found axially symmetric self-similar solution captures very well the behaviour of the perturbation in a vicinity of singularity. The perturbations with the amplitudes below the threshold - decay, although a substantial transient growth is possible for the initial perturbations close

to the threshold. Upon finding the boundaries of the manifolds of collapsing initial conditions for a few classes of simple initial conditions we were able to extrapolate the results to get an idea of the overall picture. For the situations with negligible dissipation we benefit from having analytical sufficient condition in integral form which we analyse. There are just two main parameters of the initial perturbations: the amplitude and maximal width. On the amplitude-width plane the domain of collapsing initial conditions is confined by a hyperbola from below; the threshold amplitude decreases as inverse width of the perturbation and for very wide perturbations tends to zero. In the context of collapses of special interest is a class of axially-symmetric initial perturbations which are stationary solutions stationary solutions of the 2d-BO equation (Abramyan et al. [1992]), sometimes referred to as the 'ground solitons'; in the absence of dissipation such initial conditions always collapse, there is no threshold.

Unexpectedly, the conditions of collapse proved to be very sensitive to dissipation. The account of even small dissipation might raise the amplitude threshold quite substantially, often beyond the range of weakly nonlinear theory. This implies that, as long as the main focus is on collapses, the attention should be confined to the situations with small Rayleigh friction, since otherwise collapses occur only outside the domain of weakly nonlinear regimes and validity of the evolution equation. The smallness of the relevant values of viscosity hints at a possibility of an analytic perturbation approach, however, exploring such a possibility requires a dedicated work. The unexpectedly strong sensitivity of the evolution to small Rayleigh friction can be explained by the combination of a large duration of evolution and a cumulative character of the dissipation action. In the simulations with small Rayleigh friction we found that a broader range of initial conditions exhibits a transient growth, which might also be a route to transition, however we didn't pursue this line further, since a dedicated study is required. Note, that for the flows with zero curvature at the boundary the dissipation drops to the next order, such flows require a different scaling and the resulting evolution equation will have a qualitatively different dissipation term. This particular class of situations (which includes Blasius boundary layer) requires a special consideration and will be examined elsewhere.

Our main conclusion is that the collapses we considered might be a plausible mechanism of three-dimensional patterns observed in boundary-layer transition and play an important yet to be established role in by-pass laminar-turbulent transition.

The work gives rise to a lot of questions to which we currently do not have answers. The main outstanding question concerned with the role of the modelled collapses in the bigger picture of transition splits into a number of more specific ones. In particular, our evolution equation is a weakly nonlinear asymptotic model, currently we do not know the eventual outcome of the found collapses in the full Navier-Stokes equations. Most likely, the collapses cause localised transition to turbulence. However, we cannot exclude the possibility that under certain circumstances collapses might lead to formation of long-lived coherent strongly nonlinear patterns. A dedicated direct numerical simulation study is in progress to clarify this issue.

All collapsing perturbations tend to axially symmetric self-similar distributions, which resemble the coherent patterns observed in wind tunnels. At the foot of these patterns they, as can be seen in the snapshots of the numerical simulation (2.6), also exhibit features typical of lambda vortices routinely observed in wind tunnels at certain stage of laminar turbulent transition (e.g. Kachanov [1994]). Is this resemblance just a coincidence or the model does capture elements of essential physics of the phenomenon? Although the model does predict emergence of 3d patterns resembling those observed in the tunnel by Kachanov [1994] (see figure 2.1), at the moment we could claim only a rough qualitative agreement. The validity of the model has been proved only for laterally stretched perturbations.

Our study leaves aside the question on how the initial perturbation was produced which we took as given. There are many possible scenarios, in particular, there is a room for usual linear long-wave instabilities to play, for example, as a result of inflectional long-wave instability plane wave perturbations propagating streamwise might emerge and grow until the nonlinearity becomes strong enough to balance dispersion, then, at first the plane Benjamin-Ono solitons are likely to emerge, the latter are transversally unstable; under the right conditions this instability leads to their collapse (Pelinovsky and Shrira [1995]). We understand all the phases of

this scenario, but here we just mention it, its elaboration goes beyond the scope of this work. Initial perturbations leading to collapses can be also generated by perturbations of the boundary. We assumed the boundary to be flat, but the model could be easily extended to take into account long-wave perturbations (steady or unsteady) of the boundary. It would be interesting to examine what perturbations of the boundary trigger collapses, but this should be a subject of a dedicated work.

Let us very briefly discuss the limitations of the model and how the model can be extended. The main limitation, apart from the already mentioned weak nonlinearity constraint, is the total neglect of nonparallel effects. It is relatively straightforward to incorporate weakly non-parallel effects into the employed asymptotic scheme. This has been done in (Shrira et al. [2005]) for free surface boundary layer in water with the main effect being an additional Rayleigh friction term, this term has been included into an effective dissipation. The approach can be extended for the no-slip boundary conditions as well, where we expect qualitatively similar effect; but at present this remains to be done.

The present work was confined to the simplest generic boundary layer. It is also possible to extend the developed approach to other types of boundary layers, which will be carried in the next chapters.

Chapter 3

Collapses in a confined boundary layer as described by the two-dimensional 'intermediate long-wave equation'

The chapter is based on the results of a study published in the Springer Journal of Theoretical and Mathematical Physics (Oloo & Shrira, 2020), the work is reproduced here with minor modifications.

3.1 Introduction

In the previous chapter we confined our study of nonlinear dynamics 3d longwave perturbations in boundary layers to semi-infinite boundary layers. The flows confined between two parallel plates are ubiquitous in nature and engineering context. Understanding the dynamics of confined boundary layers is crucial for controlling bypass laminar-turbulent transition. Very little is known about the effects of the boundary layer confinement on occurrence of collapses of 3d longwave perturbations. Here, in

continuation of the line of Chapter 2 we focus on nonlinear growth of 3d linearly decaying perturbations.

The basic model we consider is the *'2d Intermediate long-wave equation'* (2d-ILW), which was derived in Voronovich et al. [1998], see Eqs. (35,36,52). This equation is a member of a broader family of two-dimensional nonlinear evolution equations derived in Voronovich et al. [1998], the 2d-ILW equation describes evolution of weakly nonlinear long wave perturbations of a generic boundary layer in homogeneous fluid confined between two parallel planes separated by a distance $D (D \gg d)$ for a wide range of the Reynolds numbers. Its derivation is straightforward. In the previous chapter section §2.3.3 we showed that the slow motion outside the boundary layer is governed by the following equation specifying function f dependence on the slow variable Z_1,

$$\partial^2_{Z_1 Z_1} \hat{f}(\boldsymbol{k}) - k^2 \hat{f}(\boldsymbol{k}) = 0, \qquad (k = |\boldsymbol{k}|), \tag{3.1}$$

where $\hat{f}(\boldsymbol{k}, Z_1)$ is the Fourier transform of $f(x, y, Z_1)$. For the semi-infinite boundary layers examined in the previous chapter we employed the boundary conditions of vanishing at infinity, $\hat{f}(\boldsymbol{k})|_{Z_1 \to \infty} = 0$, while here we require vanishing of $\hat{f}(\boldsymbol{k}, Z_1)$ at $Z_1 = D$, hence,

$$\hat{f}(\boldsymbol{k})|_{Z_1 = D} = 0, \quad \hat{f}(\boldsymbol{k})|_{Z_1 = 0} = 1. \tag{3.2}$$

Its solution satisfying the boundary condition (3.2) has the form

$$\hat{f}(\boldsymbol{k}, Z_1) = \sinh k(Z_1 + D) / \sinh (kD). \tag{3.3}$$

This solution yields the modified kernel $Q(k)$ of the integral operator describing dispersion, instead of $Q(k) = k$ for semi-infinite boundary layers, we now get

$$Q(k) = k / \tanh kD, \qquad (k = |\boldsymbol{k}|, \quad k^2 = k_x^2 + k_y^2). \tag{3.4}$$

The procedure is nearly identical to that of the previous chapter yields the nonlinear evolution equation which we refer to as '2d Intermediate long-wave equation' (2d-ILW). We will be examining the 2d-ILW equation in this chapter. Since in this chapter we focus on elucidating the effects of the boundary layer confinement, we

neglect the Rayleigh friction term which is the same as in the previous chapter and leads to qualitatively similar effects.

One dimensional version of the 2d-ILW equation, known as the *Intermediate long-wave equation* (ILW) or *Joseph equation*, was derived independently in Joseph [1977] and in T. Kubota and Dobbs [1978] for long waves in stratified inviscid fluid of finite depth, for the situations when the stratification is confined to a thin layer. It has an infinite number of integrals of motions and has soliton and multi-soliton solutions (e.g. Joseph and Egri [1978],Matsuno [1979], Chen and Lee [1979]). The equation has a non-dimensional parameter D characterizing the overall depth of the fluid. In the limit of large and small D it reduces, respectively, to the integrable Benjamin-Ono and Korteweg-de Vries equations.

In contrast to its well studied 1d reduction, the 2d-ILW equation has never been studied, apart from finding numerically its localized 2d axially-symmetric solitary wave solutions in Voronovich et al. [1998]. In the linear limit the solutions of the 2d-ILW equation are a superposition of harmonic waves satisfying the following dispersion relation linking the frequency ω and wavevector $\boldsymbol{k}\{k_x, k_y\}$,

$$\omega = -k_x|\boldsymbol{k}|\coth(|\boldsymbol{k}|D),$$

where D is the dimensionless distance between two parallel planes confining the boundary layer. It is easy to see that as $D \to \infty$, this relation reduces to the dispersion relation of the linearized 2d Benjamin-Ono equation, i.e. $\omega = -k_x|\boldsymbol{k}|$, Shrira [1989]. In the opposite limit, $D \to 0$, we get $\omega = -k_x(1/D - D|\boldsymbol{k}|^2)$, which (after the Galilean transformation) corresponds to that of the linearized 2d Zakharov-Kuznetsov equation Zakharov and Kuznetsov [1974]. Correspondingly, the 2d-ILW equation reduces to the 2d Benjamin-Ono equation for large D, and, after the same Galilean transformation, to the 2d Zakharov-Kuznetsov (ZK) equation for small D.

D'yachenko and Kuznetsov [1995] showed that the essentially 2d Benjamin-Ono equation derived by Shrira (1989) describes collapses of initially localized two-dimensional perturbations. Pelinovsky and Shrira [1995] derived explicit description of the collapse in the 2d Benjamin-Ono equation employing Whitham's adiabatic

approach. In contrast, the localized in two dimensions solitary wave solutions of the 2d-ZK equation are considered to be stable Zakharov and Kuznetsov [2012]. Here, we consider the open question of what is the result of the evolution of initially localized perturbations in the framework of the 2d-ILW equation.The specific open questions we aim at clarifying are:

1. What is the outcome of the evolution of initially localized 3d long-wave perturbations within framework of the 2d-ILW equation?

2. Can the 2d-ILW equation describe collapses, and if yes, then under what conditions, and what type of singularity one could expect?

The Chapter is organized as follows. Section §3.2 sets up the physical model of a generic confined boundary layer and explains the assumptions underpinning the asymptotic derivation of the 2d-ILW equation. §3.3 describes its basic properties. In §3.4, following D'yachenko and Kuznetsov [1995], we argue that collapses in the 2d-ILW equation occur whenever the Hamiltonian is negative and unbounded, on this basis we explicitly find the domains of collapses and decay in the parameter space for the Gaussian and Lorentzian initial perturbations. In §3.5 we describe our numerical simulation of the 2d-ILW equation and provide an example of numerical simulation of collapse. This example demonstrates the self-similar character of the collapse in 2d-ILW equation. We also compare the direct numerical simulations within the 2d-ILW equation with the analytical self-similar solution and show very good agreement, the vicinity of collapse is asymptotically described by the self-similar solution of the 2d-BO equation. In the final section, §3.6, we summarize our results.

3.2 The Model

3.2.1 Boundary layer between two parallel planes

We consider a generic unidirectional boundary layer shear flow confined between two parallel planes separated by a distance D. In the Cartesian frame with the origin at

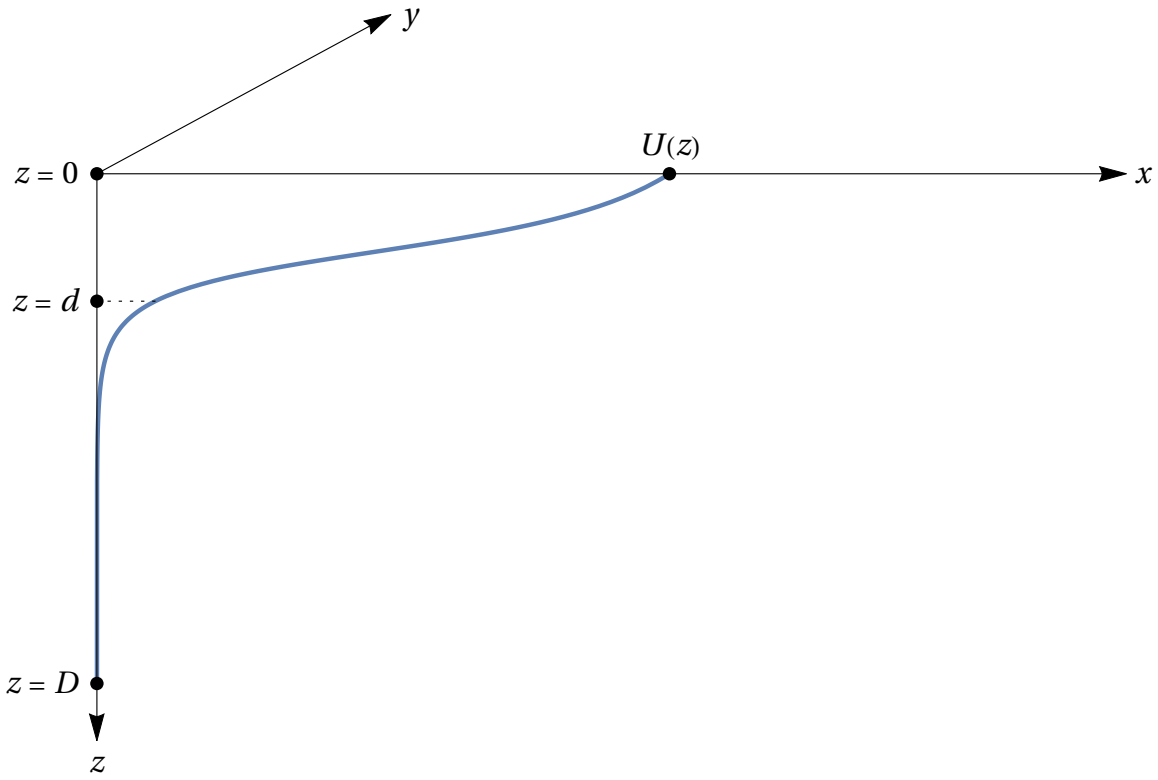

FIGURE 3.1: Sketch of geometry of a generic confined boundary layer profile with the shear localized in a thin boundary layer of thickness d and confined by a second boundary set at distance D. For certainty only, the sketch shows the boundary layer in free surface water flows. For the boundary layers typical of situations with no slip boundary (e.g. wind tunnels) sketch holds after the Galilean transformation: $U(0)$ should be set to zero, while $U(D)$ becomes the free stream velocity.

the upper boundary with z, $0 \leq z \leq D$, directed downwards with x and y directed streamwise and spanwise, respectively (Fig 3.1). The labeling of directions as vertical or horizontal is adopted for convenience only. Without loss of generality, we assume the unperturbed unidirectional boundary layer velocity $U(z)$ to be adjacent to the top boundary and localized with characteristic thickness $d, (d \ll D)$. It is also assumed that the flow profile $U(z)$ has no inflection points. In this setting the nonlinear evolution of long-wave perturbations having comparable scales in x an y is described by the 2d ILW equation derived in Voronovich et al. [1998] from the Navier-Stokes equations,

$$A_\tau - \alpha_1 A A_x - \beta_1 \hat{G}[A_x] = 0, \tag{3.5}$$

where $A(x, y, \tau)$ is the amplitude of the streamwise velocity component of the perturbation, τ is slow time, $\alpha_1 = U'(0)$, $\beta_1 = U^2(0)/U'(0)$ and the integral operator

$\hat{G}[\psi]$ is,

$$\hat{G}[\psi(\mathbf{r})] = \frac{1}{4\pi^2}\int_{-\infty}^{+\infty}\int_{-\infty}^{+\infty} k\coth(kD)\psi(\boldsymbol{r}_1)e^{(i\boldsymbol{k}(\boldsymbol{r}-\boldsymbol{r}_1))}\mathrm{d}\boldsymbol{k}\mathrm{d}\boldsymbol{r}_1, \quad (\boldsymbol{r}=\{x,y\}), \quad (3.6)$$

where $k = |\boldsymbol{k}| = (k_x^2 + k_y^2)^{1/2}$. Note the specific way the streamwise perturbation velocity $u(x, y, z, t)$ is expressed in terms of the amplitude $A(x, y, t)$: to leading order,

$$u(x,y,z,t) = -\left(f(x,y,z) * A(x,y,\tau)\right)\cdot U'(z),$$

$$f(x,y,z) = \frac{1}{4\pi^2}\int_{\infty}^{\infty}\left[\frac{\sinh k\,(\varepsilon z + D)}{\sinh(kD)}\right]e^{(-i\boldsymbol{k}\mathbf{r}))}\mathrm{d}\boldsymbol{k},$$

where $f * g$ is the convolution in the $\boldsymbol{r}$ space and $\varepsilon \ll 1$ is the small parameter of nonlinearity, defined as the ratio of the maximal streamwise velocity of the perturbation to the maximal velocity of the basic flow. Other components of velocity could be also expressed in terms of $A(x, y, \tau)$ (for details, see Voronovich et al. [1998]).

On re-scaling the variables by setting $d = 1$, we cast the 2d-ILW equation into the form which contains a single nondimensional parameter D in the kernel of the operator $\hat{G}$, specified by (3.6),

$$A_\tau + AA_x - \hat{G}[A_x] = 0. \quad (3.7)$$

This form of the 2d ILW equation provides the mathematical framework of the present study.

3.3 Basic properties of the 2d-ILW equation

The 1d-ILW equation is a well studied weakly nonlinear pseudo-differential equation which governs the evolution of long internal waves in a stratified fluid of finite depth (e.g. Joseph [1977], T. Kubota and Dobbs [1978]). In contrast, the 2d-ILW equation has not been studied, apart from a brief analysis in passing in Voronovich et al. [1998] of its steady state solutions, it was found that the 2d-ILW equation has axially symmetric solitary wave solutions. For waves propagating in any chosen direction

the 2-d ILW equation (3.7) reduces to the one-dimensional ILW equation and was shown to have an infinite set of integrals of motion, multi-soliton solutions and other properties typical of integrable systems (e.g. Joseph and Egri [1978], Chen and Lee [1979], Matsuno [1979], Ablowitz and Segur [1981]).

The notable feature of the 1d-ILW equation is that in the shallow water limit (i.e. when $D \to 0$), it tends to the classical Korteweg-de Vries equation, while at the deep water limit ($D \to \infty$), it reduces to the Benjamin-Ono equation. Similarly, the 2d-ILW, with $k \equiv |\boldsymbol{k}| = (k_x^2 + k_y^2)^{1/2}$ in the operator $\hat{G}$, reduces to the 2d Benjamin-Ono equation in the limit $kD \gg 1$. In the opposite limit, $kD \ll 1$, it is easy to see that the leading terms of the Taylor expansion of the kernel $k \coth(kD)$ are $\frac{1}{D}(1+\frac{k^2D^2}{3})$, which reduces the integral operator $\hat{G}$ to the 2d Laplace operator $\Delta = \partial_{xx}^2 + \partial_{yy}^2$; hence, for $kD \ll 1$ the 2d-ILW tends to the 2d-ZK equation. The ZK equation was originally derived to describe low frequency ion-acoustic waves in magnetized plasma Zakharov and Kuznetsov [1974], but later was found to occur in many other physical contexts Melkonian and Maslowe [1989], Nozaki [1981], Petviashvili [1980], Toh et al. [1989] and Gottwald [2003]. Note that, strictly speaking, it is not legitimate to consider the 2d-ILW equation in the ZK limit, although the equation itself does allow such a consideration and indeed reduces to the ZK equation, the asymptotic procedure employed in the derivation of the 2d-ILW equation breaks down for small D.

We can write the 2d-ILW equation (3.7) in the Hamiltonian form as follows,

$$A_\tau = \partial_x \left[\hat{G}[A] - \frac{1}{2}A^2 \right] = \partial_x \frac{\delta H}{\delta A}, \tag{3.8}$$

where the Hamiltonian H is made of two constituents I_1 and I_2,

$$H = \frac{1}{2}I_1 - \frac{1}{6}I_2, \quad I_1 = \int A\hat{G}[A]\,\mathrm{d}\boldsymbol{r}, \qquad I_2 = \int A^3\,\mathrm{d}\boldsymbol{r}, \quad (\mathrm{d}\boldsymbol{r} \equiv \mathrm{d}x\mathrm{d}y). \tag{3.9}$$

Besides the Hamiltonian, the 2d-ILW equation (3.7) conserves the streamwise and spanwise components of the 'momentum' $\boldsymbol{P}$ and the mass flux M,

$$P_x = \frac{1}{2}\int\int A^2\,\mathrm{d}x\mathrm{d}y, \quad P_y = \frac{1}{2}\int\int A\phi_y\,\mathrm{d}x\mathrm{d}y, \quad (\phi_x \equiv A), \quad M = \int\int A\,\mathrm{d}x\mathrm{d}y. \tag{3.10}$$

The way these integrals depend on parameters of the perturbations enables us in the next section to infer the existence of collapses for certain initial conditions and to outline the domain of collapsing initial conditions for particular *a priori* chosen classes of initial conditions.

3.4 Collapses in the 2d-Intermediate long-wave equation. Domain of collapses in the parameter space

3.4.1 Domain of collapses in the $a - \sigma$ space in the generic case

The existence of collapses in the 2d Benjamin-Ono equation, which is a particular limit of the 2d-ILW equation, has been shown by Dyachenko & Kusnetsov (1995). The conditions of collapse within the framework of the 2d-BO equation were thoroughly examined in the previous section 2.4. Here, we extend this approach to the 2d-ILW equation.

The plane soliton solution of the 2d-ILW equation is stable within the framework of the 1d-ILW equation, but is unstable with respect to transverse modulations within the 2d-ILW equation we are studying here. In contrast to the 2d Benjamin-Ono equation, for which the transverse stability of plane wave solutions was thoroughly studied in Pelinovsky and Stepanyants [1994], Gaidashev and Zhdanov [2004] there was no dedicated analysis of transverse instabilities for the 2d-ILW equation. Here we skip this element of analysis, since the plane soliton transverse instability clearly

manifests itself in numerical simulations of the 2d-ILW equation and we know *a priori* the scaling of the instability growth rate.

The key finding by Dyachenko & Kusnetsov (1995) is that the existence of collapses is linked with the unboundedness of the Hamiltonian from below as the amplitude of the perturbation increases. For any chosen localized initial conditions the necessary and sufficient condition for the collapse to occur is that the Hamiltonian has to be negative. The reasoning of D'yachenko and Kuznetsov [1995] is applicable to the case of the 2d-ILW equation in its entirety. By means of direct numerical simulations of the 2d-ILW equation (which we describe below) we verify that this criterion indeed predicts the emergence of collapse. Moreover, this criterion enables us to get a good *a priori* idea how the fate (i.e. collapse or decay) of an initial perturbation depends on its parameters. To outline these dependencies we examine a few simple axisymmetric distributions: the Gaussian and Lorentzian pulses,

$$A_G(x,y) = ae^{-(x^2+y^2)/2\sigma^2}, \qquad A_L(x,y) = \frac{a}{1+4(x^2/\sigma^2+y^2/\sigma^2)}. \tag{3.11}$$

These initial perturbations are fully characterized by just two parameters: amplitude a and characteristic half-width σ, which we will refer to as the 'width' for brevity.

It is easy to see that in the Hamiltonian H given by (3.9), both its constituent integrals, the dispersion one, I_1, and the nonlinear one, I_2, can be expressed in terms of amplitude a and perturbation width σ. On re-scaling the variables,

$$\tilde{x} = \frac{x}{\sigma}, \qquad \tilde{y} = \frac{y}{\sigma}, \qquad A(\tilde{x},\tilde{y}) = a\,\mathcal{A}, \quad \left(\mathcal{A}_G = e^{-(\tilde{x}^2+\tilde{y}^2)/2}, \quad \mathcal{A}_L = \frac{1}{1+4(\tilde{x}^2+\tilde{y}^2)}\right)$$

we re-write our integrals as,

$$I_1 = a^2\sigma\tilde{I}_1, \qquad \tilde{I}_1 = \int\int \mathcal{A}\,\hat{G}\,[\mathcal{A}]\,\mathrm{d}\tilde{x}\mathrm{d}\tilde{y}, \qquad I_2 = a^3\sigma^2\tilde{I}_2, \qquad \tilde{I}_2 = \int\int \mathcal{A}^3\mathrm{d}\tilde{x}\mathrm{d}\tilde{y},$$

where $\tilde{I}_1$ depends implicitly on σ through the kernel of the integral operator, $\coth\left(\frac{kD}{\sigma}\right)$, while $\tilde{I}_2$ is a constant that is evaluated analytically or numerically; for the Gaussian initial conditions $\tilde{I}_2 = \frac{2}{3}\pi$. The integral $\tilde{I}_1$ cannot be evaluated analytically and is dealt with numerically for the whole range of D and σ.

If the dispersion and nonlinear contributions in the Hamiltonian are in exact balance, i.e. $3\,I_1 - I_2 = 0$, the Hamiltonian vanishes, and thus yields a nonlinear 'neutral curve' separating the domains of collapse and decay on the $a - \sigma$ plane,

$$a^2\sigma(3\,\tilde{I}_1 - a\sigma\tilde{I}_2) = 0. \tag{3.12}$$

The relationship between the amplitude threshold a_{thr} and perturbation width σ prescribed by equation (3.12) reads,

$$a_{thr}(\sigma) = \frac{3\,\tilde{I}_1}{\tilde{I}_2\,\sigma}. \tag{3.13}$$

To better understand this relationship we expand $\coth\left(\frac{kD}{\sigma}\right)$ for $\sigma \gg 1$ and $\sigma \ll 1$. By retaining the first two terms in the Laurent series of $\coth s$, when $s = \frac{kD}{\sigma} \ll 1$ we find, $\frac{1}{s} + \frac{1}{3}s - .....$ Similarly, for short waves, $\sigma \ll 1$, i.e. when $s \gg 1$, $\coth s \approx 1$ with exponentially small discrepancy (e.g. Abramowitz and Stegun [1964]).

3.4.2 Domain of collapses in the ZK limit

Note that the transition from 2d-ILW equation to 2d-ZK is not entirely smooth, since to leading order we have large constant translation term $1/s$, which can be eliminated by switching to the moving coordinate frame. By writing the equation in the Hamiltonian form we scale the integrals of motion using parameters of the initial conditions, the amplitude a and width σ. Thus, it is easy to see that the Hamiltonian H in the ZK limit consists of three terms (the constant translational term I_3, the dispersion one, I_4, and the nonlinear one, I_2) which can be expressed in terms of amplitude a and width of the perturbation σ,

$$I_3 = 3\,a^2\sigma^2\tilde{I}_3/D, \qquad \tilde{I}_3 = \int\int \mathcal{A}^2\,\mathrm{d}\tilde{x}\mathrm{d}\tilde{y},$$

$$I_4 = D\,a^2\tilde{I}_4, \qquad \tilde{I}_4 = \int\int \mathcal{A}\,\hat{G}_1\,[\mathcal{A}]\,\mathrm{d}\tilde{x}\mathrm{d}\tilde{y},$$

$$I_2 = a^3\sigma^2\tilde{I}_2, \qquad \tilde{I}_2 = \int\int \mathcal{A}^3\mathrm{d}\tilde{x}\mathrm{d}\tilde{y}.$$

Recall that in the ZK limit the dispersion operator $\hat{G}_1$ in the Fourier space is $k^2 \equiv |\boldsymbol{k}|^2 = k_x^2 + k_y^2$. The factor $\tilde{I}_3$ is evaluated analytically or numerically; for the Gaussian initial conditions its exact value is π. The integral $\tilde{I}_4$ is dealt with numerically, yielding a constant.

If the dispersion and nonlinear contributions in the Hamiltonian are in exact balance, i.e. $I_3 + I_4 - I_2 = 0$, the Hamiltonian vanishes, which yields a nonlinear 'neutral curve' separating the domains of collapse and decay on $a - \sigma$ plane,

$$a^2 \left(\frac{3\,\sigma^2 \tilde{I}_3}{D} + D\tilde{I}_4 - a\sigma^2 \tilde{I}_2 \right) = 0. \tag{3.14}$$

Thus, in the long-wave limit the nonlinear neutral curve specifying the amplitude threshold $a_{thr}(\sigma)$ corresponding to the Z-K equation tends to a constant independent of σ,

$$a_{thr} = \frac{3\,\tilde{I}_3}{D\,\tilde{I}_2} + \frac{D\tilde{I}_4}{\sigma^2 \tilde{I}_2}. \tag{3.15}$$

Note that the asymptotic expression of the threshold amplitude equation (3.15) corresponding to 2d-ZK equation was found to be in good agreement with that obtained from the 2d-ILW given by equation (3.12). Therefore the amplitude threshold in this particular limit depends primarily on D (it tends to infinity as $1/D$ as $D \to 0$), while the dependence on the width σ is vanishing. In the limit of $\sigma \gg 1$ the amplitude threshold ceases to depend on σ.

In the opposite limit ($\sigma \ll D$), the neutral curve is the hyperbola,

$$a_{thr} = \frac{3\,\hat{I}_1}{\hat{I}_2\,\sigma}. \tag{3.16}$$

We obtained the neutral curves for the intermediate values of D by evaluating integrals I_1 and I_2 numerically for the axisymmetric Gaussian and Lorentzian initial pulses. Plots of the results are shown in figure (3.2). Perturbations with a and σ above the neutral curve invariably collapse, those with a, σ below the curve – decay. Note that the curves for the Gaussian and Lorentzian initial conditions are very

similar; the quantitative discrepancy is rather small. We emphasize two features of these plots:

1. The amplitude threshold monotonically raises with the decrease of D and tends to infinity as D tends to zero, and

2. For any non-zero D the amplitude threshold monotonically raises with the decrease of σ.

In the limit of small D corresponding to the ZK equation, the threshold amplitude ceases to depend on σ and tends to a large $O(1/D)$ constant. Since the 2d-ILW equation was derived assuming weak nonlinearity, for small D a considerable portion of the 'collapse domain' is beyond the range of validity of the equation. Note that here we considered whether a given initial perturbation lump of amplitude a and width σ would collapse assuming a and σ to be independent. The conclusion is that the threshold amplitude tends to zero as the width tends to infinity. However, if we allow σ to depend on a, we get, at a first glance, a different picture. For example if we choose the lump solitary wave solutions reported in Voronovich et al. [1998] as our initial condition, then their Hamiltonian is always negative, hence, all such initial conditions collapse, whatever the initial amplitude. Thus, for this class of initial perturbations there is no amplitude threshold. In fact, there is no contradiction with the conclusions obtained for simple shape initial distributions, just when $\sigma = \sigma(a)$, the picture becomes somewhat distorted: for the lump solitons of Voronovich et al. [1998], $\sigma \to \infty$ as $a \to 0$. That is, for the infinitely long initial perturbations of whatever shape the amplitude threshold tends to zero.

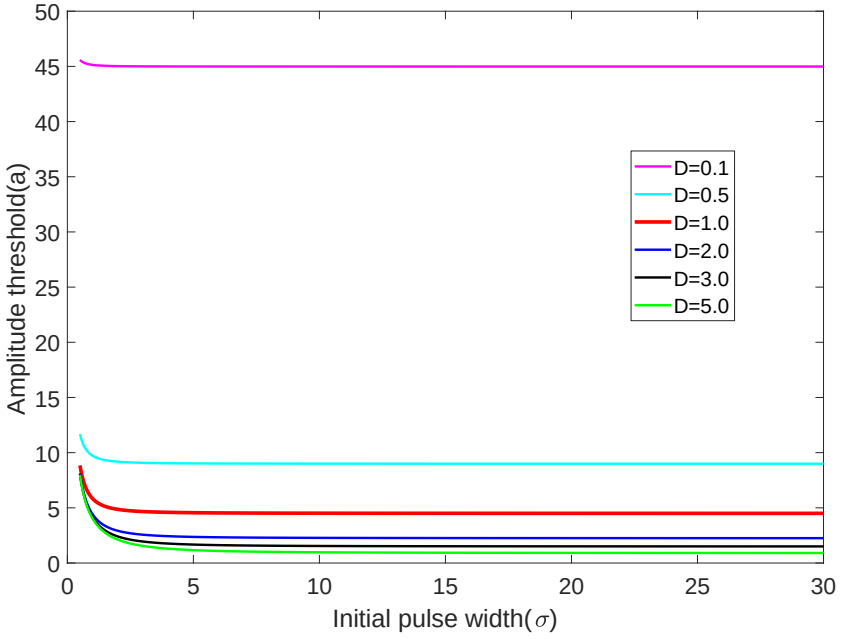

(a)

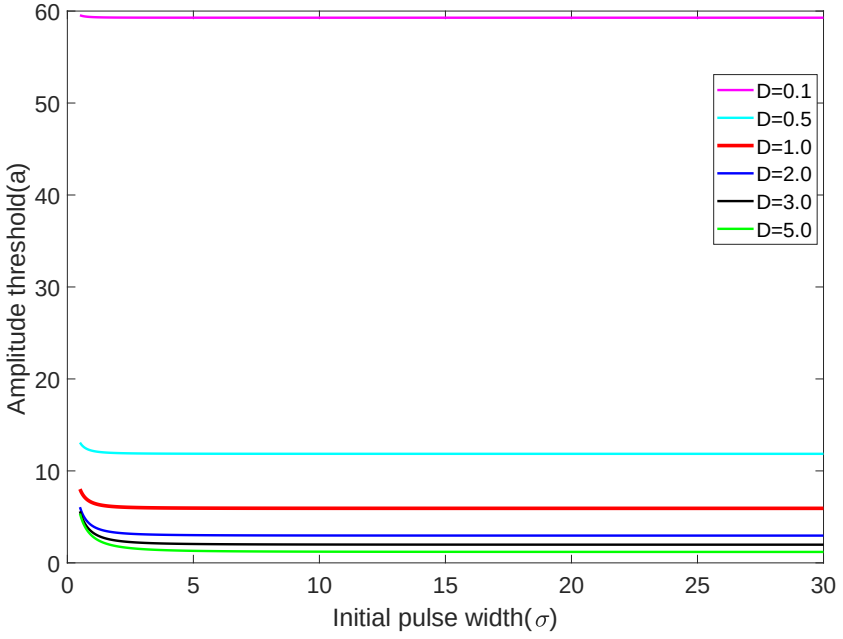

(b)

FIGURE 3.2: 'Neutral curves' separating the domains of collapse and decay for different values of D ($D = 0.1, 0.5, 1, 2, 3, 5$) for: (a) the Gaussian and (b) the Lorentzian initial conditions.

3.5 Self-similar solution and numerical simulation of collapses

3.5.1 Self-similar solution

It is natural to expect a self-similar behaviour of the solution in the vicinity of the singularity. In D'yachenko and Kuznetsov [1995] a self-similar solution of the 2d Benjamin-Ono was put forward. In this section we show that the same logic applies to the 2d-ILW equation and find the self-similar solution of (3.5).

We consider the spatial and temporal dependence of collapsing perturbation in a certain vicinity of the blow-up singularity occurring at $\boldsymbol{r} = \boldsymbol{r}_0\,\{x_0, y_0\}$. Introduce time to singularity $\check{\tau}$ and distance to singularity $\check{x} = x - x_0$, $\check{y} = y - y_0$. We look for a self-similar solution in the form

$$A(\mathbf{r}, \check{\tau}) = \check{\tau}^{\lambda} g(\boldsymbol{\xi}), \quad \boldsymbol{\xi} = \frac{\boldsymbol{r}}{\check{\tau}^{\mu}}. \tag{3.17}$$

On substituting ansatz (3.17) into the 2d-ILW in the form (3.7) and ensuring the equation remains invariant, it is easy to show that $\lambda = -\frac{1}{2}$ and $\mu = \frac{1}{2}$. Thus,

$$u(\boldsymbol{r}, \check{\tau}) = \check{\tau}^{-\frac{1}{2}} g(\boldsymbol{\xi}), \quad \boldsymbol{\xi} = \frac{\boldsymbol{r}}{\check{\tau}^{\frac{1}{2}}}, \tag{3.18}$$

where $g(\boldsymbol{\xi})$ is specified by the equation,

$$\frac{\boldsymbol{\xi} g}{2} + \frac{g^2}{2} + \hat{G}[\,g\,] = 0.$$

We have thus obtained an explicit self-similar solution of the 2d-ILW equation which predicts the $1/\sqrt{\tau_0 - \tau}$ singularity in time and the shrinking spatial distribution given by $g(\boldsymbol{\xi})$, its width tends to zero as $\sqrt{\tau_0 - \tau}$. This is (up to a typo in the time dependence exponent in D'yachenko and Kuznetsov [1995]) the self-similar solution of the 2d Benjamin-Ono equation obtained in D'yachenko and Kuznetsov [1995]. Our equation for g specifying the shape of the distribution has a simpler form, since we integrated our equation once.

Hence, we obtained the same self-similar solution for an essentially different equation because the asymptotics of two different equations coincide near the singularity. Here, the shrinking spatial scale of the solution implies infinite growth of the dominant wave numbers and, hence, $kD \to \infty$. Thus, in the 2d-ILW equation the vicinity of the singularity is always (for non-zero D) governed by the 2d Benjamin-Ono equation. We leave open the question whether there might exist other interesting self-similar regimes for the 2d-ILW equation corresponding to an unidentified yet intermediate asymptotics.

In our numerical experiments we also considered the axisymmetric 'ground solitons' of 2d-ILW found in Voronovich et al. [1998] as the initial conditions, the Hamiltonian for such distributions is negative, hence they collapse and there is no threshold in amplitude. This holds for any non-zero D. When $D \to 0$ the 2d-ILW ground soliton morphs into that of the 2d-ZK. Although the Hamiltonian of the ground soliton remains negative, the unboundness of the Hamiltonian disappears in the 2d-ZK limit(see Zakharov and Kuznetsov [2012],Kuznetsov [2018]), which suggests that the 2d-ZK ground soliton is stable. There is a number of numerical studies of the 2d-ZK equation, where its ground solitons were used as the initial conditions and found to be stable (e.g Jorge et al. [2005]).

We do not discuss the 2d-ZK equation further here, because the 2d-ILW equation, as mentioned, becomes inapplicable in this limit.

3.5.2 Numerical simulation

To simulate numerically the 2d-ILW equation for localized initial perturbations we use the pseudo-spectral method (see e.g.,Orszag [1969],Kopriva [2009]). The pseudo-spectral method with periodic boundary conditions uses efficient fast Fourier transform (FFT) routines in handling dependencies on x and y, while for the time evolution the classic fourth order Runge-Kutta method is employed.

In our context, it was found to be optimal to use large rectangular box of length 256π and width 64π. We re-iterate that the choice of our box size for the simulation

here is different from the previous analysis because the initial condition is axisymmetric i.e., in this case, $\sigma_x = \sigma_y = \sigma$. This choice provides sufficient domain for the spatial decay of the localized perturbations we were simulating and also to allow the perturbation sufficient time to move along the streamwise direction during the evolution. To resolve the rapidly growing and increasingly localized amplitudes we used 4096×1024 grid points. We were solving numerically the 2d-ILW equation (3.7) in the moving coordinate frame. It is convenient to present our evolution equation in the flux-conservation form,

$$A_\tau + F_x = 0.$$

where the flux $F = -\hat{G}[A] + \frac{1}{2}A^2$. The integral operator $\hat{G}[A]$ was dealt with in the Fourier space, while nonlinear terms were considered in the physical space on collocation points with the 'two-third de-aliasing rule' Orszag [1969]. The accuracy of the simulations was controlled by ensuring that the integrals of motion (3.9, 3.10) remain constant with the error not exceeding $O(10^{-4})$.

3.5.3 Evolution scenarios

On obtaining in §3.4 nonlinear neutral curves separating the domain of collapse and decay, we verified the findings by numerical simulations of the evolution of axially symmetric Gaussian pulse initial conditions (3.11). By choosing the initial perturbations slightly above and slightly below the curve, we confirmed that, indeed, the initial perturbations with the amplitudes exceeding the threshold collapse, that is, such perturbations evolve into a short-lived pattern which tends to a localized self-similar solution with a point singularity. The 'subcritical' initial conditions decay, although a temporary transient growth, sometimes substantial, can also occur.

In figures (3.4) and (3.3), we illustrate a typical evolution of a collapsing pulse for a localized initial condition. Figure (3.3) shows the typical time dependence of a collapsing pulse amplitude simulated for the axisymmetric Gaussian initial condition and $D = 4$. Note that for most of its evolution the amplitude grows slowly, the sharp growth occurs just immediately prior to the singularity. The figure also gives a good

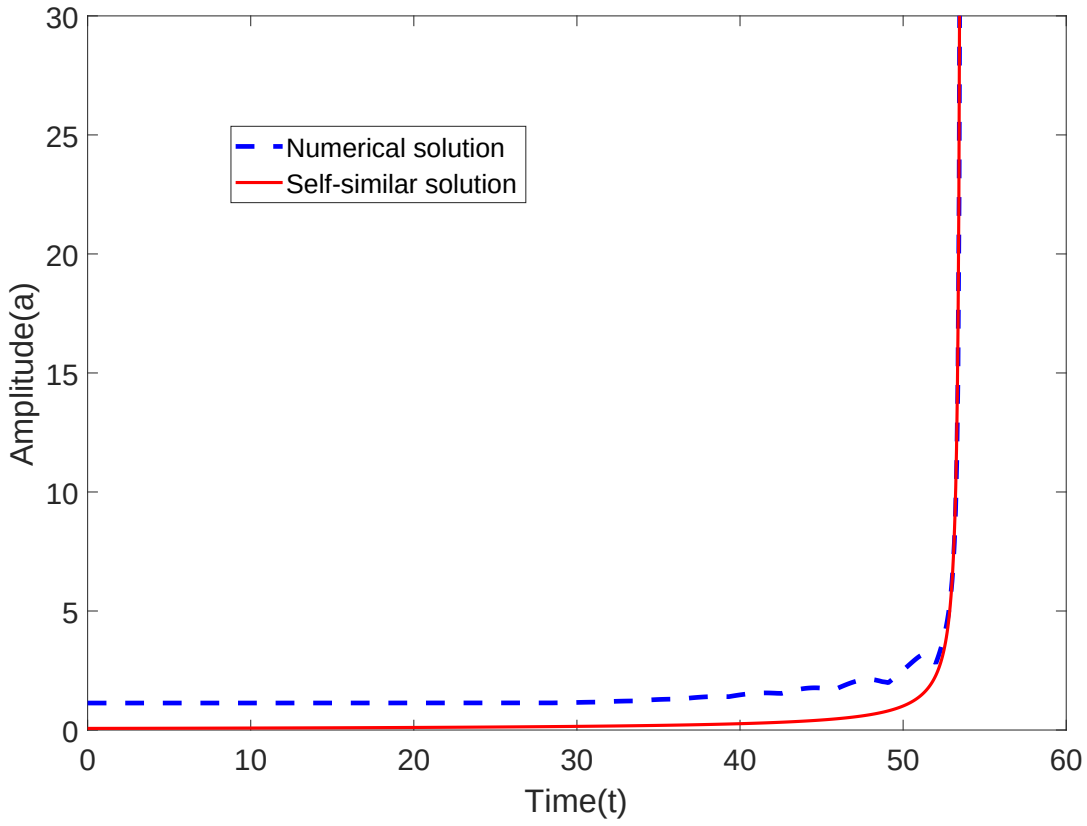

FIGURE 3.3: Example of time evolution of the amplitude of a collapsing pulse with finite D. Blue dashed line: simulated evolution of the amplitude of a collapsing pulse with the Gaussian initial condition ($a = 1.1340, \sigma = 25$) for $D = 4$. Red solid line: the self-similar solution (3.18) for $D = \infty$.

idea how surprisingly well the self-similar solution (3.18) of the 2d Benjamin-Ono equation captures the evolution governed by the 2d ILW equation. A complementary view of the evolution is provided by Figure (3.4), which shows a sequence of snapshots of a collapsing pulse.

Here, we emphasize two notable features. Although the initial condition is perfectly axially symmetric, the emerging pattern on figure 3.5 is not: at the pedestal, the pulse radiates at two distinguished directions; the resulting pattern resembles 'hair-pin' or 'lambda' vortices routinely observed in the wind tunnels (e.g.Kachanov [1994]). The top of the pulse evolves in an axially symmetric self-similar manner tending to a point singularity at the end. Asymmetric initial conditions also have these properties.

Figures 2.8 and 3.5 are showing the evolution of the perturbation cross-sections for the semi-infinite 2.8 and confined cases. At the initial moment (t=0) the perturbation is the same axially symmetric gaussian lump. A quick comparison enables us to make the following qualitative observations. The same well-confined initial lump is laterally dispersing quite differently. In both cases, during the evolution, we see a sequence of different patterns which at the foot of the perturbation resemble hairpin vortices usually observed in wind tunnel experiments during the laminar-turbulent transition. In the confined case these patterns are more pronounced. In contrast, in both cases, the top part of the perturbations becomes more and more symmetric as the perturbation approaches the collapse. As expected near the collapse when nonlinear localizing effects dominate over dispersion, all the patterns evolve into a well-localized axially symmetric shape before their eventual collapse. We could summarise the differences by saying that confinement of the boundary layer strongly affects the cross-section evolution, it results in the emergence of quite complicated patterns at the foot of collapsing lumps. In contrast, the self-similar evolution near the singularity remains qualitatively similar, the pulses tend to become axially symmetric.

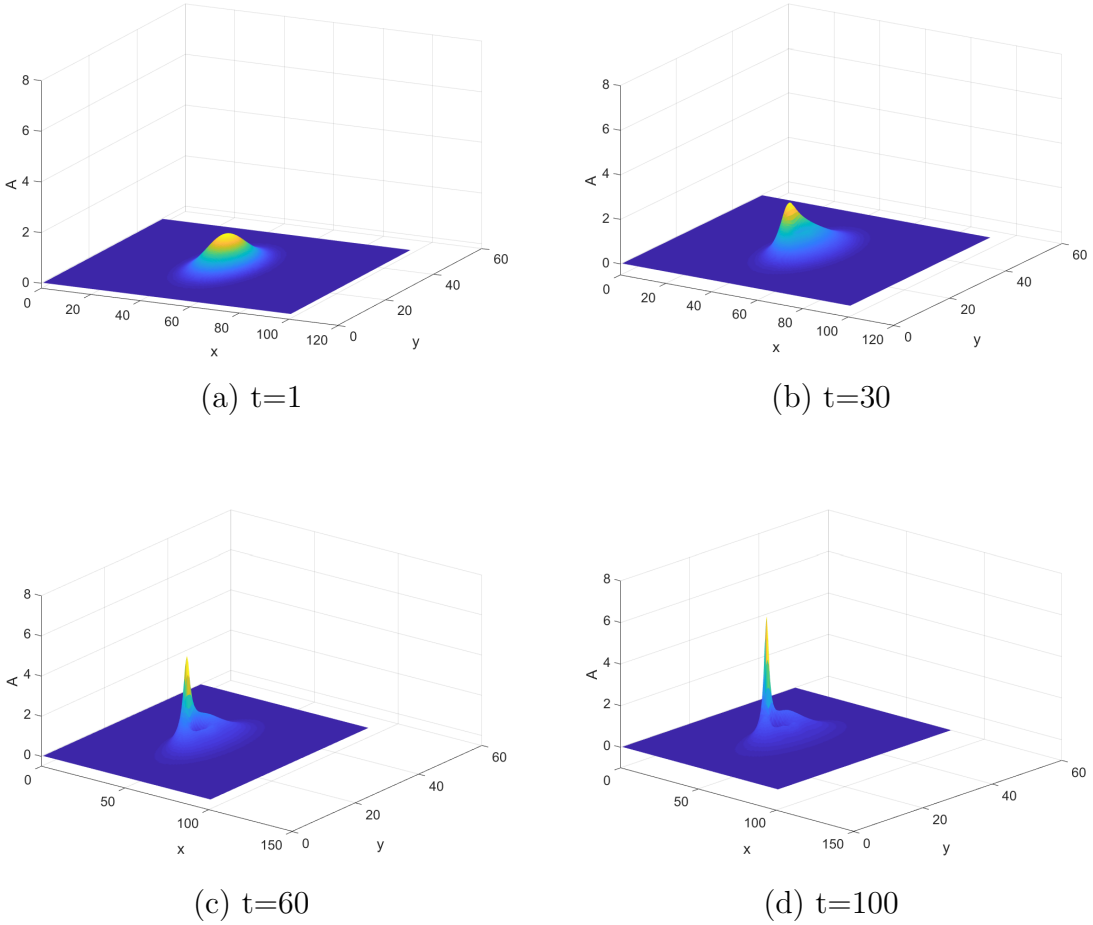

(a) t=1 (b) t=30

(c) t=60 (d) t=100

FIGURE 3.4: Example of evolution of $A(x, y, t)$ for a collapsing pulse with the Gaussian initial distribution for the initial conditions and parameters of Figure 3.3

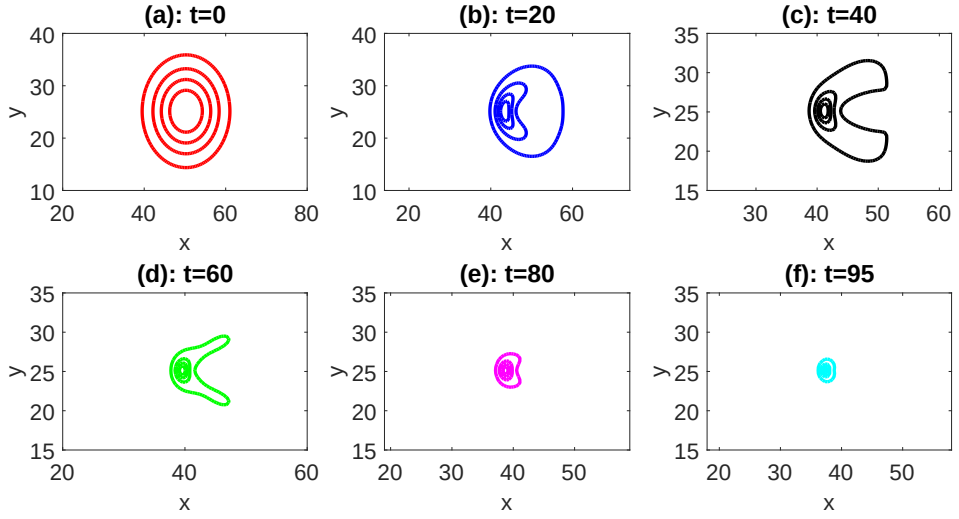

FIGURE 3.5: Evolution of the amplitude cross-sections of a collapsing pulse with Gaussian initial distribution taken at six-different moments showing hair-pin or lambda vortices. The initial conditions are the same as in figure 3.4.

3.6 Conclusions

In this chapter we examined collapses in a confined homogeneous boundary layer as described by 2d-ILW equation. This equation is a member of a broader family of two-dimensional nonlinear evolution equations derived in Voronovich et al. [1998], the 2d-ILW equation describes evolution of weakly nonlinear long-wave perturbations of a generic boundary layer in homogeneous fluid confined between two parallel planes separated by a distance $D(D \gg d)$ for a wide range of the Reynolds numbers. In contrast to its well studied 1d reduction, the 2d-ILW equation has never been studied, apart from finding numerically its localized 2d axially-symmetric solitary wave solutions in Voronovich et al. [1998]. In this section based on our analytical and numerical examination of collapses of 3d perturbations in 2d-ILW equation we summarise our findings.

1. We have shown using the methodology of D'yachenko and Kuznetsov [1995], that within the framework of the 2d-ILW equation the localized initial perturbations with negative values of the Hamiltonian H collapse for all non-zero values of parameter D. That is, we showed that a wide class of initial conditions evolves into growing coherent patterns resembling 'hairpin vortices' and

'spikes' often observed in aerodynamic tunnels Kachanov [1994]. These patterns collapse (blow up in finite time) in a self-similar manner, forming a point singularity.

2. We examined this scenario of collapse by numerically simulating the 2d-ILW equation. By using the criterion $H = 0$, which we verified numerically, we delineated the domains of collapse and decay in the a, σ, D parameter space. For axially symmetric Gaussian and Lorentzian initial distributions the results proved to be qualitatively similar and numerically close and can be summarized as follows. For large D the amplitude threshold a_{thr} as a function of the horizontal scale of the initial distribution σ is prescribed by a hyperbola: $a_{thr} = const/\sigma$. Any decrease of D raises the threshold. For small D, when the 2d ILW equation tends to the Zakharov-Kuznetsov equation, the threshold ceases to depend on σ and tends to infinity as $1/D$.

3. Our main conclusion is that physically relevant collapses are possible only for relatively large D and σ, because the threshold for small values of D and σ is too high for any part of the evolution leading to collapse to be weakly nonlinear. We also recall that the derivation of the 2d-ILW equation itself breaks down for small D.

4. The initial conditions for the solitary waves has no amplitude threshold. For example if we choose the lump solitary wave solutions reported in Voronovich et al. [1998] as our initial condition, then their Hamiltonian is always negative, hence, all such initial conditions collapse, whatever the initial amplitude. Thus, for this class of initial perturbations there is no amplitude threshold. In fact, there is no contradiction with the conclusions obtained for simple shape initial distributions, just when $\sigma = \sigma(a)$, the picture becomes somewhat distorted: for the lump solitons of Voronovich et al. [1998], $\sigma \to \infty$ as $a \to 0$. That is, for the infinitely long initial perturbations of whatever shape the amplitude threshold tends to zero.

Chapter 4

Nonlinear dynamics of three-dimensional(3d) long-wave perturbations in weakly stratified boundary layers

4.1 Introduction

In the previous chapters nonlinear dynamics of linearly decaying 3d long-wave perturbations in a generic unidirectional boundary layer flow has been examined. The main results are the novel Whitham-type evolution equations which under certain conditions predict collapse of initial 3d perturbations. The boundary layers are often stratified both in nature, e.g. surface and bottom boundary layers in the ocean (the surface boundary layer becomes stratified because of the direct solar heating and interaction with atmosphere [see Miropol'Sky [2001], Komen et al. [1996], Soloviev and Lukas [2013]], gets buoyancy because of air bubble entrainment from breaking

wind-wave, while the bottom layer becomes stratified through entrainment of sediments) and atmosphere (there is a density stratification in the atmospheric boundary layer), there are many examples of stratified flows in the engineering context. In this chapter we examine a generic weakly stratified semi-infinite boundary layer leaving aside the issue of links of this model to specific geophysical and engineering contexts. To our knowledge there was no studies of weakly stratified boundary layers with the small Richardson numbers (Ri). Physically in the context of hydrodynamic stability, Richardson number is a ratio between the square of buoyancy force ($N^2(z)$) to the square of shear ($(U')^2$). Often the flows with the Richardson number less than 1/4 are considered to be linearly unstable, although this condition is just the necessary condition for the linear instability and not sufficient [see e.g., Miles [1961], Howard [1961]]. In our consideration the linear instabilities play no role in virtue of the same arguments as in the case of homogeneous boundary layers: the growth rates of long-wave perturbations are too small compared to the time scales of nonlinear dynamics we are focussing upon.

The main question we want to address is whether the account of weak stratification changes qualitatively the nonlinear dynamics of 3d long-wave perturbations. The specific open questions we aim at clarifying are:

1. Can the effect of weak stratification on boundary layer 3d long-wave dynamics be captured by a single evolution equation?

2. Is the boundary layer collapse found for the homogeneous flow sufficiently robust to survive in the presence of weak stratification?

3. If the collapses are possible, in what ways do they differ from the collapses in the homogeneous boundary layer? What is the role of the stratification?

To address these questions, in this chapter we derive a novel 2d nonlinear evolution equation which is essentially two-dimensional Whitham type equation with explicit account of stratification in the boundary layer. We also take into account the viscous linear decay and examine its role in the evolution of perturbations. By numerical simulations of the derived equation we show that an initial localised perturbation

of any given shape collapses, blows up forming a point singularity in finite time, provided its initial amplitude exceeds a certain threshold specific for each particular initial shape and the stratification. The initial perturbations exceeding the threshold collapses, while the perturbations with the amplitudes below the threshold - decay. Such collapses might be a plausible mechanisms of laminar-turbulent transition. We find that indeed the collapses occur much faster than linear instabilities in stratified flows when Richardson number is less than 1/4. Linear stability of stratified shear flows has been studied for many years, primarily in the inviscid setting, and is summarised in many monographs and reviews [see. e.g., Howard and Maslowe [1973], Turner [1979], LeBlond and Mysak [1981], Carpenter et al. [2011]]

4.1.1 Linear stability of waves in stratified shear flows

The interplay between shear and buoyancy force plays a key role in the dynamics of a multitude of boundary layers including near-surface layer of the ocean. The shear effect creates a destabilizing effect, while the buoyancy tends to stabilize the disturbance created by the shear effect. The most fundamental basic model to examine the effects of buoyancy is a stratified, plane parallel shear flow which is a classical problem of hydrodynamics (see, for example, Drazin and Reid [2004]).

Numerous linear inviscid models have been thoroughly studied with the focus on the possibility of unstable modes in stratified shear flows (e.g. Turner [1979], Carpenter et al. [2010] Carpenter et al. [2011]). Among the most studied models of stratification are two layer models flows of different densities and shear profiles, these models revealed the existence of unstable modes either through Kelvin-Helmholtz instability or Holmboe instability (H-I and KH-I)[see Holmboe [1962], Drazin and Reid [2004], Carpenter et al. [2011]].

4.1.1.1 Introduction to linear stability and Taylor-Goldstein equation

In the context of geophysical fluid dynamic, shear instability is known to be important for understanding the physics underpinning transition to turbulence and mixing in

the atmospheric and oceanic boundary layers. Since oceanic and atmospheric flows are generally density stratified, the instability process often involves the interplay of shear and density stratification. The first step towards the study of a stratified shear flow is to perform a linear stability analysis to determine whether small perturbations applied to the flow will grow in time. This has been carried out in many contexts primarily using the well known Taylor-Goldstein equation that was derived as an extension of the Rayleigh equation to incorporate variations in density. There are well known three types of linear instabilities in the inviscid stratified shear flows: Kelvin-Helmholtz (KH) (in its nonlinear stage it produces overturning billows through vorticity-vorticity interaction), Holmboe (H) instability results from the interaction of a vorticity and a gravity wave and Taylor-Caulfield (T-C) for two interacting internal gravity waves. A general classification of the unstable interactions in inviscid stratified shear flows was given in [e.g Caulfield [1994], Carpenter et al. [2010]] in terms of three fundamental mechanisms: (i) the Kelvin-Helmholtz (KH) interaction of two vorticity waves, (ii) the Holmboe (H) interaction of an internal gravity wave and a vorticity wave, and (iii) the Taylor-Caulfield (TC) interaction of two internal gravity waves. The most common analytical tool used to investigate the linear stability is the normal mode approach. The equations of motion (the Navier-Stokes or Euler equations) are first linearized around a plane parallel shear flow, and after performing the Fourier transform with respect to the streamwise and spanwise spatial variables and imposing appropriate boundary conditions, analysis of stability reduces to the analysis of the resulting boundary value problem. Since the equations are linear the evolution of every harmonic could be studied separately. By means of the normal mode approach, one can determine the phase velocity $c = c_r + ic_i$ of the internal waves, together with their growth rates (stable, unstable and neutral modes). The real part c_r represents the phase speed of the perturbation, while a positive imaginary component c_i indicates an exponential growth in time, with a growth rate given by the imaginary component of the complex frequency $\omega_i = kc_i$. The biggest shortcoming of linear stability analysis is that it is only valid when the perturbations are very small. When the amplitudes become larger, the nonlinear effects can accumulate and become dominant; this case goes beyond the domain of applicability of linear theory.

It is therefore very important and reasonable to begin the analysis of parallel flows with the linear analysis in order to understand the nature of the modes that are likely to grow or become neutral in case of a disturbance. In inviscid stratified shear flows, the main equation that describes the normal modes for linear stability is the Taylor-Goldstein equation with the appropriate boundary conditions. In our study, we will focus primarily on the stably stratified shear flow, meaning that the density variation with depth is considered and the Boussinesq approximation can be applied. The original form of Taylor-Goldstein equation was first derived in 1931 independently by Taylor and Goldstein [Craik [1988]] in the context studies of stability of stratified shear flows; it is the same form that is still being used today. The Taylor-Goldstein (TG) equation is derived from the linearized Euler equations, under the assumptions of inviscid, Boussinesq fluid; the equation for the vertical structure is linearized about vertical profiles of horizontal velocity and density representing the basic state. Two boundary conditions supplementing the TG equation yield the TG boundary value problem. The normal mode analysis to the TG boundary value problem has revealed its properties in terms of stable, unstable and neutral modes of the internal waves in a stratified shear flow. The coefficients of the equation have a singularity at the critical value $z = z_c$, where the horizontal value of the phase speed $c = U(z_c)$, this makes the TG boundary value problem singular. The TG equation is not easy to handle analytically, asymptotically and numerically for arbitrary profiles of stratification and shear. Very few analytical solutions exist, primarily, for special circumstances with piece-wise and constant profiles of shear and stratification. Previous studies have shown that the use of Frobenius expansion [e.g. LeBlond and Mysak [1981]; Sutherland [2010]; Massel [2015]] in solving the TG boundary value problem reveals the behavior of its solutions near the critical value z_c. It has been shown that for inviscid plane-parallel flows the Richardson number Ri

$$Ri = \frac{N^2}{(U')^2}. \tag{4.1}$$

where N^2 is the buoyancy (Brunt–Väisälä) frequency squared and U' is the basic flow shear, is the key parameter controlling the stability of the normal modes in stratified shear flows. When $Ri > \frac{1}{4}$ for all z the flow remains stable, while if $Ri < \frac{1}{4}$ for for

some z, the flow might become unstable. When $Ri = 0$, the scenario is somewhat complicated since we could have neutral modes belonging to continuous spectrum and to the discrete spectrum. When there are discrete neutral modes we will necessarily have also unstable modes. We also do have unstable modes for $Ri = 0$ when the shear has inflection points (see the Rayleigh criterion). Hence the TG BVP can be used to predict the dispersion relation and the structure of the internal waves in inviscid stratified shear flows for stable, unstable and neutral solutions.

We conclude our brief overview of linear stability of stratified flows by pointing to the outstanding questions relevant for our study. To our knowledge there are practically no studies of the viscous weakly stratified flows with small Richardson numbers, the only exception we are aware of is the work by Danyi [2018]. In particular, there was no attempt of obtaining asymptotic expansion in small wave numbers to extend the results established for the zero Richardson number Healey [2017]. In principle, it is straightforward, since the weak stratification enters into the boundary value problem as a regular perturbation. However such an analysis would be quite involved and is beyond the scope of the present study. For our purposes it would be sufficient to know that the growth rates of longwave perturbations with wavenumbers $O(\varepsilon)$ remains to be $O(\varepsilon^3)$ as in the case of homogeneous flows. Although we do not have the rigorous proof, there are strong arguments that this is the case: the account of weak stratification acts as a regular perturbations and is expected to decrease the growth rate.

4.1.2 Long nonlinear waves in stratified shear flows

To our knowledge there are very few works on the study of the effect of shear on solitary waves taking into account both stratification and shear effects in the boundary layer. The pioneering work was conducted by Maslowe and Redekopp [1980]. They considered the propagation of solitary waves in the presence of shear within a thin strongly stratified boundary layer and weak stratification outside the infinite bottom layer. Nonlinear internal waves propagating along a shallow thermocline above a weakly stratified deep lower layer may radiate internal waves into the lower layer,

thereby damping the nonlinear waves. This problem was formulated by Maslowe and Redekopp [1980], who derived the inhomogeneous Benjamin-Ono equation and found adiabatic solutions for the decay rate of the solitary waves of the homogeneous equation. For a comprehensive review of observation and laboratory experiment on long nonlinear internal solitary waves with a sole focus on KdV models [see Helfrich and Melville [2006]]. The scenario is quite distinct to the work in this chapter in the following respects:

1. The Maslowe & Redekopp (1980) stratification was assumed to be strong ($Ri \gtrapprox 1$). Here we focus on the situations with $Ri \ll 1$.
2. The viscous effects were ignored, in our consideration their account is crucial.
3. Maslowe & Redekopp (1980) assumed weak stratification outside the boundary layer; we assume none.
4. Their model was concerned with propagation of one-dimensional (1d) perturbation. Here we consider essentially two-dimensional (2d) model with comparable streamwise and span-wise scales.

Taking into account these factors becomes apparent in comparing laboratory measurements and the simplest two-layer inviscid KdV models. In such cases the Reynolds numbers may be considered large but finite that viscous boundary-layer effects (including the interface) can be formulated to modify the evolution equation, with satisfactory results when compared with experimental measurements.

4.2 The Model, Assumptions, Scaling and Asymptotic scheme

4.2.1 Model Formulation

We consider the evolution of three-dimensional localised finite-amplitude perturbations of a steady unidirectional boundary layer shear flow $\boldsymbol{U}$ adjacent to an infinite

flat boundary. Inside the thin boundary layer we have a weakly decaying stratification $N^2(z)$ that is localised in the main boundary layer. The motion is governed by the Standard Navier-Stokes equations for incompressible fluid of variable density ρ, $\rho = \rho_0(z) + \bar{\rho}(x, y, z, t)$; $|\bar{\rho}| \ll \rho_0$, mass conservation equation and incompressibility equation. In this section the notation ρ_0 represents equilibrium density or reference density that depends only on the fast vertical scale z while $\bar{\rho}$ is the perturbation density of the fluid that depends on both streamwise and spanwise coordinates x, y and vertical coordinate z as well as time t. In the Cartesian frame with the fluid in the half space $z > 0$ and with x and y directed streamwise and spanwise, respectively, the equations take the form,

$$\rho_0[D_t u + wU'] + p_x = -\bar{\rho}[D_t u + wU'] - \rho_0(\boldsymbol{u}\cdot\nabla)u - \bar{\rho}(\boldsymbol{u}\cdot\nabla)u + \nu\nabla^2 u \tag{4.2a}$$

$$\rho_0 D_t v + p_y = -\bar{\rho} D_t v - \rho_0(\boldsymbol{u}\cdot\nabla)v - \bar{\rho}(\boldsymbol{u}\cdot\nabla)v + \nu\nabla^2 v \tag{4.2b}$$

$$\rho_0 D_t w + p_z + \bar{\rho}g = -\bar{\rho} D_t w - \rho_0(\boldsymbol{u}\cdot\nabla)w - \bar{\rho}(\boldsymbol{u}\cdot\nabla)w + \nu\nabla^2 w \tag{4.2c}$$

$$D_t\bar{\rho} + w\rho_0' = K\nabla^2\bar{\rho} - (\boldsymbol{u}\nabla)\bar{\rho} \tag{4.2d}$$

$$\nabla\cdot\boldsymbol{u} = 0. \tag{4.2e}$$

where $\boldsymbol{U} = (U(z), 0, 0)$ is the basic flow, $\boldsymbol{u} = (\boldsymbol{q}, w) = (u, v, w)$ and p are, respectively, the velocity and pressure perturbations, $D_t = \partial_t + U\partial_x$ is the material derivative. ρ_0 is the equilibrium density in equation (4.2), $\bar{\rho}$ is perturbation density. The notation $\nabla^2 = \partial^2_{xx} + \partial^2_{yy} + \partial^2_{zz}$ stands for the three-dimensional Laplacian operator. The gravitational acceleration g is a constant, ν is the fluid viscosity, while K is the mass diffusivity coefficient, which is the driving force for diffusion.

The prime denotes the derivatives with respect to z. We impose no particular restrictions on $\boldsymbol{U}(z)$ apart from the assumption that the flow is plane parallel (in this work we exclude consideration of non-parallel effects and three-dimensional boundary layers). In contrast to the original derivations in (Shrira [1989], Voronovich et al. [1998]), we do not require the profile $U(z)$ to have no inflection points. The boundary conditions for the perturbations $\boldsymbol{u}$ at $z = 0$ are of two main types:

1. The "no-flux" ("rigid lid") conditions typical of environmental flows,

$$w(z=0)=0, \tag{4.3}$$

complemented by the constant stress condition

$$u'(z=0)=v'(z=0)=0. \tag{4.4}$$

2. The more common "no-slip" conditions imply

$$\boldsymbol{u}(z=0)=0. \tag{4.5}$$

The boundary condition at infinity is that of vanishing perturbation velocity, it is the same for both types of the boundary layers

$$\boldsymbol{u}\to 0, \quad \text{as} \quad z\to\infty. \tag{4.6}$$

We complete the formulation of our initial problem by specifying the perturbation velocity field at the initial moment, $\boldsymbol{u}(\boldsymbol{x},0)$. We are primarily interested in localised initial perturbations

$$\boldsymbol{u}(\boldsymbol{x},0)\to 0, \quad \text{as} \quad x,y\to\infty. \tag{4.7}$$

The Navier-Stokes equations (4.2) with the initial and boundary conditions (4.5, 4.6) or (4.3, 4.4, 4.6) differing only in the boundary condition at the surface $z=0$ constitute the mathematical formulation of the problem.

The conventions for the "no-slip" and "no-flux" boundaries differ. Usually, for the no-flux case the maximum of $U(z)$ is at the surface $z=0$ with $U(z)$ vanishing as $z\to\infty$, while for the no-slip case, U is vanishing at $z=0$ and tends to a finite "free stream velocity" U_∞ as $z\to\infty$. Mathematically these conventions are equally legitimate, one can switch from one to another by a galilean transformation, as is illustrated by figure (4.1). We assume the boundary layer profile $U(z)$ to be given, but do not specify it until an illustrative example is needed.

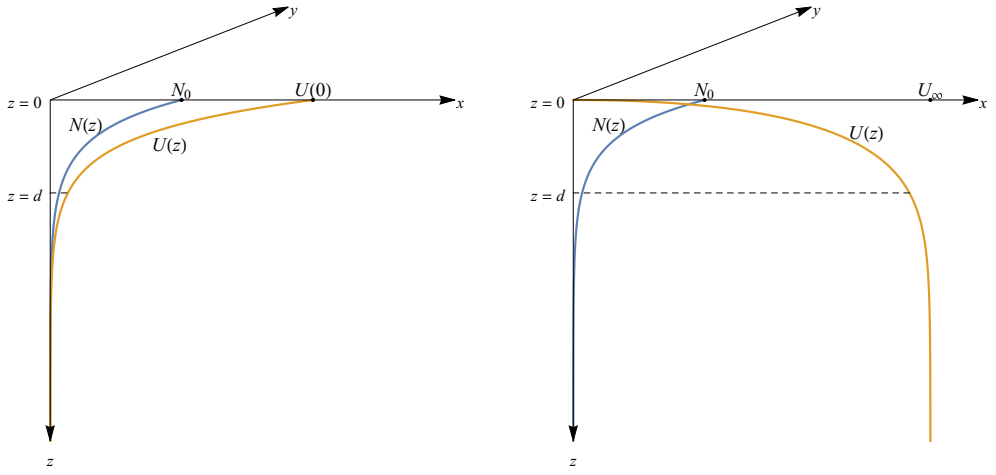

FIGURE 4.1: Sketch of geometry of a generic boundary layer profile with the shear and stratification localised in a thin layer of thickness d. (a) A typical free surface boundary layer with the maximum of velocity is attained at the surface $U_{max} = U(0)$. (b) Sketch of a boundary layer with a no-slip boundary. U_∞ is the free stream velocity. N_0 is a typical value of the buoyancy frequency taken at the boundary

4.2.2 Scaling

We begin by specifying the scaling. The basic flow $U(z)$ has a characteristic velocity we denote as V_0. N_0 is a typical value of the buoyancy frequency taken at the boundary. For the no-flux/constant stress boundary layers we choose it as the speed at the boundary $U(0)$, while for the no-slip case the natural choice for V_0 is U_∞. The characteristic streamwise and spanwise scales of perturbations we denote as L, while as the cross-boundary scale we choose the boundary layer thickness d. Here we are considering long perturbations with $L \gg d$. We non-dimensionalise the dependent variables as follows:

$$\tilde{u} = \frac{u}{V_0}, \quad \tilde{v} = \frac{v}{V_0}, \quad \tilde{w} = \frac{w}{V_0}, \quad \tilde{x} = \frac{x}{L}, \quad \tilde{y} = \frac{y}{L}, \quad \tilde{z} = \frac{z}{d}, \quad \tilde{U} = \frac{U}{V_0}, \quad \tilde{t} = \frac{V_0}{L}t,$$

$$\tilde{N} = \frac{N}{N_0}, \quad \tilde{p} = \frac{p}{\rho_0 V_0^2}, \quad \tilde{\rho} = \frac{\rho}{\rho_0}. \tag{4.8}$$

where quantities with tildes denote non-dimensional variables. To proceed, we first estimate the magnitudes of the perturbation from the basic governing equations ((4.2)). To this end we first write the incompressibility equation in non-dimensional form

omitting the tildes. Then the magnitude of the vertical velocity perturbation $[\,w\,]$ expressed in terms of the magnitudes of the horizontal components $[\,\mathrm{q}\,]$,

$$[\,w\,] = \frac{d}{L}[\,q\,]. \tag{4.9}$$

The momentum equation (4.2a) yields the characteristic time scale,

$$[\,t\,] = \frac{L}{V_0}. \tag{4.10}$$

Next we multiply mass conservation equation (4.2d) by gravitational acceleration g and divide by the reference density ρ_0, and substitute $N^2 = -\frac{g}{\rho_0}\frac{\partial \rho_0}{\partial z}$ for buoyancy frequency using Boussinesq approximation to get the expression below,

$$g\,D_t\left(\frac{\bar{\rho}}{\rho_0}\right) - w\,N^2(z) = g\frac{K}{\rho_0}\nabla^2\bar{\rho} - \frac{g}{\rho_0}\,(\mathbf{u}\nabla)\bar{\rho}, \tag{4.11}$$

To proceed we express (4.11) in dimensionless form and substitute equation (4.9) and (4.10), re-arrange to get the expression of typical density perturbation magnitude

$$\left[\frac{\bar{\rho}}{\rho_0}\right] = \frac{N_0^2 d}{g}\frac{[\,q\,]}{V_0}, \tag{4.12}$$

In the derivation, we will employ the Boussinesq approximation, whereby, if not multiplied by g, the terms in the equations due to the equilibrium density ρ_0 variations are negligibly small. This approximation is valid in oceanic and atmospheric applications where density variations are small. The Boussinesq approximation holds under the assumptions

$$\frac{N_0^2}{g/d} \ll \frac{[\,q\,]}{V_0}, \tag{4.13}$$

This condition allows us to drop small nonlinear buoyancy terms. Stratification is considered to be localised in the boundary layer. The viscosity is small but finite, it is supposed to affect, but not to dominate, the dynamics of perturbations of chosen

scales inside the boundary layer at the timescale comparable to that of nonlinear effects.

After some algebra, upon eliminating pressure from the equations (4.2), we get a single nonlinear equation for the vertical velocity perturbation w,

$$D_t^2\,\partial_{zz}^2\,w - U''\,D_t\,\partial_x w = \mathcal{N} - \left(\frac{N_0\,d}{V_0}\right)^2 N^2\nabla_\perp^2 w + \left(\frac{d}{L}\,Re\right)^{-1} D_t\,\partial_{zzzz}^4 w + \mathcal{M}. \quad (4.14)$$

where the horizontal gradient operators $\nabla_\perp = (\partial_x, \partial_y)$ and $\nabla_\perp^2 = \partial_{xx}^2 + \partial_{yy}^2$ while,

$$\mathcal{N} = \frac{[\,q\,]}{V_0}\,D_t\,\partial_z\,\nabla_\perp[(\boldsymbol{u}\nabla)\boldsymbol{q}] - \left(\frac{d}{L}\right)^2 D_t^2\,\nabla_\perp^2 w - \left(\frac{d}{L}\right)^2 \frac{[\,q\,]}{V_0}\,D_t\nabla_\perp^2(\boldsymbol{u}\nabla)w,$$

$$\mathcal{M} = \left(\frac{N_0\,d}{V_0}\right)^2 \frac{[\,q\,]}{V_0}\nabla_\perp^2(\boldsymbol{u}\nabla)\bar{\rho} + Sc\left(\frac{N_0\,d}{V_0}\right)^2 \frac{[\,q\,]}{V_0}\nabla_\perp^2\bar{\rho}'', \quad Re = \frac{\rho_0 V_0 d}{\nu},$$

The dimensionless parameter, Sc is the Schmidt number defined as the ratio of the kinematic viscosity and mass diffusivity,

$$Sc = \frac{K}{V_0\,d},$$

For more detailed derivation of equation (4.14) refer to Appendix **??**. Note, that the equation is closed only in the linear approximation and just the leading order viscous term and the leading order density diffusion term are retained. We re-iterate here that the diffusion of density (mass) contribution with a dimensionless number $Sc \sim O(1)$ as the coefficient, will be shown to be negligible in our asymptotic analysis since density is a 'passive scaler'. It will be dropped after the specification of small parameters. This will enable us to justify why the two terms of equation (4.14) denoted by $\mathcal{M}$ are negligibly small in our analysis.

Thus, in the most general formulation of the problem, there are four independent non-dimensional parameters specifying respectively the smallness of nonlinearity ($[\,q\,]/V_0 = \varepsilon \ll 1$, dispersion ($d/L = \varepsilon_D \ll 1$), stratification ($\sqrt{\varepsilon_b} = \frac{N_0\,d}{V_0} \ll 1$) and dissipative effects ($Re^{-1} \ll 1$). Aiming to describe dynamics of three-dimensional perturbations in the boundary layer taking into account nonlinearity, dispersion, stratification and

viscous effects in the distinguished limit we set

$$\varepsilon = \frac{[\,q\,]}{V_0} \ll 1, \quad \varepsilon_D = \frac{d}{L} = O(\varepsilon), \quad \sqrt{\varepsilon_b} = \frac{N_0\, d}{V_0} \ll 1, \quad Re^{-1} \sim \frac{d}{L}\frac{[\,q\,]}{V_0} = O(\varepsilon^2). \tag{4.15}$$

This key assumption enables us to proceed with deriving the evolution equation employing an asymptotic expansion in terms of the single small parameter ε and uniquely determines the scaling of dependent variables in the boundary layer.

4.2.3 Asymptotic expansion

To rationalise the specific choice of the asymptotic expansion in powers of ε we will adopt, we use the scales derived in the previous Chapter 2 of the thesis for pressure p, streamwise and spanwise velocities u, v, vertical velocity w (see Eqs. (2.13)) and in addition derive the scaling of density from the linearised inviscid reduction of the Navier-Stokes equation. First, it is straightforward to express perturbation density in terms of vertical velocity w from the linearised equation (4.11) according to,

$$gD_t\left(\frac{\bar\rho}{\rho_0}\right) = N^2 w, \implies g(U-c)\partial_x\bar\rho = \underbrace{\rho_0}_{O(1)}\underbrace{N^2 w}_{O(\varepsilon^3)}, \quad \bar\rho \sim O(\varepsilon^2). \tag{4.16}$$

Therefore, we adopt the following asymptotic expansion,

$$u = U(z) + \varepsilon u_1 + \varepsilon^2 u_2 + \varepsilon^3 u_3 + \ldots \tag{4.17a}$$

$$w = \varepsilon^2 w_2 + \varepsilon^3 w_3 + \varepsilon^4 w_4 + \ldots \tag{4.17b}$$

$$v = \varepsilon^3 v_3 + \varepsilon^4 v_4 + \ldots \tag{4.17c}$$

$$p = \varepsilon^3 p_3 + \varepsilon^4 p_4 + \ldots \tag{4.17d}$$

$$\bar\rho = \varepsilon^2 \bar\rho_2 + \varepsilon^3 \bar\rho_3 + \ldots \tag{4.17e}$$

where u_i, v_i, w_i, p_i and $\bar\rho_i$ are $O(1)$ functions of x, y, z, t.

The scaling (4.17) will be employed inside the boundary layer, outside the boundary layer and in the immediate vicinity of the boundary, in the viscous sub-layer, the scaling is different and will be specified in the next section.

4.3 Derivation of the nonlinear evolution equation

In this section we derive the nonlinear evolution equation for longwave three-dimensional perturbations employing 'triple deck' asymptotic approach (see e.g., Ruban [2017] , Sobey [2000]). As is common for this approach, we distinguish three domains in z, often called decks, with different balance between the terms in (4.14). The domains are sketched in figure (2.3) [see Chapter 2 for detail]. In contrast to the triple deck convention we do not scale our variable in terms of powers of inverse Reynolds number, in our context we prefer to use the scaling in powers of ε. The derivation largely follows that in (Shrira [1989], and Voronovich et al. [1998]), with three major differences:

1. The presence of weak stratification in the boundary layer (main deck) is taken into account;
2. The case of the 'no-slip' boundary conditions is incorporated into consideration;
3. No assumption regarding the absence of inflection points is required.

We begin with analysis of the motion in the main deck.

4.3.1 Inside the boundary layer. The main deck

The scaling ((4.17)) based upon the distinguished limit which balances nonlinearity, weak dispersion, stratification and viscosity, provides the basis of our asymptotic analysis inside the main deck. On substituting the already adopted relations between the small parameters $\varepsilon_D = \varepsilon_b = \varepsilon$ and introducing re-scaled Reynolds number denoted

as Re_*, $Re_* = \varepsilon^2 Re$, into equation (4.14), we make the scaling of each term more explicit,

$$D_t^2\,\partial_{zz}^2\,w - U''\,D_t\,\partial_x w = \varepsilon\,D_t\,\partial_z\,\mathcal{N}_L - \varepsilon N^2\nabla_\perp^2 w + \frac{\varepsilon}{Re}\,D_t w^{iv} - \varepsilon^2 D_t^2\,\nabla_\perp^2 w + \mathcal{M}_1, \quad (4.18)$$

where $\nabla_\perp = (\partial_x,\, \partial_y)$, $w^{iv} \equiv \partial^4_{zzzz} w$,

$$\mathcal{M}_1 = \varepsilon^2\nabla_\perp^2(\boldsymbol{u}\nabla)\bar{\rho} + \varepsilon^2 Sc\,\nabla_\perp^2\bar{\rho}'' - \varepsilon^3\,D_t\nabla_\perp^2(\boldsymbol{u}\nabla)w,$$

and,

$$\mathcal{N}_L = [\partial_x(u\partial_x u + v\partial_y u + w\partial_z u) + \partial_y(u\partial_x v + v\partial_y v + w\partial_z v)],$$

$$= [\varepsilon\partial_x(\varepsilon^3 u\partial_x u + \varepsilon^5 v\partial_y u + \varepsilon^3 w\partial_z u) + \varepsilon\partial_y(\varepsilon^5 u\partial_x v + \varepsilon^7 v\partial_y v + \varepsilon^5 w\partial_z v)]$$

$$= \varepsilon^4[\partial_x(u\partial_x u + w\partial_z u)] + \varepsilon^6[\partial_x(v\partial_y u) + \partial_y(u\partial_x v + w\partial_z v + \varepsilon^2 v\partial_y v)].$$

Although the streamwise and spanwise scales are assumed to be comparable, according to ((4.17)) the spanwise velocity is two orders of magnitude smaller, which enables us to split the nonlinear term $\mathcal{N}_L$ into three parts and neglect the $O(\varepsilon^6)$, $O(\varepsilon^7)$ and $O(\varepsilon^8)$ terms. The extra small terms $\varepsilon^2\nabla_\perp^2(\boldsymbol{u}\nabla)\bar{\rho}$, $\varepsilon^2 Sc\,\nabla_\perp^2\bar{\rho}''$ and $\varepsilon^3\,D_t\nabla_\perp^2((\boldsymbol{u}\nabla)w)$, on the right-hand-side of (4.18) corresponds to $O(\varepsilon^7)$ and above will also be neglected in our further analysis. Upon these simplifications, recalling that $w = O(\varepsilon^2)$, we re-write equation (4.18) explicitly pulling out ε,

$$\underbrace{D_t^2\,\partial_{zz}^2\,w - U''\,D_t\,\partial_x w}_{\text{terms of } O(\varepsilon^4)} = \varepsilon^5\,D_t\,\partial_z\,\partial_x[u\partial_x u + w\partial_z u] - \varepsilon^5 N^2\nabla_\perp^2 w + \ldots$$

$$+ \frac{\varepsilon^5}{Re}\,D_t w^{iv} - \varepsilon^6 D_t^2\,\nabla_\perp^2 w. \quad (4.19)$$

Since $v = O(\varepsilon^3)$ and $u = O(\varepsilon^1)$, it is easy to see that by virtue of the continuity equation: $\partial_x u = -\partial_z w + O(\varepsilon^4)$. To solve equation (4.19) we adopt a moving coordinate frame and use standard multiple-scale method by introducing fast and slow non-dimensional independent variables,

$$Z_1 = \varepsilon\tilde{z} = \frac{1}{L}z, \qquad \tau = \varepsilon\frac{V_0}{L}t, \qquad \tilde{x} = \frac{x-ct}{L}, \qquad \tilde{y} = \frac{y}{L}, \quad \tilde{z} = \frac{z}{d}, \qquad \tilde{c} = \frac{c}{V_0} \tag{4.20}$$

where c is the speed of the long waves which will be specified later and the tildes denote non-dimensional quantities. Upon the introduction of the slow-spatial variable Z_1 and slow time τ, it is easy to see that the material derivative D_t^2 and ∂_{zz}^2 in terms of the tilde variables takes the form,

$$D_t^2 = \frac{V_0^2}{L^2}[(\tilde{U}-\tilde{c})\partial_{\tilde{x}}+\varepsilon\partial_\tau]^2 = \frac{V_0^2}{L^2}\tilde{D}_t^2 \sim \varepsilon^2\tilde{D}_t^2, \qquad \partial_{zz}^2 = \frac{1}{d^2}(\partial_{\tilde{z}}+\varepsilon\partial_{Z_1})^2 = \frac{1}{d^2}\partial_{\tilde{z}\tilde{z}}^2 \sim \partial_{\tilde{z}\tilde{z}}^2,$$

From this moment we operate only with non-dimensional variables and omit tildes. The equation for the $z-$ component of velocity w (4.19) reduces to

$$D_t^2\partial_{zz}^2 w - U''D_t\partial_x w = \varepsilon D_t\partial_z\partial_x[u\partial_x u + w\partial_z u] - \varepsilon N^2\nabla_\perp^2 w + \frac{\varepsilon}{Re}D_t w'''' - \varepsilon^2 D_t^2\nabla_\perp^2 w, \tag{4.21}$$

where

$$D_t = (U-c)\partial_x + \varepsilon\partial_\tau, \qquad \partial_z = \partial_z + \varepsilon\partial_{Z_1}. \tag{4.22}$$

We assume the mean flow $U(z)$ and stratification $N(z)$ to be entirely localised in the boundary layer and, correspondingly, to depend only on the fast scale z. The situations with U, N having also dependence on the slow scale can be easily incorporated into the scheme, but are not considered here.

Here, for the time being, for both the free-surface-type flows with the no-flux boundary conditions and the flows with the no-slip conditions we impose the no-flux condition at $z = 0$. We will deal with the true boundary conditions at the boundary in section §4.3.3. We also require vanishing of velocity as $Z_1 \to \infty$. In addition, we introduce 'inner boundary conditions', the condition of matching at the outer boundary of the boundary layer. Thus,

$$w(z=0) = 0; \qquad w(z\to\infty) = const = w(Z_1 \to 0), \qquad w(Z_1 \to \infty) \to 0. \tag{4.23}$$

We will seek an asymptotic solution to the boundary value problem (4.21), (4.22)

and (4.23) employing power series in ε (4.17). On finding the solution to (4.21) for w at a certain order in ε, we find u, v and p with the corresponding accuracy from the basic equations,

$$D_t u + wU' + p_x = -\varepsilon(\boldsymbol{u}\cdot\nabla)u + \frac{\varepsilon}{Re}u'' \tag{4.24a}$$

$$D_t v + p_y = -\varepsilon(\boldsymbol{u}\cdot\nabla)v + \frac{\varepsilon}{Re}v'' \tag{4.24b}$$

$$gD_t\left(\frac{\bar\rho}{\rho_0}\right) = N^2 w + g\frac{K}{\rho_0}\nabla^2\bar\rho - \frac{g}{\rho_0}(\mathbf{u}\nabla)\bar\rho \tag{4.24c}$$

$$\partial_x u + \partial_y v + \partial_z w = 0 \tag{4.24d}$$

It is important to re-iterate here, that from the density equation (4.24c) the variations of $\bar\rho$ feels the effect of velocity w but its leading order term containing buoyancy N^2 only enters the equation for the velocity field w given by equation (4.21), while the terms containing derivative and horizontal gradients of $\bar\rho$ drops out. Therefore $\bar\rho$ is a "passive scalar". It is one of the key simplifications: the equation for $\bar\rho$ splits out. The solutions for u, v and p, accurate to a corresponding order in ε, are further used for the derivation of the next order terms for w, the cycle is repeated as many times as necessary. At the first step we get the following. On substituting (4.17) into equation (4.21) and setting $\varepsilon = 0$, we see that in the leading order nonlinearity, buoyancy/stratification, and viscous dissipation drop out. Taking into account (4.22) we obtain for w_2 the longwave limit of the Rayleigh equation,

$$(U-c)\partial_{xx}[(U-c)w_2'' - U''w_2] = 0, \tag{4.25}$$

where derivative with respect to the fast variable z are denoted by primes. It can be easily seen from (4.25) that the x and z dependencies can be separated. Assuming that the disturbance to be localized in the streamwise direction, similar to the Section 2 the general solution to equation (4.25) is convenient to present in the form,

$$w_2 = (f(x,y,Z_1) * \partial_x A(x,y,\tau))\cdot(U(z)-c), \tag{4.26}$$

where $*$ designates the convolution of two functions

$$\varphi * \psi = \int_{-\infty}^{+\infty} \int_{-\infty}^{+\infty} \varphi(\hat{x}, \hat{y}) \psi(x - \hat{x}, y - \hat{y}) \mathrm{d}\hat{x} \mathrm{d}\hat{y}.$$

The analysis follows the same line as in chapter 2 of this thesis (see section 2.3.2). Here, as it will be made explicit at the next step a few lines below, $A(x, y, \tau)$ is the amplitude of the x-component of velocity perturbation, while the arbitrary function $f(x, y, Z_1)$ in (4.26) is the general representation of a function of (x, y, Z_1, τ) localized or periodic in (x, y). The fundamental properties of the presentation (4.26) become more transparent on making Fourier transform of the solution (4.26). The standard way of representing a function of (x, y, Z_1, τ) is to decompose it into a set of spatial orthogonal functions with time-dependent amplitudes. We chose Fourier in (x, y) and a particular function f specifying each Fourier mode that depends on the slow cross-boundary spatial variable Z_1. The specific dependence on the slow spatial scale $f(Z_1)$ will be found below.

The boundary condition $w_2(z = 0) = 0$ specifies the eigenvalue c,

$$c = U|_{z=0}. \tag{4.27}$$

The mode we are considering is to leading order a vorticity wave, modified in the next orders by stratification and viscosity. To leading order its speed is the mean flow velocity at $z = 0$, which is its maximal value for the typical 'no-flux, constant stress' flows and zero for the no-slip ones. In any case, it plays no role in our further analysis since its only significance is in specifying the reference frame, it will be removed by the galilean transformation at the next step. The slow function $f(Z_1)$ will be specified later.

To proceed further, we first find the other components of perturbation wave field from equation (4.24) taking into account the asymptotic expansion of (4.17),

Substituting the leading order solution for w_2 into (4.24) we get the other components of the perturbation field,

$$u_1 = -U'(f * A), \tag{4.28a}$$

$$v_2 = 0, \tag{4.28b}$$

$$p_2 = 0. \tag{4.28c}$$

Note that (4.28a) clarifies the physical sense of amplitude A, it is indeed, up to a factor $-U'$, amplitude of the x-component of perturbation velocity. The above relations show that to leading order the motion is extremely simple: the particles of the vorticity wave motion oscillate, mainly, in the streamwise direction, while the cross-boundary and, especially, spanwise velocities and pressure perturbations are much smaller in the adopted long-wave approximation. This extraordinary feature is specific for long vorticity waves (see Voronovich et al. [1998]). Such a simplicity of the motion of interest in the leading order is the key element enabling for a remarkably simple description of nonlinear dynamics of vorticity waves which we will discuss below.

Substituting into (4.21) the expressions (4.26) for w_2 and (4.28a) for u_1 we get an equation for w_3,

$$w_3'' - \frac{U''}{U-c} w_3 = -M\,\frac{U''}{U-c} + \frac{P}{Re}\,\frac{U''''}{U-c} - Q\,\tilde{k}^2\,\frac{N^2(z)}{U-c} - T\,\frac{[(U-c)^2]'}{U-c} + R\,\frac{[(U')^2 - (U-c)U'']'}{U-c}, \tag{4.29}$$

where,

$$M = (f * A_\tau), \qquad P = (f * A), \qquad Q = (f * A_x), \qquad T = (f_{Z_1} * A_x),$$

$$R = (f * A)(f * A_x), \qquad \tilde{k}^2 = \frac{k_x^2 + k_y^2}{k_x^2} \tag{4.30}$$

The subscripts x and τ stand for the corresponding derivatives. The buoyancy frequency $N^2(z)$ is localised in the boundary layer. The specific dependence $N^2(z)$ is arbitrary, the only requirement is

$$N^2(z) \to 0, \quad \text{as} \qquad z \to \infty. \tag{4.31}$$

while at the boundary if $z = 0$ the buoyancy frequency $N(z = 0) = N_0$ is maximum. The general solution to equation (4.29) can be written as,

$$w_3 = M - T(U-c)\int_z^\infty \mathrm{d}\xi + B(U-c)\int_z^\infty \frac{\mathrm{d}\xi}{(U-c)^2} + \frac{P}{Re}(U-c)\int_z^\infty \left[\frac{U'''}{(U-c)^2}\right]\mathrm{d}\xi - Q\,\tilde{k}^2\,(U-c)\int_z^\infty \left[\frac{S(\xi)}{(U-c)^2}\right]\mathrm{d}\xi - RU'. \tag{4.32}$$

where ξ is a dummy variable of integration while the integral $S(z)$ yields the contribution from stratification,

$$S(z) = \int_z^\infty N^2(z)\mathrm{d}\xi. \tag{4.33}$$

B is an arbitrary constant specifying the "amplitude" of the second homogeneous solution to the Rayleigh equation in the longwave limit. To eliminate singularity in the integrals in (4.32), we chose B in such a way that the equation for w_3 takes the form,

$$w_3 = M - T\,(U-c)\int_z^\infty [1 - Y(U-c)^{-2}]\mathrm{d}\xi + \frac{P}{Re}\,(U-c)\int_z^\infty \left[\frac{U'''}{(U-c)^2}\right]\mathrm{d}\xi ... - Q\,\tilde{k}^2\,(U-c)\int_z^\infty \left[\frac{S(z)}{(U-c)^2}\right]\mathrm{d}\xi - R\,U' \tag{4.34}$$

where integration constant Y has been chosen to be the same for both types of the boundary conditions. For the no-slip boundary $U(0) = 0$, it is chosen as,

$$Y = \lim_{z\to 0}(U-c)^2 = c^2 = U^2|_{z=\infty} = U_\infty^2 = U_0^2, \qquad N(z)|_{z\to\infty} = 0, \tag{4.35}$$

where $U_\infty = U_0$ is free stream velocity for the "no-slip" boundary.

For free surface or "no-flux" boundary the constant is chosen as,

$$Y = \lim_{z\to\infty}(U-c)^2 = c^2 = U_0^2. \tag{4.36}$$

Next we proceed with the derivation of the evolution equation valid for both "no-slip" and "no-flux" boundaries. To evaluate the singular integrals above in (4.34) we assume that near the boundary $z = 0$ we can expand $U - c$ as $U'(0)z = U_0'z$ and $U''' \approx U'''(0) \neq 0$. It is important to note that for Blasius flow profiles the third derivative of the mean flow taken at the surface vanishes, i.e. $U'''(0) = 0$, but for pressure driven flows described by Falkner-Skan profiles we obtain a nonzero constant [see e.g Schlichting and Gersten [2016]]. Upon applying the condition at the boundary, $w|_{z=0,Z_1=0} = 0$, to equation (4.34), after some algebra, we get an equation for the amplitude A containing so far unspecified function $f(Z_1)$ of the slow cross-boundary variable Z_1,

$$\begin{aligned}(f(0) * A_\tau) - U'(0)\left(\Big(f(0) * A\Big)\Big(f(0) * A_x\Big)\right) + \left(\frac{U_0^2}{U'(0)}\right)\Big(f_{Z_1}(0) * A_x\Big)\ldots \\ - \tilde{k}^2\left(\frac{N_0^2\, d}{2\,U'(0)}\right)\Big(f(0) * A_x\Big) + \frac{1}{Re}\left(\frac{U'''(0)}{U'(0)}\right)\Big(f(0) * A\Big) = 0\end{aligned} \tag{4.37}$$

where $f(0) \equiv f(x, y, Z_1 = 0)$.

4.3.2 The outer flow

To specify the dependence of the solution (4.26) and (4.34) on the slow variable Z_1, first we need to proceed to the next order in ε in equation (4.21) for w_2. The procedure is nearly identical to that of Chapter 2. Following the same asymptotic procedure and using (4.26) and (4.34) we express u, v, p in terms of amplitude A,

$$u_2 = -Y(f_{Z_1} * \nabla_\perp^{-2} A_{xx})(U-c)^{-1} + (f_{Z_1} * A)U' \int_z^\infty \Big[1 - Y(U-c)^{-2}\Big]\mathrm{d}\xi$$

$$+\frac{1}{2}(f*A)^2U''+\hat{G}_2[P]\frac{S(z)}{U-c}+\hat{G}_2[P]U'\int_z^\infty\left(\frac{S(z)}{(U-c)^2}\right)\mathrm{d}\xi$$

$$-\frac{\bar{P}U'}{Re}\int_z^\infty\left(\frac{U'''}{(U-c)^2}\right)\mathrm{d}\xi-\frac{\bar{P}}{Re}\frac{U'''}{(U-c)}, \tag{4.38}$$

$$v_3=-Y(f_{Z_1}*\nabla_\perp^{-2}A_{xy})(U-c)^{-1}+\hat{G}_3[(f*A)]\,S(z)\,(U-c)^{-1}, \tag{4.39}$$

$$p_3=Y\,(f_{Z_1}*\nabla_\perp^{-2}A_{xx})-\hat{G}_2[(f*A)]\,S(z), \tag{4.40}$$

where $\hat{G}_2$ and $\hat{G}_3$ are integral operators, while $\bar{P}=(f*\partial_x^{-1}A)$. In Fourier space the integral operator $\hat{G}_2=\tilde{k}^2$ and $\hat{G}_3=\hat{k}\tilde{k}^2$, where, $\hat{k}=\frac{k_y}{k_x}$, P,Y,$\tilde{k}^2$ and $S(z)$ are given by the expressions (4.30) and (4.33).

Now consider the next order term for the cross-boundary velocity, w_4. After some algebra it can be brought to the form,

$$\partial_x[(U-c)w_4''-U''w_4]=-(f_{Z_1Z_1}*A_{xx})(U-c)^2 \\ -(f*\nabla_\perp^2A_{xx})(U-c)^2+F(x,y,\tau,z,Z_1), \tag{4.41}$$

where $F(x,y,\tau,z,Z_1)$ given by a bulky expression tends to zero faster as $z\to\infty$ than $|z|^{-1}$. In contrast, for an arbitrary function of $f(x,y,Z_1)$ the first two terms on the right-hand side of equation (4.41) do not tend to zero as $z\to\infty$. As a result, the integration of (4.41) yields secular growth of the correction w_4 as $z\to\infty$, which does not allow the matching condition $w(z\to\infty,Z_1)\to$ const to be satisfied. We put these secular terms to zero, which gives us an equation determining the dependence of the unspecified yet function f on the slow variable Z_1,

$$(f_{Z_1Z_1}*A_{xx})+(f*\nabla_\perp^2A_{xx})=0. \tag{4.42}$$

The equation is complemented by the boundary condition at infinity

$$w(Z_1 \to \infty) = 0. \tag{4.43}$$

To find $f(Z_1)$ we perform the Fourier transform with respect to x, y in the boundary problem (4.42) and (4.43). Making the Fourier transform of the convolution and omitting the amplitude A, we get the boundary value problem,

$$\partial^2_{Z_1 Z_1} \hat{f}(\boldsymbol{k}) - k^2 \hat{f}(\boldsymbol{k}) = 0, \tag{4.44}$$

with the boundary conditions,

$$\hat{f}(\boldsymbol{k})|_{Z_1 \to \infty} = 0, \quad \hat{f}(\boldsymbol{k})|_{Z_1 = 0} = 1. \tag{4.45}$$

Here $\hat{f}(\boldsymbol{k}, Z_1)$ is the Fourier transform of $f(x, y, Z_1)$

$$f(x, y, Z_1) = \frac{1}{4\pi^2} \int_{-\infty}^{+\infty} \int_{-\infty}^{+\infty} \hat{f}(k_x, k_y, Z_1) e^{(i(k_x x + k_y y))} \mathrm{d}k_x \mathrm{d}k_y, \tag{4.46}$$

and $k = |\boldsymbol{k}|$, $k^2 = k_x^2 + k_y^2$. The boundary condition $\hat{f}(\boldsymbol{k})|_{Z_1=0} = 1$ has been introduced for convenience to normalize the motion in the outer deck $\hat{f}(k_x, k_y, Z_1)$ near the boundary. As one could anticipate, the motion in the outer layer is potential and satisfies the Laplace equation (4.44). Hence, the boundary value problem (4.44), (4.45) is easily solvable. Its solution satisfying the boundary condition (4.45) has the form

$$\hat{f}(\boldsymbol{k}, Z_1) = e^{-kZ_1} \qquad Z_1 \to \infty. \tag{4.47}$$

Next we designate $\partial_{Z_1} \hat{f}(\boldsymbol{k}, 0) \equiv Q(k_x, k_y)$ and take into account that at the boundary $\hat{f}(0) = \delta(x)\delta(y)$. The solution to equation (4.44) readily yields the kernel of the integral operator $Q(k) = -k$ in the long wave limit. Substituting these notations into (4.37), we obtain nonlinear evolution equation for the amplitude of three-dimensional long-wave boundary layer perturbations in the distinguished limit,

$$A_\tau - \alpha_1 A A_x - \beta_1 \hat{G}_1[A_x] - \beta_2 \hat{G}_2[A_x] + \gamma A = 0 \tag{4.48}$$

where $\alpha_1 = U'(0)$, $\beta_1 = \frac{U_0^2}{U'(0)}$, $\gamma = \frac{1}{Re}\frac{U'''(0)}{U'(0)}, \beta_2 = \frac{N_0^2\, d}{2\, U_0'}$, and the dispersion operators $\hat{G}_1$ and $\hat{G}_2$ in the integral form reads

$$\hat{G}_1[\varphi(\boldsymbol{k})] = \frac{1}{4\pi^2}\int_{-\infty}^{+\infty}\int_{-\infty}^{+\infty} |\boldsymbol{k}|\varphi(\boldsymbol{r}_1)e^{(i\boldsymbol{k}(\boldsymbol{r}-\boldsymbol{r}_1))}\mathrm{d}\boldsymbol{k}\mathrm{d}\boldsymbol{r}_1, \tag{4.49}$$

$$\hat{G}_2[\psi(\mathbf{k})] = \frac{1}{4\pi^2}\int_{-\infty}^{+\infty}\int_{-\infty}^{+\infty} \frac{k^2}{k_x^2}\psi(\mathbf{r}_1)e^{(i\mathbf{k}(\mathbf{r}-\mathbf{r}_1))}\mathrm{d}\mathbf{k}\mathrm{d}\mathbf{r}_1 \tag{4.50}$$

where, $k = |\boldsymbol{k}| = \sqrt{k_x^2 + k_y^2}$ and $k^2 = k_x^2 + k_y^2$. The explicit account of viscous dissipation and weak stratification yields both the Rayleigh friction type term and a second dispersion term of buoyancy effect in the evolution equation. Coefficients α_1 and β_1 of (4.48) can be removed by rescaling in the next section to obtain the final evolution equation that will form the framework of our study.

4.3.3 Viscous sub-layer

4.3.3.1 Divergence of the asymptotic expansion and Tollmien's rescaling

Consider more closely behaviour of the main deck solutions u_2 and v_3 of (4.38) and (4.39) as $z \to 0$. Near the boundary as $z \to 0$, we apply Taylor series to expand $(U - c) \approx U'(0)\, z$ to obtain,

$$u_2 = -\frac{U_{max}^2}{U'(0)}(f_{Z_1} * \nabla_\perp^{-2} A_{xx})\frac{1}{z} + \frac{U_{max}^2}{U'(0)}(f_{Z_1} * A)\frac{1}{z} + \frac{1}{2}(f * A)^2 U''(0), \tag{4.51}$$

$$v_3 = -\frac{U_{max}^2}{U'(0)}(f_{Z_1} * \nabla_\perp^{-2} A_{xy})\frac{1}{z} + \hat{G}_3(f * A)\frac{N_0^2\, d}{2U_0'}\frac{1}{z}, \tag{4.52}$$

First it is important to note that the last four terms due to stratification and viscosity of equation (4.38) all cancel each other, hence we recover the same form of the singular streamwise perturbation velocity equation (2.43) of the homogeneous case as $z \to 0$ obtained in Chapter 2. In contrast to the streamwise perturbation velocity u_2, the spanwise component yields a new extra singular term due to stratification N_0.

On substituting the simplified form of the singular terms of equation 4.51 (the same form of simplification as in chapter two) and taking into account their inverse Fourier

transform we obtain the ultimate simplification of the expression for u_2,

$$u_2 = \frac{U_{max}^2}{U'(0)}(f_{Z_1}(0) * \nabla_\perp^{-2} A_{yy})\frac{1}{z} + \frac{1}{2}(f * A)^2 U''(0). \tag{4.53}$$

It is easy to see that uniformity of the asymptotic expansion employed in the previous section breaks down as $z \to 0$. Indeed, according to (4.53) and (4.52) velocity components u_2 and v_3 diverge as $1/z$, unless spanwise dependence of amplitude vanishes,

$$u_2 \sim 1/z, \quad v_3 \sim 1/z. \tag{4.54}$$

The cause of this singularity is the critical layer that coincides with the boundary in the long-wave limit. It is obvious that in the generic case the scaling (4.17) adopted for the main deck is invalid near the boundary. As outlined in Chapter 2, a quick fix is to confine our consideration to quasi-planar perturbations, i.e. assume $A_y \ll A_x$. Then the singular terms in the expressions for u_2 and v_3 given by equations (4.53) and (4.52) drop into the next order.

In principle, it is also possible to derive a uniformly valid asymptotic solution for generic perturbations as well. Here we just outline how to do this. To get rid of the singularities we have to re-scale the variables appropriately and solve the Navier-Stokes equations in the region immediately adjacent to the boundary and then match them with the solutions already obtained for the main deck. By choosing the scaling we choose different regimes and, correspondingly, different thicknesses of this region. To our knowledge there was no studies of critical layer dynamics for weakly stratified flows. Here, we follow the analysis of Chapter 2 and focus upon the regime where viscosity is dominant, while nonlinearity is negligible. Here, as in Chapter 2, and (Voronovich et al. [1998]), before that, we scale the critical layer thickness δ as:

$$\delta = (\varepsilon\, Re\, U_0')^{-1/3} \sim \varepsilon^{1/3} \quad (U_0' = U'|_{z=0}),$$

which ensures that δ is small compared to the $O(1)$ overall thickness of the boundary layer δ_{BL}. For further consideration it is crucially important that

$$1 \gg \delta \gg \varepsilon. \tag{4.55}$$

which means that the thickness of viscous critical layer we are considering far exceeds the thickness of nonlinear critical layer, while it is small compared to the boundary layer thickness.

4.3.3.2 Re-scaling. Inner variable

To proceed with the study of the perturbation dynamics inside the viscous critical layer we re-scale our variables as follows,

$$\xi = \frac{z}{\delta}; \qquad T = U_0'\tau; \qquad U - c = \delta\, U_0'\,\xi + o(\delta); \qquad N^2 = (U_0')^2\,\hat{N}^2,$$

$$u = U_0'\hat{u}; \qquad v = \frac{\varepsilon}{\delta}U_0'\hat{v}; \qquad w = \delta\, U_0'\hat{w}; \qquad p = \varepsilon(U_0')^2\hat{p}, \tag{4.56}$$

In terms of the new variables after some algebra, equations for w and the complementary Navier-Stokes equations for other components of velocity take the form,

$$\xi^2\,(U_0')^3\,\partial^2_{xx}\,\partial^2_{\xi\xi}\,\hat{w} + 2\,\frac{\varepsilon}{\delta}\,\xi\,(U_0')^3\,\partial^2_{xT}\,\partial^2_{\xi\xi}\hat{w} = \frac{\varepsilon}{\delta}\,\xi\,(U_0')^3\,\partial_\xi\,\partial^2_{xx}\left[\hat{u}\,\partial_x\,\hat{u} + \hat{w}\,\partial_\xi\hat{u}\right]$$
$$- \varepsilon\,(U_0')^3\,\nabla^2_\perp\,\hat{N}^2\,\hat{w} + \frac{(\varepsilon\,Re)^{-1}}{\delta^3}\,(U_0')^2\,\partial_x\,\xi\,\partial^4_{\xi\xi\xi\xi}\,\hat{w} \tag{4.57a}$$

$$(U_0')^2\,\xi\,\partial_x\,\hat{u} + \frac{\varepsilon}{\delta}\,(U_0')^2\,\partial_T\hat{u} + (U_0')^2\,\hat{w} + \frac{\varepsilon}{\delta}\,(U_0')^2\,\hat{p}_x =$$
$$- \frac{\varepsilon}{\delta}\,(U_0')^2\left[\hat{u}\,\partial_x\,\hat{u} + \frac{\varepsilon}{\delta}\,\hat{v}\,\partial_y\,\hat{u} + \hat{w}\,\partial_\xi\,\hat{u}\right] + \frac{(\varepsilon\,Re)^{-1}}{\delta^3}\,U_0'\,\partial^2_{\xi\xi}\,\hat{u} \tag{4.57b}$$

$$\xi\,(U_0')^2\,\partial_x\,\hat{v} + (U_0')^2\,\frac{\varepsilon}{\delta}\,\partial_T\,\hat{v} + (U_0')^2\,\hat{p}_y = \\ -\,(U_0')^2\left[\frac{\varepsilon}{\delta}\hat{u}\,\partial_x\,\hat{v} + (\frac{\varepsilon}{\delta})^2\,\hat{v}\,\partial_y\,\hat{v} + \frac{\varepsilon}{\delta}\hat{w}\,\partial_\xi\,\hat{v}\right] + \frac{(\varepsilon\,Re)^{-1}}{\delta^3}\,U_0'\,\partial^2_{\xi\xi}\,\hat{v} \quad (4.57c)$$

$$U_0'\,\hat{u}_x + \frac{\varepsilon}{\delta}\,U_0'\,\hat{v}_y + U_0'\,\hat{w}_\xi = 0 \quad (4.57d)$$

It easy to see that the only difference in the rescaled equations above compared to those in chapter 2 is the appearance $O(\varepsilon)$ stratification term in equation (4.57a). Eliminating U_0' and substituting $\delta = (\varepsilon\,U_0'\,Re)^{-1/3}$, while retaining only the leading order $O(1)$ terms and ϵ/δ correction terms, equation (4.57) can be written as,

$$(\partial^2_{\xi\xi} - \xi\partial_x)\hat{w}'' = \frac{\varepsilon}{\delta}\,(\,2\,\partial_T\,\hat{w}'' - \partial_\xi\partial_x(\hat{u}\hat{u}_x + \hat{w}\hat{u}_\xi)) \quad (4.58a)$$

$$(\partial^2_{\xi\xi} - \xi\partial_x)\hat{u} = \hat{w} + \frac{\varepsilon}{\delta}(\partial_T\hat{u} + \hat{p}_x + \hat{u}\hat{u}_x + \hat{w}\hat{u}_\xi) \quad (4.58b)$$

$$(\partial^2_{\xi\xi} - \xi\partial_x)\hat{v} = \hat{p}_y + \frac{\varepsilon}{\delta}(\partial_T\hat{v} + \hat{u}\hat{v}_x + \hat{w}\hat{v}_\xi) \quad (4.58c)$$

$$\hat{u}_x + \hat{w}_\xi = -\frac{\varepsilon}{\delta}\,\hat{v}_y, \quad (4.58d)$$

where $\hat{w}'' = \partial^2_{\xi\xi}\hat{w}$.

The key point is, that the buoyancy term $\hat{N}^2$, which is of order ε, proved to be negligible in the critical layer. We re-iterate that these governing equations (4.58) are identical to their counterparts for the homogeneous flows in Chapter 2. The next step which we do not pursue here is to find solution to equation (4.58) in the form of asymptotic power series in ε/δ rather than ε, subject to the appropriate boundary conditions. At the boundary the solutions should satisfy either constant stress conditions,

$$\hat{w}|_{\xi=0} = 0, \qquad \hat{u}'|_{\xi=0} = \hat{v}'|_{\xi=0} = 0, \quad (4.59)$$

or, no-slip conditions

$$u|_{\xi=0} = v|_{\xi=0} = 0. \quad (4.60)$$

These solutions should not exhibit any singularities in the viscous sub-layer. They have to be matched with the main deck solution at $\xi \to \infty$. Hence, the resulting

matched asymptotic expansion will be uniformly valid.

4.3.4 Conclusions

The main result of this section is the nonlinear evolution equation (4.48) for long three-dimensional perturbations in semi-infinite boundary layers with explicit account of both stratification and viscous effects. The equation is universal in the sense that the specific profile of the boundary layer is immaterial. The specificity of the boundary layer retained in the coefficients in (4.48) can be further reduced by re-scaling the variables

$$\tau_1 = \tau\, U'(0), \quad d = \frac{U_0}{U'(0)}, \quad x_1 = x/d, \quad A_1 = -\frac{1}{d}\, A, \tag{4.61}$$

which yields (with the subscripts dropped) while setting $d = 1$,

$$A_\tau + AA_x - \hat{G}_1[A_x] - \widetilde{\beta}_2\, \hat{G}_2[A_x] + \widetilde{\gamma}\, A = 0, \tag{4.62}$$

the dispersion operators $\hat{G}_1$ and $\hat{G}_2$ remains the same,

$$\hat{G}_1[\varphi(\boldsymbol{k})] = \frac{1}{4\pi^2} \int_{-\infty}^{+\infty} \int_{-\infty}^{+\infty} |\boldsymbol{k}| \varphi(\boldsymbol{r}_1) e^{(-i\boldsymbol{k}(\boldsymbol{r}-\boldsymbol{r}_1))} \mathrm{d}\boldsymbol{k} \mathrm{d}\boldsymbol{r}_1, \tag{4.63}$$

$$\hat{G}_2[\psi(\boldsymbol{k})] = \frac{1}{4\pi^2} \int_{-\infty}^{+\infty} \int_{-\infty}^{+\infty} \frac{k^2}{k_x^2} \psi(\mathbf{r}_1) e^{(-i\mathbf{k}(\boldsymbol{r}-\boldsymbol{r}_1))} \mathrm{d}\boldsymbol{k} \mathrm{d}\boldsymbol{r}_1 \tag{4.64}$$

where, $k = |\boldsymbol{k}|$ and $k^2 = k_x^2 + k_y^2$. The only remaining two coefficients are,

$$\widetilde{\beta}_2 = \frac{N_0^2}{2\varepsilon^2\, (U_0')^2}, \qquad \widetilde{\gamma} = \frac{1}{\varepsilon^2 Re} \frac{U_0'''}{(U_0')^2},$$

showing the importance of both stratification due to buoyancy and the Rayleigh friction type term compared to the nonlinear one in the evolution equation. The magnitude of the stratification is weak and proportional to the ratio of buoyancy force to inertia also known as the Richardson number $\mathrm{Ri} = N_0^2/U_0'^2$, while the magnitude of the Rayleigh friction term is proportional to the ratio the vorticity curvature at the boundary and the Reynolds number. Miles' theorem states that the necessary

condition for linear stability of ideal stratified flow is given by $\mathrm{Ri} = N^2/U'^2 \geq 1/4$ everywhere in the flow. Mile's sufficient condition for linear stability has a simple physical interpretation. The Richardson's number Ri represents the ratio of buoyancy to inertia (shear), therefore the theorem effectively states that if the stabilizing influence of stratification dominates the destabilizing influence of nonlinear terms, then the flow is stable. When $\mathrm{Ri} < 1/4$ then the flow might become linearly unstable. We re-iterate, that in our context linear instabilities play no role since the nonlinear mechanism resulting to collapse we consider develop much faster than linear instability. The nonlinear evolution equation (4.62) provides the framework for studying collapses of three-dimensional perturbations and, in particular, the role of the stratification $\widetilde{\beta}_2 \neq 0$ in 4.4 and the role of Rayleigh friction term $\widetilde{\gamma} \neq 0$ in §4.5

4.4 Collapses in weakly stratified boundary layers without the Rayleigh friction

In this section we examine collapses of three-dimensional localised perturbations, lumps, within the framework of equation (4.62) with $\widetilde{\gamma} = 0$. The reduction of (4.62) to the new 2d nonlinear evolution equation is justified for larger Reynolds numbers, $Re \gg \varepsilon^{-2}$ and for the situations with sufficiently small curvature of vorticity at the boundary $\frac{U'''(0)}{(U'(0))^2}$. Note that for the Blasius boundary layers $\frac{U'''(0)}{(U'(0))^2} = 0$ [see Schlichting and Gersten [2016]].

The layout of the section is as follows. We begin in §4.4.1 with an overview of relevant earlier works. In §4.4.2 we discuss some basic properties of the new 2d nonlinear evolution equation containing an extra new dispersion term due to weak stratification and introduce a notion of 'neutral curves' and 'neutral surfaces' for collapses - the separatices delineating the manifolds of initial conditions which in the course of evolution collapse from those which decay. In §4.4.3 on examining the sufficient criterion for collapse for a few simple initial distributions we attempt at making a general picture of collapses in the new 2d evolution equation. The presence of extra dispersion modifies the evolution of the three-dimensional perturbation hence

raises the threshold of blow-up. Numerical simulation of collapse and its comparison with the self-similar solution is the subject of §4.4.4.

4.4.1 Overview of earlier studies

In this section we discuss briefly what is known about the new 2d nonlinear evolution equation that has been derived and its numerical solution is the subject of discussion in the next section. The equation we are referring to is (4.62) when $\widetilde{\gamma} = 0$.

$$A_\tau + AA_x - \hat{G}_1[A_x] - \widetilde{\beta}_2\,\hat{G}_2[A_x] = 0, \tag{4.65}$$

The new 2d nonlinear evolution equation (4.65) is an extension of the 2d-BO equation derived by Shrira 1989, Voronovich et.al. 1998. To our knowledge equation (4.65) is new and has not been studied. In this work we incorporated stratification inside the boundary layer resulting in a new dispersion term with an integral dispersion operator $\hat{G}_2$. In Fourier space the integral operator $\hat{G}_2 = \frac{k_y^2}{k_x^2}$. It is important to stress that the derivation of equation (4.62) does not assume paraxial approximation, the smallness of (k_y/k_x), as it does in the Kadomtsev-Petviashvilli equation [see Kadomtsev and Petviashvili [1970]]. The general properties of the low frequency modes (vorticity waves) we are interested in and were earlier considered by Shrira 1989 in the context of the upper ocean, is that the transverse components of the velocity fluctuation v are much smaller in comparison with the longitudinal one u. When transverse wavenumber is much less than that of the streamwise wavenumber i.e $k_y \ll k_x$, the new 2d nonlinear evolution equation reduces to the well known one-dimensional Benjamin Ono equation(BO). The one dimensional Benjamin-Ono equation (hereinafter BO) is one of the few celebrated universal weakly nonlinear long-wave evolution equation which emerge in various physical contexts, it was originally derived in the context of long internal waves in deep stratified fluid with a thin layer with stronger stratification Benjamin [1967], Davis and Acrivos [1967] and Ono [1975]. The BO equation is integrable, possesses both multi-soliton and multi-periodic wave solution and conserves an infinite set of integrals of motion and other properties typical of integrable systems

(e.g., Case [1978],Case [1979], Ablowitz and Segur [1981],Matsuno [1984]).The solitons are very robust in the one-dimensional setting. A weakly two-dimensional generalisation of the Benjamin-Ono equation was derived in Ablowitz and Segur [1980] for waves in isotropic media, leading to a Kadomtsev-Petviashvili type extension with a similar pattern of longwave transverse instability in case of positive dispersion [see Kadomtsev and Petviashvili [1970],Kadomtsev [2001]]. The anisotropic essentially-two-dimensional Benjamin-Ono equation(2d-BO) first derived by Shrira [1989] has been comprehensively studied and the results presented in Chapter 2 of this thesis, that is, the evolution equation (4.65) with $\widetilde{\beta}_2 = 0$. We apply a similar approach to investigate the nonlinear stability of equation (4.65), it can also be expressed in the Hamiltonian form. Next we overview the results of the studies of 2d-BO equation which is a special limit of (4.65) without explicit account of stratification ($\widetilde{\beta}_2 = 0$). An obvious class of its exact solutions - all steady and unsteady oblique plane wave solutions of the one-dimensional Benjamin-Ono. However, such solutions proved to be unstable to long transverse perturbations Pelinovsky and Stepanyants [1994]. In particular, for instability of plane solitary waves the maximal growth rates are $\sim V^2$, while the range of unstable transverse wavenumbers is between zero and the $O(V)$ cut-off wavenumber, where V is the solitary wave speed in the frame of reference moving with the speed of long waves. A more detailed analysis of this instability was carried out in Gaidashev and Zhdanov [2004]. Abramyan et al. [1992] found that the 2d-BO equation possesses steady axially symmetric solitary wave solutions. In that work the attention was focussed on the 'zero mode' or 'ground mode' solitary waves, which decay monotonically as $x^2+y^2 \to \infty$, although solutions with oscillatory decay also exist. These steady solutions proved to be unstable. D'yachenko and Kuznetsov [1995] were the first to show that the 2d-BO equation describes collapses: localised perturbations collapse provided the nonlinearity is stronger than dispersion. It has also been shown that the equation also possesses self-similar solutions which describe emergence of axially symmetric singularity in finite time. An explicit description of the collapse evolving as a result of transverse instability of plane solitary waves was derived employing Whitham's adiabatic approach in Pelinovsky and Shrira [1995].

The sufficient condition of collapse for any chosen initial condition is that the Hamiltonian should be negative (Zakharov and Kuznetsov [2012]). However, the integral condition of negativity of the Hamiltonian is implicit, *a priori* it is not obvious what initial perturbations collapse and what decay. For any chosen shape of the perturbation there is a threshold in amplitude above which the perturbation collapse. In this section we will find dependence of the threshold on the parameters of the perturbation and outline the range of parameters where the threshold does not exceed the limitations imposed by the weakly nonlinear nature of the equation.

4.4.2 Basic properties and 'neutral curves'

By extending the results of (D'yachenko and Kuznetsov [1995]) the new 2d nonlinear evolution equation (4.65) can be written in the Hamiltonian form as follows,

$$A_\tau = \partial_x \left[\hat{G}_1[A] + \widetilde{\beta}_2 \, \hat{G}_2[A] - \frac{1}{2} A^2 \right] = \partial_x \frac{\delta H}{\delta A}, \tag{4.66}$$

where the Hamiltonian H is made of three constituent integrals I_1, I_2 and I_3, describing respectively dispersion and nonlinearity,

$$H = \frac{1}{2} I_1 + \frac{\widetilde{\beta}_2}{2} I_2 - \frac{1}{6} I_3, \tag{4.67}$$

where,

$$I_1 = \int A \hat{G}_1[A] \, \mathrm{d}x\mathrm{d}y, \qquad I_2 = \int A \hat{G}_2[A] \, \mathrm{d}x\mathrm{d}y, \qquad I_3 = \int A^3 \, \mathrm{d}x\mathrm{d}y, \qquad (\boldsymbol{dr} \equiv \mathrm{d}x\mathrm{d}y).$$

Besides the Hamiltonian, the new 2d nonlinear evolution equation (4.65) conserves three other integrals of motion: the streamwise and spanwise components of the 'momentum' $\boldsymbol{P}$ and the mass flux M,

$$P_x = \frac{1}{2} \int\int A^2 \, \mathrm{d}x\mathrm{d}y, \quad P_y = \frac{1}{2} \int\int A \phi_y \, \mathrm{d}x\mathrm{d}y, \quad (\phi_x \equiv A), \quad M = \int\int A \, \mathrm{d}x\mathrm{d}y. \tag{4.68}$$

The way these integrals depend on parameters of the perturbations enables us to infer the existence of collapses for certain initial conditions and to outline the manifolds of collapsing initial conditions for particular *a priori* chosen classes of initial conditions.

4.4.3 Domains of collapses in parameter space

Here, we apply the sufficient condition of collapse, $H < 0$, to find separatrices delineating the domains of collapse (supercritical region) and domains of decay (subcritical region) in the parameter space. We will refer to the curves or surfaces where the Hamiltonian vanishes as nonlinear neutral curves/surfaces. By means of direct numerical simulations of the new 2d nonlinear evolution equation (4.65) (which we describe below) we verify that this criterion indeed predicts the emergence of collapse or decay of initial perturbations. Applying this criterion to a few simple asymmetric distributions enables us to get a good *a priori* idea how the outcome of the evolution (i.e. collapse or decay) of an initial perturbation depends on its parameters. To outline these dependencies we first examine a few simple asymmetric distributions: the Gaussian and Lorentzian pulses,

$$A_G(x,y) = a e^{-\left(\frac{x^2}{2\sigma_x^2}+\frac{y^2}{2\sigma_y^2}\right)}, \qquad A_L(x,y) = \frac{a}{1+4(x^2/\sigma_x^2+y^2/\sigma_y^2)}. \tag{4.69}$$

These initial perturbations are fully characterized by just three parameters: amplitude a and characteristic half-widths σ_x and σ_y, which we will refer to as the 'widths' for brevity.

It is easy to see that in the Hamiltonian H given by (4.67), its constituent integrals, the dispersion ones, I_1, I_2 and the nonlinear one, I_3, can be expressed in terms of the perturbation initial amplitude a and perturbation widths σ_x and σ_y. On re-scaling the variables,

$$\tilde{x} = \frac{x}{\sigma_x}, \qquad \tilde{y} = \frac{y}{\sigma_y}, \qquad A(\tilde{x},\tilde{y}) = a\,\mathcal{A}, \quad \left(\mathcal{A}_G = e^{-(\tilde{x}^2+\tilde{y}^2)/2}, \quad \mathcal{A}_L = \frac{1}{1+4(\tilde{x}^2+\tilde{y}^2)}\right)$$

we re-write our integrals as,

$$I_1 = \alpha a^2 \sigma_x \tilde{I}_1, \quad \tilde{I}_1 = \int\int \mathcal{A}\,\hat{G}_1\,[\mathcal{A}]\,\mathrm{d}\tilde{x}\mathrm{d}\tilde{y}, \quad I_2 = \alpha a^2 \sigma_x^2 \tilde{I}_2, \quad \tilde{I}_2 = \int\int \mathcal{A}\,\hat{G}_2\,[\mathcal{A}]\,\mathrm{d}\tilde{x}\mathrm{d}\tilde{y},$$

$$I_3 = \alpha a^3 \sigma_x^2 \tilde{I}_3, \qquad \tilde{I}_3 = \int\int \mathcal{A}^3 \mathrm{d}\tilde{x}\mathrm{d}\tilde{y}, \qquad \alpha = \frac{\sigma_y}{\sigma_x},$$

where the first and second integrals $\tilde{I}_1$, $\tilde{I}_2$ depends implicitly on the ratio α through the kernel of the integral operator, $\hat{G}_1$ and $\hat{G}_2$. In the Fourier space $\hat{G}_1 = \left(k_x^2 + \frac{1}{\alpha^2}k_y^2\right)^{1/2}$ while $\hat{G}_2 = \frac{1}{\alpha^2}\frac{k_y^2}{k_x^2}$. The third integral $\tilde{I}_3$ is a constant which is evaluated analytically or numerically; for the Gaussian initial conditions $\tilde{I}_2 = \frac{2}{3}\pi$. The dispersion integrals $\tilde{I}_1$ and $\tilde{I}_2$ cannot be evaluated analytically and is dealt with numerically. It is easy to see that I_1 depends on σ_x linearly, while I_2 and I_3 both have quadratic dependence on σ_x. The parameter α is the ratio of spanwise half-width σ_y to that of the streamwise half-width σ_x. From now on, we will drop the subscript and denote σ_x by σ and proceed to finding nonlinear neutral curves/surfaces in terms of amplitude a, width σ and aspect ratio α, for each value of the stratification parameter that is specified by $\widetilde{\beta}_2$.

Recall that the Hamiltonian vanishes when $3\,I_1 + 3\,\widetilde{\beta}_2 I_2 - I_3 = 0$, which thus yields nonlinear 'neutral surfaces' separating the domains of collapse and decay in the $a - \sigma - \widetilde{\beta}_2$ space,

$$a^2\sigma(3\,\tilde{I}_1 + 3\,\widetilde{\beta}_2\,\sigma\tilde{I}_2 - a\sigma\tilde{I}_3) = 0. \tag{4.70}$$

It proved to be convenient to present the results of such an analysis as cross-sections with fixed values of asymmetry parameter α and stratification parameter $\widetilde{\beta}_2$. Then the relationship between the amplitude threshold a_{thr} and perturbation width σ prescribed by equation (4.70) for constant values of α and $\widetilde{\beta}_2$ is hyperbola.

$$a_{thr} = \frac{3\,\tilde{I}_1}{\sigma\,\tilde{I}_3} + \frac{3\,\widetilde{\beta}_2\tilde{I}_2}{\tilde{I}_3}, \tag{4.71}$$

This amplitude threshold depends on both the stratification $\widetilde{\beta}_2$ and asymmetry parameter α. A set of cross-sections for different values of asymmetry parameter α (i.e., $\alpha = 0.25, 0.5, 1.0, 1.5, 2.0, 4.0, 8.0$) and stratification $\widetilde{\beta}_2$ ($\widetilde{\beta}_2 = 0.005$) for the

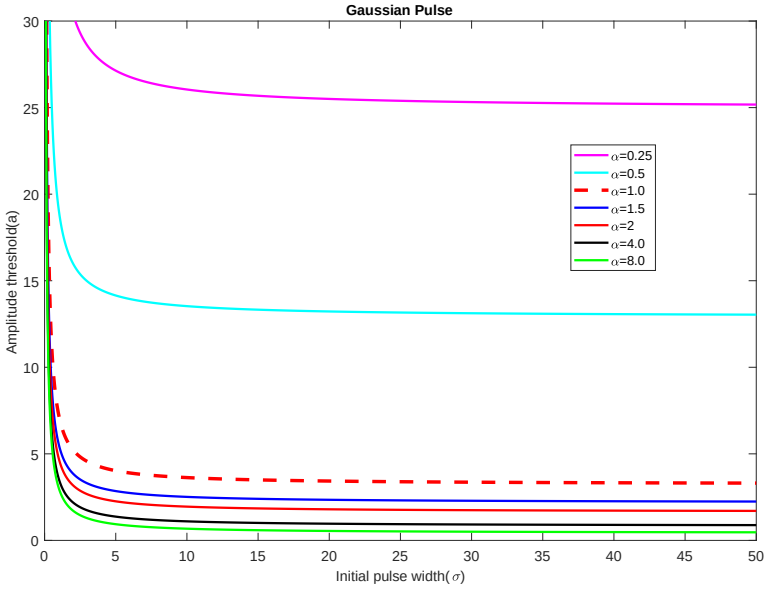

(a)

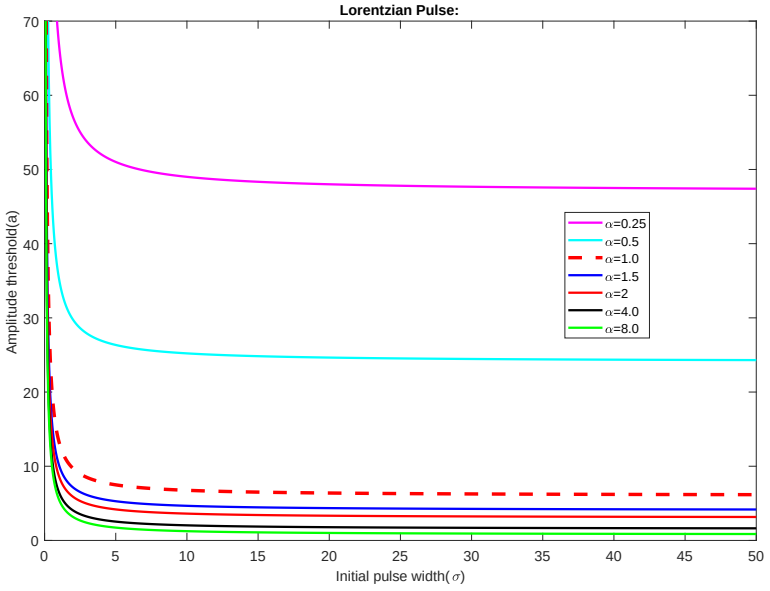

(b)

FIGURE 4.2: 'Neutral curves' separating the domains of collapse and decay for different values of α ($\alpha = 0.25, 0.5, 1, 1.5, 2, 4, 8$) and $\widetilde{\beta}_2 = 0.005$ for: (a) the Gaussian and (b) the Lorentzian initial conditions.

Gaussian and the Lorentzian initial conditions are shown in figure 4.2. The figure illustrates several salient features of the separatrices in the $a - \sigma$ plane. For every value of the stratification parameter $\widetilde{\beta}_2$ the cross-sections are hyperbola. The role of the stratification is to raise the threshold of the nonlinear neutral curve, while α lowers the threshold of blow-up. The initial pulses with a, σ above the curve collapse. For larger σ the threshold decreases slowly for any asymmetric Gaussian or Lorentzian pulses. The slow decay of the hyperbola is attributed to how stratification weakens the decay of these long perturbations. Since the main mechanism of the collapse is self-focussing asymmetry quite noticeably affects the threshold: as expected, the threshold decreases for the pulses stretched in the spanwise direction ($\alpha > 1$), it increases for the pulses stretched in the streamwise direction ($\alpha < 1$). For the evolution to be weakly nonlinear and to allow for a substantial growth, the initial amplitude should be sufficiently small. The neutral curves for the Gaussian and Lorentzian initial pulses are qualitatively very similar. However, quantitatively, the Gaussian pulses for moderate values of σ have a noticeably smaller threshold. The comparison of the neutral curves for the Gaussian and Lorentzian initial pulses suggests that their behaviour is robust and at the qualitative level we can generalise and to expect to see the same salient features: a decrease of the amplitude threshold for collapse with the increase of both spatial scales, crucially, $a_{thr} \to 0$ as σ or α tend to infinity. Recall that for the plane wave soliton solutions of the 2d-BO equation of any amplitude $H = 0$ and, hence these solutions are at the boundary of the domain of collapsing initial conditions even for vanishingly small amplitudes. The transverse instabilities of plane solitons within the framework of the 2d-BO equation are known to be possible for any amplitude of the solitary waves (Pelinovsky and Stepanyants [1994]), Gaidashev and Zhdanov [2004]), although the instability growth rate is proportional to the soliton amplitude and, hence, tends to zero as the amplitude tends to zero. Within the framework of the 2d-BO equation this instability is known to end up in collapse (Pelinovsky and Shrira [1995]), at present we don't have analytic results for the transverse instability of planar solitons for the equation accounting for weak stratification (4.65).

4.4.4 Collapse and self-similarity within the framework of the 2d nonlinear evolution equation for weakly stratified boundary layers: self-similar solution and examples of simulation

In this section we find the self-similar solution of (4.65) describing formation of the blow up singularity and outline the numerical procedure used to investigate the collapse in the 2d nonlinear evolution equation with explicit account of weak stratification. First we demonstrate that the evolution equation (4.65) has self-similar solution which captures the behaviour of the perturbation amplitude in the vicinity of the singularity at time τ_0 and space (x_0, y_0).

4.4.4.1 Self-similar solution

Consider the spatial and temporal dependence of a collapsing perturbation in a certain vicinity of the blow-up singularity occurring at $\boldsymbol{r} = \boldsymbol{r}_0\{x_0, y_0\}$. Introduce time to singularity $\check{\tau}$ and distance to singularity $\check{x} = x - x_0$, $\check{y} = y - y_0$. There is a self-similar solution in the form

$$A(\boldsymbol{r}, \check{\tau}) = \check{\tau}^{-\frac{1}{2}} h(\check{\boldsymbol{\xi}}), \quad \check{\boldsymbol{\xi}} = \frac{\check{\boldsymbol{r}}}{\check{\tau}^{\frac{1}{2}}}. \tag{4.72}$$

where $h(\check{\boldsymbol{\xi}})$ is specified by the equation,

$$\frac{1}{2}\check{\boldsymbol{\xi}} h'' + (h'^2 + hh'') - \hat{G}_1[h''] - \beta_2 h'' = 0 \tag{4.73}$$

This self-similar solution for the stratified equation is similar to a known self-similar solution of the 2d-BO equation which predicts the $1/\sqrt{\tau_0 - \tau}$ singularity in time and the shrinking spatial distribution given by $h(\check{\boldsymbol{\xi}})$, its width shrinks as $\sqrt{\tau_0 - \tau}$. Our equation for the spatial scale h specifying the shape of the distribution has a much more complicated form than its counterpart for the 2d-BO derived in 2.4.4.1.

4.4.4.2 Numerical simulation

To simulate numerically the 2d equation (4.65) for localized initial perturbations we use the same pseudo-spectral method as in Chapter 2. As in Chapter 2, the employed pseudo-spectral method with periodic boundary conditions uses efficient fast Fourier transform (FFT) routines in handling dependencies on x and y, while for the time evolution the classic fourth order Runge-Kutta method is employed, hence the temporal accuracy is fourth order.

In our context it was found to be optimal to use a rectangular box of length 512π and width 128π. This choice provides sufficient domain for the spatial decay of the localized perturbations we were simulating and also to allow the perturbation sufficient time to move in the streamwise direction during the evolution. To resolve the rapidly growing and increasingly localized amplitude distribution we used 4096×1024 grid points. It is convenient to present our evolution equation in the flux-conservation form,

$$A_\tau + F_x = 0$$

where the flux $F = -\hat{G}_1[A] - \widetilde{\beta}_2 \hat{G}_2[A] + \frac{1}{2}A^2$. The integral operators $\hat{G}_1[A]$ and $\hat{G}_2[A]$ are dealt with in the Fourier space, while nonlinear terms were considered in the physical space on collocation points with the 'two-third de-aliasing rule' (e.g.Orszag [1969]). The accuracy of the simulations was controlled by ensuring that the integrals of motion (4.68) remain constant with the error not exceeding $O(10^{-4})$.

4.4.4.3 Evolution scenarios

Our simulations suggest that the phase space of the evolution equation of (4.65) is organised very simply: there are just two attractors corresponding to basic flow and the point singularity, there are no nontrivial long-lived states. On obtaining in §4.4.3 the boundaries separating the domains of the initial conditions resulting in collapse or decay, we verified the findings by numerical simulations of the evolution of symmetric and asymmetric Gaussian pulse initial conditions (4.69). By choosing the initial perturbations slightly above and slightly below the hyperbola, we confirmed that,

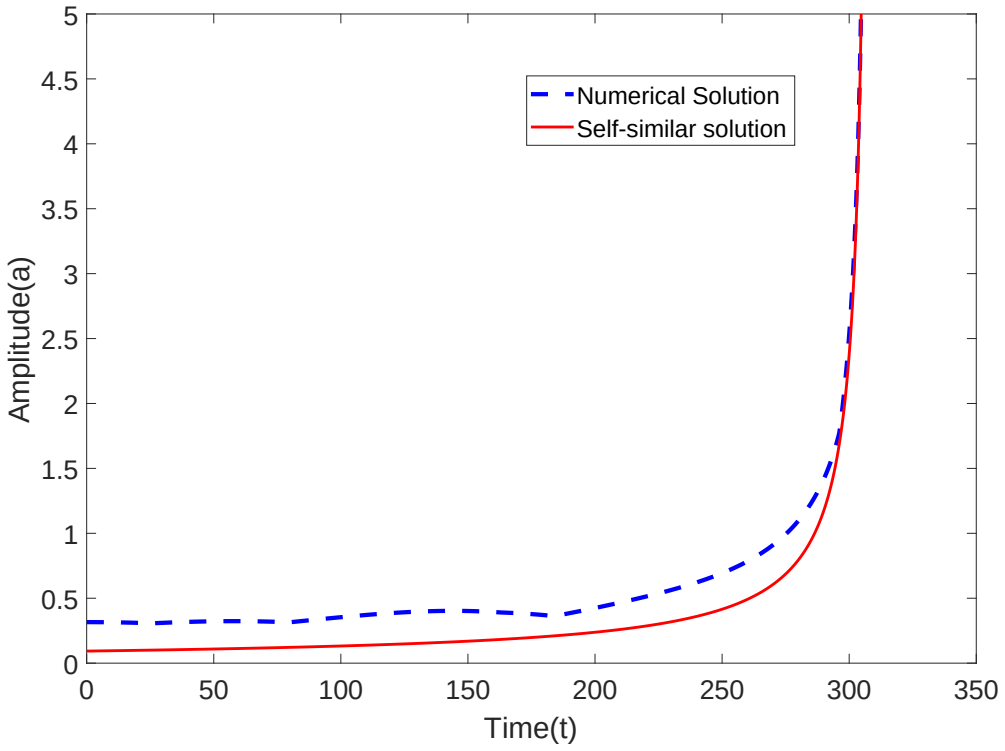

FIGURE 4.3: Example of time evolution of the amplitude of a collapsing laterally stretched pulse with $\alpha = 2$. Blue dashed line: simulated evolution of the amplitude of a collapsing pulse with the asymmetric Gaussian initial condition ($a = 0.3159, \widetilde{\beta}_2 = 0.005, \sigma_x = 25, \sigma_y = 50, \widetilde{\gamma} = 0$). Red solid line: the self-similar solution (4.72)

indeed, the initial perturbations with the amplitudes exceeding the threshold collapse, that is, such perturbations evolve into a short-lived pattern which tends to a localized self-similar solution with a point singularity. The initial conditions with amplitude below the threshold decay, although, for the initial conditions close to the threshold surface, a temporary transient growth, sometimes substantial, can also occur. We do not illustrate it here. Figure (4.3) shows the simulated time dependence of a collapsing pulse amplitude for the same example along with the self-similar solution (4.72). Note that during the most of the pulse evolution the amplitude grows very slowly, the sharp growth occurs just immediately prior to the singularity. The figure also gives an idea how well the self-similar solution (4.72) captures the evolution. The fact that evolution of any supercritical localised perturbation tends to the self-similar solution, it not only proves the existence of singularity, it also shows that the universal character of the singularity captured by the analytical solution (4.72). We illustrate

a typical collapse scenario by providing snapshots of amplitude cross-sections based upon our simulations of the evolution of a collapsing pulse for a localized asymmetric initial conditions. The initial condition is a laterally stretched Gaussian pulse $\alpha = 2$ corresponding to $\sigma_x = 25$, $\sigma_y = 50$, $a = 0.3159, \widetilde{\beta}_2 = 0.005, \widetilde{\gamma} = 0$. Here, we highlight two features. Although the initial condition is a smooth well confined lump, the emerging pattern shown on figure (4.5) is not : at the pedestal, the pulse radiates at two distinguished directions; the resulting pattern resembles 'hair-pin' or 'lambda' vortices routinely observed in the wind tunnels (e.g. Kachanov [1994]). The top of the pulse evolves in an axially symmetric self-similar manner tending to a point singularity at the end. We also provide a sequence of snapshots of amplitude evolution at four different moments on figure 4.4.

Figures 2.8 and 4.4 are showing the evolution of the perturbation cross-sections for homogeneous 2.8 and stratified cases. At the initial moment (t=0) the perturbation is the same axially symmetric gaussian lump. A quick comparison enables us to make the following qualitative observations. The same well-confined initial lump is laterally dispersing quite differently. In both cases, during the evolution, we see a sequence of different patterns which at the foot of the perturbation resemble hairpin vortices usually observed in wind tunnel experiments during the laminar-turbulent transition. In the stratified case these patterns are much more pronounced and have a more complicated form. In contrast, in both cases, the top part of the perturbations becomes more and more symmetric as the perturbation approaches the collapse. As expected near the collapse when nonlinear localizing effects dominate over dispersion, all the patterns evolve into a well-localized axially symmetric shape before their eventual collapse. We could summarise the differences by saying that cross-section evolution is strongly dependent on stratification, stratification results in the emergence of quite complicated patterns at the foot of collapsing lumps. In contrast, the self-similar evolution near the singularity remains qualitatively similar.

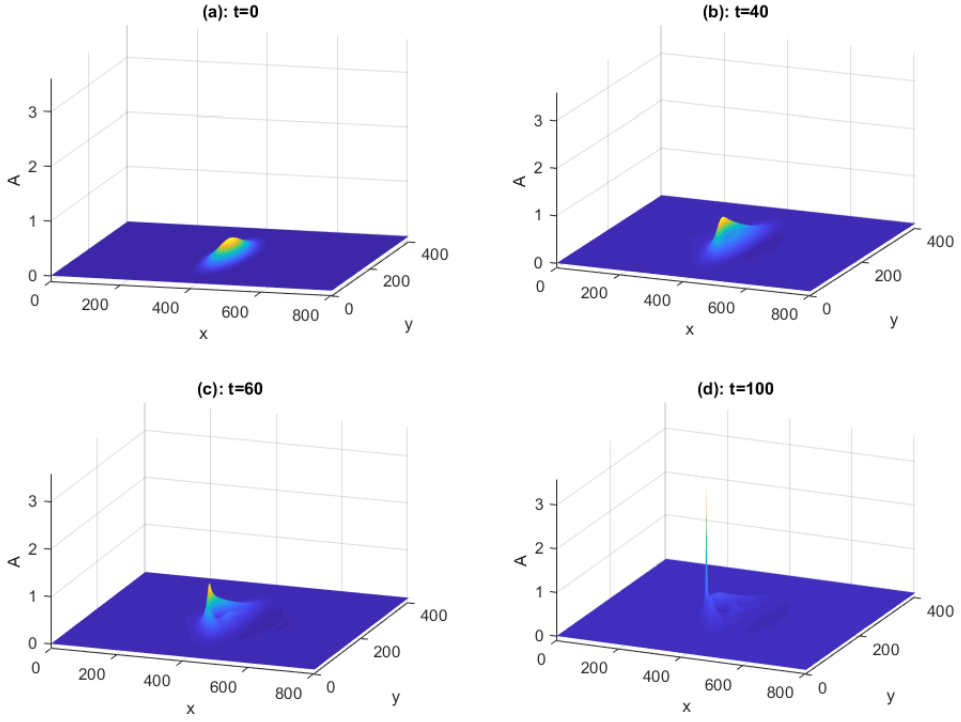

FIGURE 4.4: Snapshots showing the evolution of the amplitude $A(x, y, t)$ of a collapsing laterally stretched ($\alpha = 2$) pulse taken at the start of evolution ($t = 0$) and finally at t=100 of the maximal amplitude at four-different moments. The simulation is for supercritical asymmetric Gaussian initial condition ($a = 0.3159, \sigma_x = 25, \sigma_y = 50, \widetilde{\gamma} = 0$).

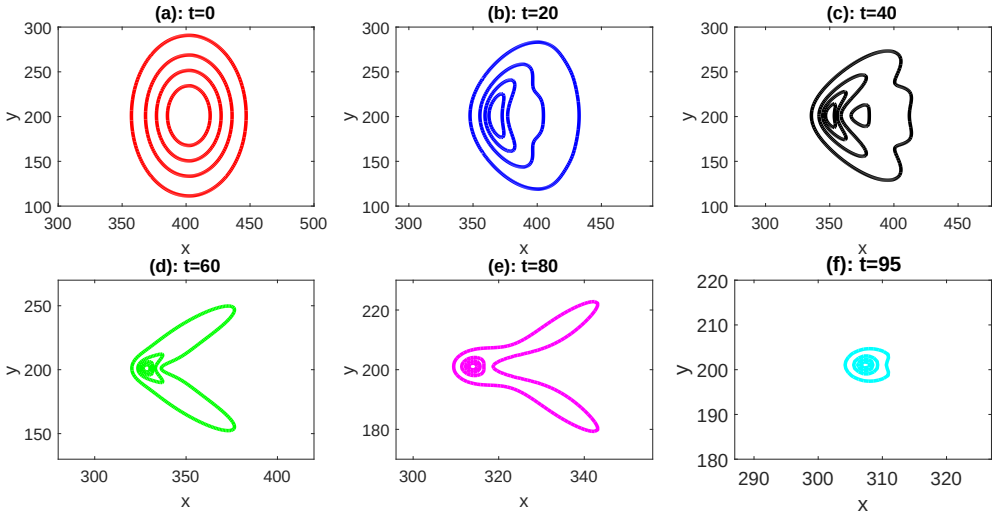

FIGURE 4.5: Evolution of the cross-section of a collapsing laterally stretched pulse $\alpha = 2$ taken at the start of evolution($t = 0$) and finally at t=95 of the maximal amplitude at six-different moments showing hair-pin or lambda vortices. The simulation is for supercritical asymmetric Gaussian initial condition ($a = 0.3159, \sigma_x = 25, \sigma_y = 50, \widetilde{\beta}_2 = 0.005, \widetilde{\gamma} = 0$).

4.5 Collapses with the account of the Rayleigh friction term ($\widetilde{\gamma} \neq 0$)

The aim of this section is a preliminary analysis of equation (4.62),

$$A_\tau + AA_x - \hat{G}_1[A_x] - \widetilde{\beta}_2 \hat{G}_2[A_x] + \widetilde{\gamma} A = 0, \tag{4.74}$$

The evolution equation (4.62) has not been studied before. First, it is easy to see that the new 2d evolution equation (4.74) with explicit account of Rayleigh friction term differs from its homogeneous counterpart equation (2.55) only by the presence of the second dispersion term with coefficient $\widetilde{\beta}_2$ resulting from the account for stratification. The main open questions are:

1. How is the phase space of this equation organised?
2. Are there collapses? If yes, in what respect do they differ from their counterparts without the Rayleigh friction and stratification?
3. In what range of the dissipation parameter $\widetilde{\gamma}$ the collapse might occur and how does the amplitude threshold depend on $\widetilde{\gamma}$?

Our limited amount of simulations strongly suggests that the phase space of the evolution equation (4.74) is qualitatively similar to that of the models without the stratification and the Rayleigh friction: any initial perturbation evolves either to the unperturbed state or collapses forming a point singularity. Although at a first glance there are no analytical tools for studying (4.74) we have shown that the self-similar solution (4.72) obtained in the limit $\widetilde{\gamma} = 0$ perfectly captures the character of the singularity when $\widetilde{\gamma} \neq 0$. An increase in $\widetilde{\gamma}$ raises the threshold for the collapse to occur and increases the duration of the evolution. The second dispersion due to stratification has a qualitatively similar effect. The threshold proved to be extremely sensitive to small variations of $\widetilde{\gamma}$, the threshold grows sharply with increase of $\widetilde{\gamma}$ and might go beyond the range of validity of weakly nonlinear theory. A comprehensive mapping

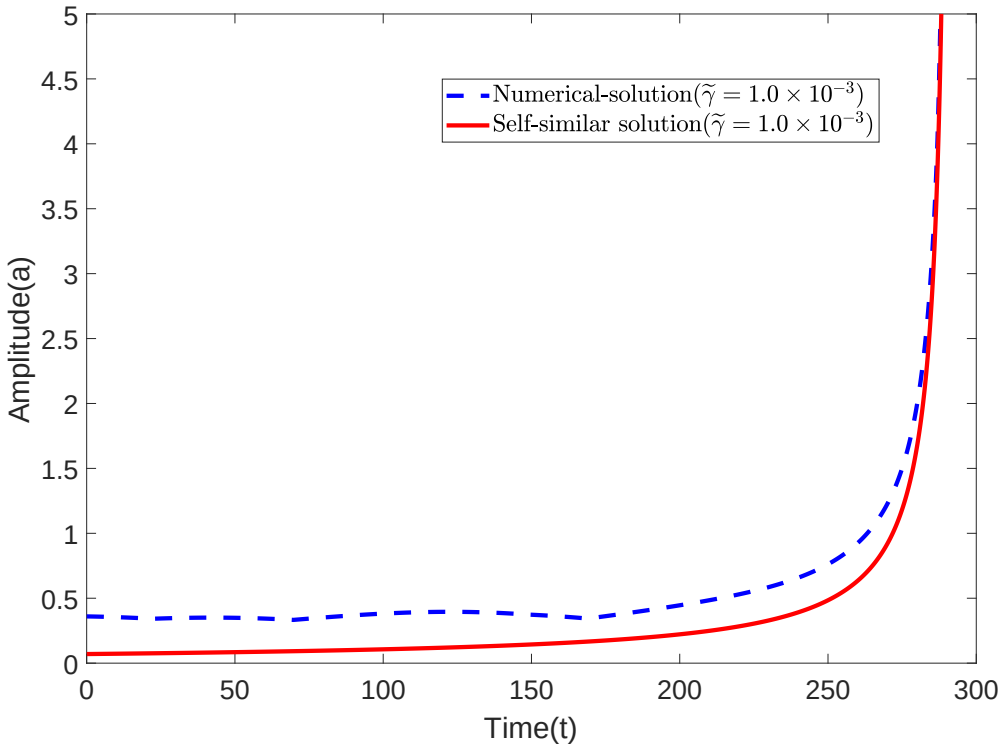

FIGURE 4.6: Example of time evolution of the amplitude of a collapsing laterally stretched pulse with $\alpha = 2$. Blue dashed line: simulated evolution of the amplitude of a collapsing pulse with the asymmetric Gaussian initial condition ($a = 0.3600, \sigma_x = 25, \sigma_y = 50, \widetilde{\beta}_2 = 5.0 \times 10^{-3}, \widetilde{\gamma} = 1.0 \times 10^{-3}$). Red solid line: the self-similar solution (4.72)

of the collapsing initial conditions requires a dedicated study and goes beyond the scope of present work.

4.6 Conclusions

In this Chapter we extended the approach introduced in Chapter 2 for homogeneous boundary layer, and derived a novel 2d nonlinear evolution equation which is essentially two-dimensional Whitham type equation with explicit account of stratification in the boundary layer. We also took into account the viscous linear decay and examined its role in the evolution of 3d perturbations. In this section based on our analytical and numerical examination of collapses of 3d perturbations in new

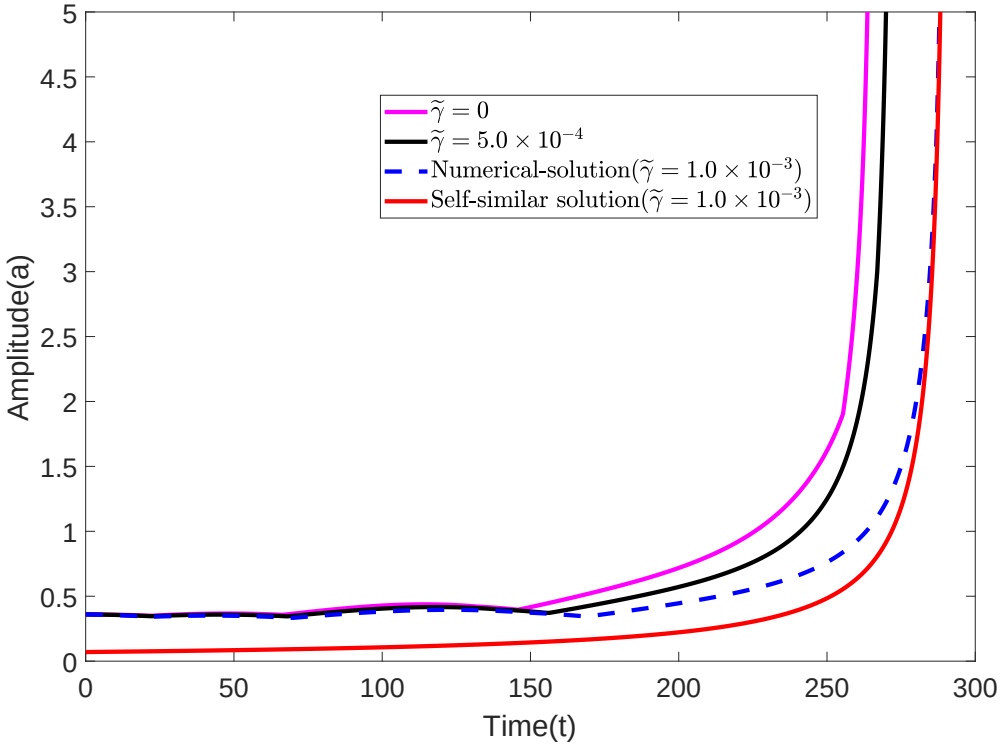

FIGURE 4.7: Example of time evolution of the amplitude of a collapsing laterally stretched pulse with $\alpha = 2$. Magenta line: simulated evolution of the amplitude of a collapsing pulse with the asymmetric Gaussian initial condition $(a = 0.3600, \sigma_x = 25, \sigma_y = 50, \widetilde{\beta}_2 = 5.0 \times 10^{-3}, \widetilde{\gamma} = 0$: (Black solid line), $\widetilde{\gamma} = 5.0 \times 10^{-4}$: (Blue dashed line), $\widetilde{\gamma} = 1.0 \times 10^{-3}$. Red solid line: the self-similar solution (4.72)

two-dimensional weakly stratified and strong dissipation equation we summarise our findings.

1. A novel model describing dynamics of 3d longwave perturbations in generic weakly stratified semi-infinite boundary layers for finite Reynolds numbers has been derived by a systematic asymptotic procedure. The model represents a 2d Whitham type pseudo-differential nonlinear evolution equation obtained in the distinguished limit where the nonlinearity, two types of dispersion and dissipation described by the Rayleigh friction term are all in balance.

2. It has been shown that within the framework of the model the initial perturbations either collapse, i.e. blow up forming a point singularity or decay. An analytical self-similar solution describing behaviour of the collapsing solutions

has been derived. By means numerical simulations it has been found that the collapsing perturbations tend to the obtained self-similar solutions and, hence, have analytically described singularity.

3. It has been found that stratification and the Rayleigh friction terms do not arrest the collapse, but they raise the amplitude of initial perturbations required for collapse to occur and increase the duration of evolution. The dependence of the amplitude threshold on the parameters has been examined.

Chapter 5

Conclusions and Discussion

5.1 The main conclusions

1. By means of a systematic asymptotic procedure a family of novel weakly nonlinear self-contained models describing dynamics of 3d long-wave perturbations in generic boundary layers has been derived in the distinguished limit assuming balance of the nonlinearity, dispersion and dissipation. Each model represents a 2d pseudo-differential evolution equation for the amplitude $A(x, y)$ of a single longwave mode which is weakly decaying in the linear setting, while the dependence on the cross-boundary coordinate z is provided by an explicit solution of the corresponding boundary-value problem. The new equations are generalisations of the two-dimensional Benjamin-Ono (2d-BO) equation with the Rayleigh-type dissipation. They cover the situations of semi-infinite and confined boundary layers, both homogeneous and weakly stratified boundary layers and are equally valid for the no-slip and constant stress conditions at the boundary. The employed asymptotic expansions have been shown to be uniformly valid for perturbations strongly laterally stretched, i.e. for the perturbations with $|A_y| \ll |A_x|$. For the perturbations with $|A_x| \sim |A_y|$ the question

of validity of the derived equations remains open, nevertheless the equations have been thoroughly examined for the whole range of parameters.

2. The derived models are valid for a wide range of the Reynolds numbers, the account of the finite Reynolds number leads to the Rayleigh-type dissipation in the evolution equation. In all models considered so far the Rayleigh-type dissipation is proportional to the ratio of the curvature of the basic flow vorticity at the boundary and product of the Reynolds number and nonlinearity parameter squared. A key parameter $\widetilde{\gamma}$ characterising the relative magnitude of the dissipative and nonlinear terms has been identified.

3. It has been shown that the novel evolution equations admit collapses occurring for a broad class of initial conditions. The phase space of the evolution equations is found to be very simply organised: there are two attractors corresponding to the unperturbed basic flow and the blow-up singularity. An initial 'lump' of a given shape collapses, i.e. blows up forming a point singularity in finite time, provided its initial amplitude exceeds a certain threshold. This threshold is specific for each particular initial shape and the value of parameter $\widetilde{\gamma}$. The initial perturbations exceeding the threshold collapse in a self-similar manner, the derived axially symmetric self-similar solution captures very well the behaviour of the perturbation in a substantial neighbourhood of the singularity. The perturbations with the amplitudes below the threshold - decay, although a substantial transient growth is possible for the initial perturbations close to the threshold. To find the boundary in parameter space between the domains of collapse and decay an analytical sufficient condition in integral form was used for the not uncommon situations with zero $\widetilde{\gamma}$. On the amplitude-width plane the domain of collapsing initial conditions is found to be confined by a hyperbola from below; the threshold amplitude decreases as inverse width of the perturbation and for very wide perturbations tends to zero. For the asymmetric initial perturbations the boundary is more complicated but exhibits the same trends. Collapses in dissipative evolution equations have not been studied before and there are no suitable mathematical tools. By numerical simulation of the evolving perturbations and by constructing an analytical self-similar solution it has

been shown that the explicit account of dissipation in the evolution equation does not preclude the occurrence of singularity, it does not alter the character of the singularity either, but it considerably increases the time needed for the singularity to emerge and raises the amplitude threshold, sometimes beyond the range of applicability of weakly nonlinear theory.

4. The examined collapses provide a robust mechanism for growth of 3d patterns resembling the 3d coherent structures often observed in wind tunnels at intermediate stages of transition. The collapses might be considered as a plausible candidate for the key role in scenarios of by-pass laminar-turbulent transition in generic boundary layers.

5.2 Discussion

To put our results into context, here we briefly discuss a broader picture, the new questions they generate, and the directions of further research which we view as the most promising.

The work gives rise to a lot of questions to which we currently do not have answers. The main outstanding question is concerned with the role of the modelled collapses in the bigger picture of transition, this main question splits into a multitude of more specific ones. In particular, our evolution equations are an element of a weakly nonlinear asymptotic model, currently we do not know the eventual outcome of the collapses occurring within the framework of the model when the solution goes beyond the limit of applicability of the the model. In other words, what happens in the full Navier-Stokes equations? Most likely, the collapses cause localised transition to turbulence. However, we cannot exclude the possibility that under certain circumstances collapses might lead to formation of long-lived 3d coherent strongly nonlinear patterns. A dedicated direct numerical simulation study is in progress to clarify this crucial issue.

All collapsing perturbations tend to axially symmetric self-similar distributions, which resemble the coherent patterns observed in wind tunnels. At the foot of these

patterns they, as can be seen in the cross-sections of the numerical simulation (2.8), also exhibit features typical of lambda vortices routinely observed in wind tunnels at an intermediate stage of laminar turbulent transition (e.g. Kachanov [1994]). Is this resemblance just a coincidence or the model does capture elements of essential physics of the phenomenon?

Although the model does predict emergence of 3d patterns resembling those observed in the wind tunnels, at the moment we could claim only a rough qualitative agreement. For a quantitative comparison the model has to be extended to take into account non-parallel effects. The work in this direction is currently in progress, we return to this point below.

Our study leaves aside the question on how the initial perturbation might be produced, which we took as given. There are many possible scenarios, in particular, there is a room for usual linear long-wave instabilities to play, for example, as a result of inflectional long-wave instability plane wave perturbations propagating streamwise might emerge and grow until the nonlinearity becomes strong enough to balance dispersion, then, at first the plane Benjamin-Ono solitons are likely to emerge, the latter are transversally unstable; under the right conditions this instability leads to their collapse (Pelinovsky and Shrira [1995]). In the similar vein the TS waves might produce first the plane Benjamin-Ono solitons (Kachanov et al. [1993]). Currently we understand all the phases of this scenario, but its elaboration requires a dedicated work. Initial perturbations leading to collapses can be also generated by perturbations of the boundary. We assumed the boundary to be flat, but the model could be easily extended to take into account long-wave perturbations (steady or unsteady) of the boundary. It would be interesting to examine what perturbations of the boundary trigger collapses, but this should be a subject of a dedicated work.

Let us very briefly discuss the limitations of the model and how the model can be extended. The main limitation, apart from the already mentioned weak nonlinearity constraint, is the total neglect of nonparallel effects. This is not an inherent difficulty of the approach, it is our conscious choice to keep the derivation simple. It seems to be relatively straightforward to incorporate weakly non-parallel effects into the employed

asymptotic scheme. This has been done in (Shrira et al. [2005]) for free surface boundary layer in water with the main effect being an additional Rayleigh friction term, this term has been included into an effective dissipation. The approach can be extended for the no-slip boundary conditions as well, where we expect qualitatively similar effect; but at present this remains to be done.

The present work was confined to the simplest generic boundary layer with unidirectional shear flow. It is also possible to extend the developed approach to other types of boundary layers. Now it has become clear how to generalise the derived evolution equations to describe more complicated hydrodynamic situations accounting for the 3d boundary layers and compliant boundaries. The fluid outside the boundary layer was assumed homogeneous and stagnant, these assumptions can be relaxed or totally lifted. The occurrence of collapses in these situations is currently being investigated.

We did not attempt a quantitative comparison with data for the coherent structures observed by Kachanov (1994). However, we mention that our simulations for the 3d perturbations in all the boundary layers we considered agrees qualitatively with the observed 3d coherent patterns. This qualitative agreements seems encouraging, but might prove to be just a coincidence. A detailed comparison with observations is needed, which requires a dedicated work. The role of the collapses in the bigger picture of the boundary-layer instabilities and laminar-turbulent transition remains the biggest open question. Resolving these outstanding questions will provide a new insight into physical mechanisms of boundary layer instabilities and laminar-turbulent transition.

Yet another seemingly possible direction of extension of the present study is concerned with turbulent boundary layers. Adopting the Boussinesq hypothesis one can reduce the description of the turbulent shear flow to that of a laminar one with an eddy viscosity. Within the framework of this approach the only difference in the mathematical formulation of the problem is that the eddy viscosity becomes a function of the cross-boundary coordinate. Correspondingly, the derivation of the evolution equations remains the same. The difficulty to be dealt with is the behaviour

of the asymptotic expansion in the critical layer. If the solution in the critical layer remains regular for the case of the coordinate dependent viscosity, which is likely, but remains to be worked through, then the approach could be easily extended to turbulent boundary layers and employed to explain bursts observed, in particular, in atmospheric boundary layer.

Appendix A

Details of the derivation of the nonlinear evolution equation for homogeneous boundary layer with explicit account of viscous effects

In this section we elaborate in detail how the viscous effects are dealt with in the procedure of deriving the nonlinear evolution equation for homogeneous boundary layer. The governing equations are the standard Navier-Stokes equations,

$$\rho[D_t u + wU'] + p_x = -\rho(\boldsymbol{u}\cdot\nabla)u + \nu\nabla^2 u \tag{A.1a}$$

$$\rho D_t v + p_y = -\rho(\boldsymbol{u}\cdot\nabla)v + \nu\nabla^2 v \tag{A.1b}$$

$$\rho D_t w + p_z + \rho g = -\rho(\boldsymbol{u}\cdot\nabla)w + \nu\nabla^2 w \tag{A.1c}$$

$$\nabla\cdot\boldsymbol{u} = 0. \tag{A.1d}$$

where density ρ is assumed to be constant, ν is the fluid viscosity and D_t is the material derivative, $D_t = \partial_t + U\partial_x$. The notation $\nabla^2 = \partial^2_{xx} + \partial^2_{yy} + \partial^2_{zz} = \frac{\partial^2}{\partial x^2} + \frac{\partial^2}{\partial y^2} + \frac{\partial^2}{\partial z^2}$ is used for the three-dimensional Laplace operator. The gravitational acceleration g is also a constant. The equation (A.1) differ from the Euler equations by the presence of

the viscous term $\nu\nabla^2\boldsymbol{u}$. To eliminate the pressure term from the set of the equations (A.1) to obtain a single nonlinear equation for vertical velocity perturbation w closed in linear approximation requires some algebra.

To proceed, we first divide both sides of equation (A.1c) by ρ and take the derivative of both sides with respect to material derivative D_t,

$$\frac{1}{\rho}D_t p_z = -D_t^2 w - D_t(\boldsymbol{u}\nabla)w + \frac{\nu}{\rho}D_t\nabla^2 w, \tag{A.2}$$

Next we divide (A.1b) and (A.1a) by ρ, take the partial derivative with respect to z, followed by taking its material derivative D_t, to obtain,

$$D_t[\partial_z D_t v] + \frac{1}{\rho}\partial_y D_t p_z = -D_t\partial_z(\boldsymbol{u}\nabla)v + \frac{\nu}{\rho}D_t\partial_z\nabla^2 v, \tag{A.3}$$

$$D_t[\partial_z D_t u] + D_t\partial_z(wU') + \frac{1}{\rho}\partial_x D_t p_z = -D_t\partial_z(\boldsymbol{u}\nabla)u + \frac{\nu}{\rho}D_t\partial_z\nabla^2 u. \tag{A.4}$$

The next step is to take partial derivative of equation (A.4) with respect to x and partial derivative of equation (A.3) with respect to y, which yields,

$$D_t[\partial_z D_t u_x] + D_t\partial_z(w_x U') + \partial_{xx}^2\left(\frac{1}{\rho}D_t p_z\right) = -D_t\partial_z\partial_x(\boldsymbol{u}\nabla)u + \frac{\nu}{\rho}D_t\partial_z\nabla^2 u_x, \tag{A.5}$$

$$D_t[\partial_z D_t v_y] + \partial_{yy}^2\left(\frac{1}{\rho}D_t p_z\right) = -D_t\partial_z\partial_y(\boldsymbol{u}\nabla)v + \frac{\nu}{\rho}D_t\partial_z\nabla^2 v_y. \tag{A.6}$$

To proceed to the next step we sum up equations (A.4) and (A.6) to obtain,

$$\begin{aligned} D_t[\partial_z D_t(u_x + v_y)] + D_t\partial_z(w_x U') + (\partial_{xx}^2 + \partial_{yy}^2)\left[\frac{1}{\rho}D_t p_z\right] = \\ - D_t\partial_z[\partial_x(\boldsymbol{u}\nabla)u + \partial_y(\boldsymbol{u}\nabla)v] + \frac{\nu}{\rho}D_t\partial_z\nabla^2(u_x + v_y). \end{aligned} \tag{A.7}$$

Next we substitute equation (A.2) into (A.7) to replace the term containing pressure,

$$\begin{aligned} D_t[\partial_z D_t(u_x + v_y)] + D_t\partial_z(w_x U') + (\partial_{xx}^2 + \partial_{yy}^2)\left[-D_t^2 w - D_t(\boldsymbol{u}\nabla)w + \frac{\nu}{\rho}D_t\nabla^2 w\right] = \\ - D_t\partial_z[\partial_x(\boldsymbol{u}\nabla)u + \partial_y(\boldsymbol{u}\nabla)v] + \frac{\nu}{\rho}D_t\partial_z\nabla^2(u_x + v_y), \end{aligned} \tag{A.8}$$

To carry out further simplification on the first and last term of equation (A.8), we substitute incompressibility equation (A.1d) by making use of the following,

$$u_x + v_y = -w_z$$

,

$$\partial_z D_t(u_x + v_y) = \partial_z D_t(-w_z) = -[\partial_t + U\partial_x]w_{zz} - U'\partial_x w_z = -D_t w_{zz} - U'\partial_x w_z$$

,

$$\frac{\nu}{\rho} D_t \partial_z \nabla^2 (u_x + v_y) = -\frac{\nu}{\rho} D_t \partial_z \nabla^2 w_z \equiv -\frac{\nu}{\rho} D_t w_{zzzz} - \frac{\nu}{\rho} D_t \nabla_\perp^2 w_{zz}$$

Substituting the above expressions into equation (A.8) we obtain,

$$D_t^2 w_{zz} - U'' D_t \partial_x w = -D_t^2 \nabla_\perp^2 w - D_t \nabla_\perp^2 (\boldsymbol{u}\nabla) w + \underbrace{\frac{\nu}{\rho} D_t \nabla_\perp^4 w}_{\text{e.s.t}} + \underbrace{\frac{\nu}{\rho} D_t \nabla_\perp^2 w_{zz}}_{\text{e.s.t}}$$
$$+ D_t \partial_z [\partial_x (\boldsymbol{u}\nabla) u + \partial_y (\boldsymbol{u}\nabla) v] + \underbrace{\frac{\nu}{\rho} D_t \nabla_\perp^2 w_{zz}}_{\text{e.s.t}} + \underbrace{\frac{\nu}{\rho} D_t w_{zzzz}}_{\text{dominant viscous term}} . \quad \text{(A.9)}$$

Finally dropping the marked extra small viscous terms, while retaining only the leading order viscosity term we obtain the following nonlinear equation closed in linear approximation,

$$D_t^2 w_{zz} - U'' D_t \partial_x w = D_t \partial_z [\partial_x (\boldsymbol{u}\nabla) u + \partial_y (\boldsymbol{u}\nabla) v] - D_t^2 \nabla_\perp^2 w - D_t \nabla_\perp^2 (\boldsymbol{u}\nabla) w + \frac{\nu}{\rho} D_t w_{zzzz}, \quad \text{(A.10)}$$

where we use the notation $\nabla_\perp^2 = \partial_{xx}^2 + \partial_{yy}^2$. The next step is to non-dimensionalise the nonlinear equation (A.10) to make explicit the order of magnitude of each term. To this end we substitute dimensionless variables tilde quantities of equation (4.8) into equation (A.10) to obtain,

$$D_t = \partial_t + U\partial_x = \frac{V_0}{L}\left[\partial_{\tilde{t}} + \tilde{U}\partial_{\tilde{x}}\right] = \frac{V_0}{L}\tilde{D}_t, \quad D_t^2 = \frac{V_0^2}{L^2}\left[\partial_{\tilde{t}} + \tilde{U}\partial_{\tilde{x}}\right]^2 = \frac{V_0^2}{L^2}\tilde{D}_t^2,$$

$$D_t^2 w_{zz} = \frac{V_0^3}{L^2 d^2}\tilde{D}_t^2 \tilde{w}_{zz}, \quad U'' D_t \partial_x w = \frac{V_0^3}{L^2 d^2}\tilde{U}''\tilde{D}_t \partial_{\tilde{x}}\tilde{w}, \quad D_t^2 \nabla_\perp^2 w = \frac{V_0^3}{L^4}\tilde{D}_t^2 \tilde{\nabla}_\perp^2 \tilde{w},$$

$$D_t\partial_z[\partial_x(\boldsymbol{u}\nabla)\,u+\partial_y(\boldsymbol{u}\nabla)v]=\frac{V_0^2}{L^2d^2}\,[\,q\,]\,D_t\partial_z[\partial_{\tilde{x}}(\boldsymbol{u}\nabla)\,\tilde{u}+\partial_{\tilde{y}}(\boldsymbol{u}\nabla)\,\tilde{v}],$$

$$D_t\nabla_\perp^2(\boldsymbol{u}\nabla)w=\frac{V_0^2}{L^2}\,[\,q\,]\,\tilde{D}_t\tilde{\nabla}_\perp^2(\boldsymbol{u}\nabla)\tilde{w},\quad \frac{\nu}{\rho}D_tw_{zzzz}=\frac{\nu}{\rho}\frac{V_0^2}{L\,d^4}\tilde{D}_t\tilde{w}_{\tilde{z}\tilde{z}\tilde{z}\tilde{z}}.$$

Substituting the above re-scaled tilde variables into equation (A.10) and upon carrying out some algebra, we obtain a single dimensionless equation closed in linear approximation which retains only the leading order viscous term,

$$D_t^2\,\partial_{zz}^2\,w-U''\,D_t\,\partial_x w=\mathcal{N}+\left(\frac{d}{L}\,Re\right)^{-1}D_t\partial_{zzzz}^4w,\tag{A.11}$$

where we dropped the tildes and Re stands for the Reynolds number defined as

$$\mathrm{Re}=\frac{\rho V_0 d}{\nu}=\frac{V_0 d}{\widetilde{\mu}},\qquad \widetilde{\mu}=\frac{\nu}{\rho},\implies \mathrm{Re}^{-1}=\frac{\widetilde{\mu}}{V_0 d}\sim\frac{d}{L}\frac{[\,q\,]}{V_0}.$$

The expression for the nonlinear term is

$$\mathcal{N}=\frac{[\,q\,]}{V_0}\,D_t\,\partial_z\,\nabla_\perp[(\boldsymbol{u}\nabla)\boldsymbol{q}]-\left[\left(\frac{d}{L}\right)^2\right]D_t^2\,\nabla_\perp^2w-\left(\frac{d}{L}\right)^2\frac{[\,q\,]}{V_0}\,D_t\nabla_\perp^2((\boldsymbol{u}\nabla)w).$$

Equation (A.11) is closed in linear approximation, on complementing it by the appropriate boundary conditions on the boundary and at infinity we arrive at the boundary value problem (2.9) which we examine in Chapter 2 .

Appendix B

Details of the derivation of the evolution equation for weakly stratified boundary layer with explicit account of viscous and diffusive effects

The two-dimensional Benjamin-Ono (2d-BO) equation was originally derived by Shrira [1989] for homogeneous shear layer flows in the context of the upper ocean dynamics. An extension of the derivation carried out in Voronovich et al. [1998] considered a more realistic model relevant to geophysical applications with arbitrary density stratification outside the boundary layer. The model also took into account the viscous effect, however the density diffusivity was neglected. Here we justify this neglect by showing that the inclusion of density diffusivity characterised by the diffusivity coefficient K is inconsequential, since it drops out due to smallness the relevant term.

Here we consider a situation where density stratification confined in the boundary layer is weak, but plays a key role in the boundary layer dynamics, while the account

of density diffusion enters the main equation as a small perturbation that drops out, since under adopted scaling the density perturbation is a "passive scalar". The dynamics of the finite-amplitude perturbations under consideration is governed by the Navier-Stokes, the mass conservation, and the incompressibility equations

$$\rho_0[D_t u + wU'] + p_x = -\bar{\rho}[D_t u + wU'] - \rho_0(\boldsymbol{u}\cdot\nabla)u - \bar{\rho}(\boldsymbol{u}\cdot\nabla)u + \nu\nabla^2 u, \tag{B.1a}$$

$$\rho_0 D_t v + p_y = -\bar{\rho} D_t v - \rho_0(\boldsymbol{u}\cdot\nabla)v - \bar{\rho}(\boldsymbol{u}\cdot\nabla)v + \nu\nabla^2 v, \tag{B.1b}$$

$$\rho_0 D_t w + p_z + \bar{\rho}g = -\bar{\rho} D_t w - \rho_0(\boldsymbol{u}\cdot\nabla)w - \bar{\rho}(\boldsymbol{u}\cdot\nabla)w + \nu\nabla^2 w, \tag{B.1c}$$

$$D_t\bar{\rho} + w\rho_0' = K\nabla^2\bar{\rho} - (\boldsymbol{u}\nabla)\bar{\rho} \tag{B.1d}$$

$$\nabla\cdot\boldsymbol{u} = 0, \tag{B.1e}$$

where ρ_0 is the equilibrium density, $\bar{\rho}$ is the perturbation density, while $D_t = \partial_t + U\partial_x$ is the material derivative. We use the short-hand notation for the three-dimensional Laplacian operator, $\nabla^2 = \partial^2_{xx} + \partial^2_{yy} + \partial^2_{zz}$, g is constant gravity acceleration, whereas K is the diffusivity coefficient.

The text below presents details of the algebra needed to exclude pressure term from the set of the equations (B.1) to obtain a single nonlinear equation for vertical velocity w closed in the linear approximation.

To proceed let us first re-write the density equation (B.1d) into the form below

$$gD_t\left[\frac{\bar{\rho}}{\rho_0}\right] = N^2 w + g\frac{K}{\rho_0}\nabla^2\bar{\rho} - \frac{g}{\rho_0}(\boldsymbol{u}\nabla)\bar{\rho}, \tag{B.2}$$

where $N^2(z) = -g\rho_0'/\rho_0$ is the buoyancy frequency squared. Note that the assumed smallness of vertical variations of ρ_0 has been utilised. Next we divide both sides of (B.2) by the gravitational constant g to obtain,

$$D_t\left[\frac{\bar{\rho}}{\rho_0}\right] = \frac{N^2 w}{g} + \frac{K}{\rho_0}\nabla^2\bar{\rho} - \frac{1}{\rho_0}(\boldsymbol{u}\nabla)\bar{\rho}. \tag{B.3}$$

To find the magnitude of the ratio of perturbation density $\bar{\rho}$ to that of the equilibrium density ρ_0 we employ equation (B.3). To proceed we express (B.3) in dimensionless

form and substitute equation (4.9) into (4.10), then assuming the buoyancy term to be dominant we get to leading order the expression of typical density perturbation magnitude in terms of horizontal velocity q,

$$\left[\frac{\bar{\rho}}{\rho_0}\right] = \frac{N_0^2 d}{g}\frac{[\,q\,]}{V_0}. \tag{B.4}$$

We employ the well-known Boussinesq approximation, whereby, if not multiplied by g, the terms in the equations due to the variations of density are negligibly small, or, $\frac{N_0^2 d}{g} \ll 1$. This approximation is valid for the overwhelming majority of oceanic and atmospheric applications. In our context the stratification is so weak that a much stronger inequality holds

$$\frac{N_0^2}{g/d} \ll \frac{[\,q\,]}{V_0} \sim \varepsilon. \tag{B.5}$$

This inequality justifies our neglect of nonlinear buoyancy terms. It is easy to see that in virtue of (B.5), there is a remarkable simplification of the density equation (B.2): the three terms on the RHS only enter into the z momentum equation through a single term of buoyancy consisting of the product of gravitational acceleration and perturbation density $g\bar{\rho}$.

To proceed, first we divide both sides of equation (B.1c) by ρ_0, while taking the material derivative D_t,

$$\frac{1}{\rho_0} D_t p_z + g D_t\left[\frac{\bar{\rho}}{\rho_0}\right] = -D_t^2 w - D_t(\boldsymbol{u}\nabla)w + \frac{\nu}{\rho_0} D_t \nabla^2 w. \tag{B.6}$$

Next we substitute the density equation (B.2) into equation (B.6) to find an expression for pressure,

$$\frac{1}{\rho_0} D_t p_z = -\left[N^2 w + g\frac{K}{\rho_0}\nabla^2\bar{\rho} - \frac{g}{\rho_0}(\boldsymbol{u}\nabla)\bar{\rho}\right] - D_t^2 w - D_t(\boldsymbol{u}\nabla)w + \frac{\nu}{\rho_0} D_t \nabla^2 w, \tag{B.7}$$

To this end we divide (B.1b) and (B.1a) by ρ_0, take the partial derivative with respect to z, then take the material derivative D_t to obtain the two closed expressions for the streamwise and spanwise velocities respectively,

$$D_t[\partial_z D_t v] + \frac{1}{\rho_0}\partial_y D_t p_z = -D_t\partial_z(\boldsymbol{u}\nabla)v + \frac{\nu}{\rho_0} D_t \partial_z \nabla^2 v, \tag{B.8}$$

$$D_t[\partial_z D_t u] + D_t\partial_z(wU') + \frac{1}{\rho_0}\partial_x D_t p_z = -D_t\partial_z(\boldsymbol{u}\nabla)u + \frac{\nu}{\rho_0}D_t\partial_z\nabla^2 u. \tag{B.9}$$

The next step is to take partial derivative of equation (B.9) with respect to x and partial derivative of equation (B.8) with respect to y respectively to obtain,

$$D_t[\partial_z D_t u_x] + D_t\partial_z(w_x U') + \partial_{xx}^2\left(\frac{1}{\rho_0}D_t p_z\right) = -D_t\partial_z\partial_x(\boldsymbol{u}\nabla)u + \frac{\nu}{\rho_0}D_t\partial_z\nabla^2 u_x, \tag{B.10}$$

$$D_t[\partial_z D_t v_y] + \partial_{yy}^2\left(\frac{1}{\rho_0}D_t p_z\right) = -D_t\partial_z\partial_y(\boldsymbol{u}\nabla)v + \frac{\nu}{\rho_0}D_t\partial_z\nabla^2 v_y, \tag{B.11}$$

To proceed to the next step we add equations (B.10) and (B.11), which yields,

$$\begin{aligned} D_t[\partial_z D_t(u_x + v_y)] + D_t\partial_z(w_x U') + (\partial_{xx}^2 + \partial_{yy}^2)\left[\frac{1}{\rho_0}D_t p_z\right] = \\ - D_t\partial_z[\partial_x(\boldsymbol{u}\nabla)u + \partial_y(\boldsymbol{u}\nabla)v] + \frac{\nu}{\rho_0}D_t\partial_z\nabla^2(u_x + v_y). \end{aligned} \tag{B.12}$$

The next step is to eliminate the pressure by substituting equation (B.7) into (B.12),

$$\begin{aligned} &D_t[\partial_z D_t(u_x + v_y)] + D_t\partial_z(w_x U') = \\ &- (\partial_{xx}^2 + \partial_{yy}^2)\left[-\left(N^2 w + g\frac{K}{\rho_0}\nabla^2\bar{\rho} - \frac{g}{\rho_0}(\boldsymbol{u}\nabla)\bar{\rho}\right) - D_t^2 w - D_t(\boldsymbol{u}\nabla)w + \frac{\nu}{\rho_0}D_t\nabla^2 w\right] \\ &\qquad - D_t\partial_z[\partial_x(\boldsymbol{u}\nabla)u + \partial_y(\boldsymbol{u}\nabla)v] + \frac{\nu}{\rho_0}D_t\partial_z\nabla^2(u_x + v_y). \end{aligned} \tag{B.13}$$

To carry out further simplification of the first and last term of equation (B.13), we split the density diffusion term into parts responsible for the horizontal and vertical diffusion respectively, thereafter employ the incompressibility equation (B.1e) ,

$$u_x + v_y = -w_z,$$

we immediately obtain

$$\partial_z D_t(u_x + v_y) = \partial_z D_t(-w_z) = -[\partial_t + U\partial_x]w_{zz} - U'\partial_x w_z = -D_t w_{zz} - U'\partial_x w_z,$$

$$\frac{\nu}{\rho_0}D_t\partial_z\nabla^2(u_x + v_y) = -\frac{\nu}{\rho_0}D_t\partial_z\nabla^2 w_z \equiv -\frac{\nu}{\rho_0}D_t w_{zzzz} - \frac{\nu}{\rho_0}D_t\nabla_\perp^2 w_{zz}.$$

On substituting the above expressions into equation (B.13) we obtain,

$$D_t^2 w_{zz} - U'' D_t \partial_x w = -D_t^2 \nabla_\perp^2 w - D_t \nabla_\perp^2 (\boldsymbol{u}\nabla) w + \underbrace{\frac{\nu}{\rho_0} D_t \nabla_\perp^4 w}_{\text{e.s.t}} + \underbrace{\frac{\nu}{\rho_0} D_t \nabla_\perp^2 w_{zz}}_{\text{e.s.t}}$$
$$- \nabla_\perp^2 N^2 w - \underbrace{g \frac{K}{\rho_0} \nabla_\perp^4 \bar{\rho}}_{\text{e.s.t}} - g \frac{K}{\rho_0} \nabla_\perp^2 \bar{\rho}'' + \frac{g}{\rho_0} \nabla_\perp^2 (\boldsymbol{u}\nabla) \bar{\rho}$$
$$+ D_t \partial_z [\partial_x (\boldsymbol{u}\nabla) u + \partial_y (\boldsymbol{u}\nabla) v] + \underbrace{\frac{\nu}{\rho_0} D_t \nabla_\perp^2 w_{zz}}_{\text{e.s.t}} + \underbrace{\frac{\nu}{\rho_0} D_t w_{zzzz}}_{\text{dominant viscous term}} , \quad \text{(B.14)}$$

Finally, on substituting equation (B.4) for the magnitude density ratio into (B.14) and retaining only the leading order viscous term after non-dimensionalisation we obtain a relatively compact expression for the boundary value problem formulated in terms of vertical velocity

$$D_t^2 \, \partial_{zz}^2 \, w - U'' \, D_t \, \partial_x w = \mathcal{N} + \mathcal{M} - \left(\frac{N_0 \, d}{V_0} \right)^2 N^2 \nabla_\perp^2 w + \left(\frac{d}{L} \, Re \right)^{-1} D_t \partial_{zzzz}^4 w. \quad \text{(B.15)}$$

where,

$$\mathcal{N} = \frac{[\,q\,]}{V_0} \, D_t \, \partial_z \, \nabla_\perp [(\boldsymbol{u}\nabla)\boldsymbol{q}] - \left[\left(\frac{d}{L} \right)^2 \right] D_t^2 \, \nabla_\perp^2 w - \left(\frac{d}{L} \right)^2 \frac{[\,q\,]}{V_0} \, D_t \nabla_\perp^2 (\boldsymbol{u}\nabla) w,$$

$$\mathcal{M} = \left(\frac{N_0 \, d}{V_0} \right)^2 \frac{[\,q\,]}{V_0} \nabla_\perp^2 (\boldsymbol{u}\nabla) \bar{\rho} + Sc \left(\frac{N_0 \, d}{V_0} \right)^2 \frac{[\,q\,]}{V_0} \nabla_\perp^2 \bar{\rho}'',$$

where the dimensionless parameter, Sc is the Schmidt number given by,

$$Sc = \frac{K}{V_0 \, d}.$$

Equation (B.15) is closed in linear approximation, on complementing it by the appropriate boundary conditions on the boundary and at infinity we arrive at the boundary value problem (4.14) which we examine in Chapter 4.

Bibliography

M J Ablowitz and H Segur. Long internal waves in fluids of great depth. *Studies in Applied Mathematics*, 62(3):249–262, 1980.

M J Ablowitz and H Segur. *Solitons and the inverse scattering transform*, volume 4. Siam, 1981.

M Abramowitz and I A Stegun. *Handbook of mathematical functions: with formulas, graphs, and mathematical tables*, volume 55. Courier Corporation, 1964.

L A Abramyan, Yu A Stepanyants, and V I Shrira. Multidimensional solitons in shear flows of the boundary-layer type. In *Soviet physics. Doklady*, volume 37, pages 575–578. Plenum, 1992.

T B Benjamin. Internal waves of permanent form in fluids of great depth. *Journal of Fluid Mechanics*, 29(3):559–592, 1967.

Luc Bergé. Wave collapse in physics: principles and applications to light and plasma waves. *Physics reports*, 303(5-6):259–370, 1998.

V I Borodulin and Yu S Kachanov. Experimental study of soliton-like coherent structures in boundary layer. In *Proc. Scientific & Methodological Seminar on Ship Hydrodynamics, 19th Session*, volume 2, pages 99–1, 1990.

V I Borodulin and Yu S Kachanov. Experimental study of soliton-like coherent structures. In *Eddy Structure Identification in Free Turbulent Shear Flows. IUTAM Symp. Poitiers*, 1992.

VI Borodulin and Yu S Kachanov. The role of the mechanism of the local secondary instability in k-breakdown of boundary layer. *Sov. J. Appl. Phys 3*, 2:70–81, 1989.

J R Carpenter, N J Balmforth, and G A Lawrence. Identifying unstable modes in stratified shear layers. *Physics of Fluids*, 22(5):054104, 2010.

J R Carpenter, E W Tedford, E Heifetz, and G A Lawrence. Instability in stratified shear flow: Review of a physical interpretation based on interacting waves. *Applied Mechanics Reviews*, 64(6), 2011.

K M Case. The N-Soliton solution of the Benjamin-Ono equation. *Proceedings of the National Academy of Sciences of the United States of America*, 75(8):3562, 1978.

K M Case. Properties of the Benjamin–Ono equation. *Journal of Mathematical Physics*, 20(5):972–977, 1979.

C P Caulfield. Multiple linear instability of layered stratified shear flow. *Journal of Fluid Mechanics*, 258:255–285, 1994.

H H Chen and Y C Lee. Internal-wave solitons of fluids with finite depth. *Physical Review Letters*, 43(4):264, 1979.

A D D Craik. A model for subharmonic resonance within wavepackets in unstable boundary layers. *Journal of Fluid Mechanics*, 432:409–418, 2001.

Alex D D Craik. Non-linear resonant instability in boundary layers. *Journal of Fluid Mechanics*, 50(2):393–413, 1971.

Alex D D Craik. *Wave interactions and fluid flows*. Cambridge University Press, 1988.

W O Criminale, T L Jackson, and R D Joslin. *Theory and computation in hydrodynamic stability*. Cambridge University Press, 2018.

Richard Danyi. *Global instability of mixing layers created by confinement*. PhD thesis, Keele University, 2018.

R E Davis and A Acrivos. Solitary internal waves in deep water. *Journal of Fluid Mechanics*, 29(3):593–607, 1967.

D J Doorley and F T Smith. Initial-value problems for spot disturbances in incompressible or compressible boundary layers. *Journal of engineering mathematics*, 26 (1):87–106, 1992.

P G Drazin. *Introduction to hydrodynamic stability*, volume 32. Cambridge university press, 2002.

P G Drazin and W H Reid. *Hydrodynamic stability*. Cambridge university press, 2004.

A I D'yachenko and E A Kuznetsov. Two-dimensional wave collapse in the boundary layer. *Physica D: Nonlinear Phenomena*, 87(1-4):301–313, 1995.

A N D'yachenko and E A Kuznetsov. Instability and self-focusing of solitons in the boundary layer. *JETP Letters*, 59(2):108–113, 1994.

Bengt Fornberg. *A practical guide to pseudospectral methods*, volume 1. Cambridge university press, 1998.

D G Gaidashev and S K Zhdanov. On the transverse instability of the two-dimensional Benjamin–Ono solitons. *Physics of Fluids*, 16(6):1915–1921, 2004.

G A Gottwald. The Zakharov-Kuznetsov equation as a two-dimensional model for nonlinear rossby waves. *arXiv preprint nlin/0312009*, 2003.

P Hall and F T Smith. On strongly nonlinear vortex/wave interactions in boundary-layer transition. *Journal of fluid mechanics*, 227:641–666, 1991.

J J Healey. Lecture notes on hydrodynamic stability. *https://fluids.ac.uk/researcher-resources.*, 2017.

K R Helfrich and W K Melville. Long nonlinear internal waves. *Annu. Rev. Fluid Mech.*, 38:395–425, 2006.

J Holmboe. On the behavior of symmetric waves in stratified shear layers. *Geophysical Publication*, 24:67–113, 1962.

L N Howard. Note on a paper of John W. Miles. *Journal of Fluid Mechanics*, 10(4): 509–512, 1961.

L N Howard and S A Maslowe. Stability of stratified shear flows. *Boundary-Layer Meteorology*, 4(1-4):511–523, 1973.

M C Jorge, Gustavo Cruz-Pacheco, L Mier-y Teran-Romero, and N F Smyth. Evolution of two-dimensional lump nanosolitons for the Zakharov-Kuznetsov and electromigration equations. *Chaos: An Interdisciplinary Journal of Nonlinear Science*, 15(3):037104, 2005.

R I Joseph. Solitary waves in a finite depth fluid. *Journal of Physics A: Mathematical and General*, 10(12):L225, 1977.

R I Joseph and R Egri. Multi-soliton solutions in a finite depth fluid. *Journal of Physics A: Mathematical and General*, 11(5):L97, 1978.

Y S Kachanov. Physical mechanisms of laminar-boundary-layer transition. *Annual review of fluid mechanics*, 26(1):411–482, 1994.

Yu S Kachanov. On the resonant nature of the breakdown of a laminar boundary layer. *Journal of Fluid Mechanics*, 184:43–74, 1987.

Yu S Kachanov and V Ya Levchenko. The resonant interaction of disturbances at laminar-turbulent transition in a boundary layer. *Journal of Fluid Mechanics*, 138: 209–247, 1984.

Yu S Kachanov, V V Kozlov, and V Ya Levchenko. Nonlinear development of a wave in a boundary layer. *Fluid dynamics*, 12(3):383–390, 1977.

Yu S Kachanov, V V Kozlov, V Ya Levchenko, and M P Ramazanov. On nature of k-breakdown of a laminar boundary layer. new experimental data. In *Laminar-turbulent transition*, pages 61–73. Springer, 1985.

Yu S Kachanov, O S Ryzhov, and F T Smith. Formation of solitons in transitional boundary layers: theory and experiment. *Journal of Fluid Mechanics*, 251:273–297, 1993.

B B Kadomtsev. Cooperative effects in plasmas. In *Reviews of Plasma Physics*, pages 1–226. Springer, 2001.

B B Kadomtsev and V I Petviashvili. On the stability of solitary waves in weakly dispersing media. In *Sov. Phys. Dokl*, volume 15, pages 539–541, 1970.

R R Kerswell. Nonlinear nonmodal stability theory. *Annual Review of Fluid Mechanics*, 50:319–345, 2018.

G J Komen, L Cavaleri, M Donelan, K Hasselmann, S Hasselmann, and PAEM Janssen. *Dynamics and modelling of ocean waves*. 1996.

D A Kopriva. *Implementing spectral methods for partial differential equations: Algorithms for scientists and engineers*. Springer Science & Business Media, 2009.

E A Kuznetsov. Wave collapse in plasmas and fluids. *Chaos: An Interdisciplinary Journal of Nonlinear Science*, 6(3):381–390, 1996.

E A Kuznetsov. Integral criteria of wave collapses. *Radiophysics and quantum electronics*, 46(5-6):307–322, 2003.

E A Kuznetsov. Stability criterion for solitons of the Zakharov–Kuznetsov-type equations. *Physics Letters A*, 382(31):2049–2051, 2018.

E A Kuznetsov and S L Musher. Effect of collapse of sound waves on the structure of collisionless shock waves in a magnetized plasma. *Zh. Eksp. Teor. Fiz*, 91:1605–1619, 1986.

P H LeBlond and L A Mysak. *Waves in the Ocean*. Elsevier, 1981.

S A Maslowe and L G Redekopp. Long nonlinear waves in stratified shear flows. *Journal of Fluid Mechanics*, 101(2):321–348, 1980.

Stanisław R Massel. *Internal gravity waves in the shallow seas*. Springer, 2015.

Y Matsuno. Exact multi-soliton solution for nonlinear waves in a stratified fluid of finite depth. *Physics Letters A*, 74(3-4):233–235, 1979.

Y Matsuno. Bilinear transformation method. *Mathematics in Science and Engineering*, 174, 1984.

S Melkonian and S A Maslowe. Two-dimensional amplitude evolution equations for nonlinear dispersive waves on thin films. *Physica D: Nonlinear Phenomena*, 34 (1-2):255–269, 1989.

A F Messiter. Boundary-layer flow near the trailing edge of a flat plate. *SIAM Journal on Applied Mathematics*, 18(1):241–257, 1970.

S J Metcalfe. *A blow-up mechanism in boundary layer transition*. PhD thesis, Keele University, 2013.

J W Miles. On the stability of heterogeneous shear flows. *Journal of Fluid Mechanics*, 10(4):496–508, 1961.

Yu Z Miropol'Sky. *Dynamics of internal gravity waves in the ocean*, volume 24. Springer Science & Business Media, 2001.

V Ya Neiland. Theory of laminar boundary layer separation in supersonic flow. *Fluid Dynamics*, 4(4):33–35, 1969.

K Nozaki. Vortex solitons of drift waves and anomalous diffusion. *Physical Review Letters*, 46(3):184, 1981.

J O Oloo and V I Shrira. Boundary layer collapses described by the two-dimensional intermediate long-wave equation. *Theoretical and Mathematical Physics*, 203:512–523, 2020.

H Ono. Algebraic solitary waves in stratified fluids. *Journal of the Physical Society of Japan*, 39(4):1082–1091, 1975.

S A Orszag. Numerical methods for the simulation of turbulence. *The Physics of Fluids*, 12(12):II–250, 1969.

D E Pelinovsky and V I Shrira. Collapse transformation for self-focusing solitary waves in boundary-layer type shear flows. *Physics Letters A*, 206(3-4):195–202, 1995.

D E Pelinovsky and Yu A Stepanyants. Self-focusing instability of nonlinear plane waves in shear flows. *Journal of Experimental and Theoretical Physics*, 78(6):883–891, 1994.

D E Pelinovsky and C Sulem. Bifurcations of new eigenvalues for the benjamin–ono equation. *Journal of Mathematical Physics*, 39(12):6552–6572, 1998.

V I Petviashvili. Red spot of jupiter and the drift soliton in a plasma. 1980.

V P Reutov. Asymptotic model for generation of three-dimensional vortex structures in a boundary layer. *Journal of applied mechanics and technical physics*, 36(2):199–209, 1995.

A I Ruban. *Fluid dynamics: part 3 boundary layers*. Oxford University Press, 2017.

O S Ryzhov. The formation of ordered vortex structures from unstable oscillations in the boundary layer. *USSR computational mathematics and mathematical physics*, 30(6):146–154, 1990.

W S Saric, J D Carter, and G A Reynolds. Computation and visualization of unstable-wave streaklines in a boundary layer. *Bull. Amer. Phys. Soc*, 26:1252, 1981.

H Schlichting and K Gersten. *Boundary-layer theory*. Springer, 2016.

P J Schmid. Nonmodal stability theory. *Annu. Rev. Fluid Mech.*, 39:129–162, 2007.

P J Schmid and D S Henningson. Stability and transition in shear flows springer-verlag. *New York*, 2001.

V I Shrira. On the 'sub-surface'waves of the mixed layer of the upper ocean. *Trans. USSR Acad. Sci., Earth Sci. Sec*, 308:276–279, 1989.

V I Shrira and I A Sazonov. Quasi-modes in boundary-layer-type flows. part 1. inviscid two-dimensional spatially harmonic perturbations. *Journal of Fluid Mechanics*, 446:133–171, 2001.

V I Shrira, G Caulliez, and D V Ivonin. A bypass scenario of laminarturbulent transition in the wind-driven free-surface boundary layer. In *IUTAM Symposium*

on Laminar-Turbulent Transition and Finite Amplitude Solutions, pages 267–288. Springer, 2005.

F T Smith. On the non-parallel flow stability of the blasius boundary layer. *Proceedings of the Royal Society of London. A. Mathematical and Physical Sciences*, 366 (1724):91–109, 1979.

F T Smith. On nonlinear effects near the wing-tips of an evolving boundary-layer spot. *Philosophical Transactions of the Royal Society of London. Series A: Physical and Engineering Sciences*, 340(1656):131–165, 1992.

F T Smith and P A Stewart. The resonant-triad nonlinear interaction in boundary-layer transition. *Journal of Fluid Mechanics*, 179:227–252, 1987.

I J Sobey. *Introduction to interactive boundary layer theory*, volume 3. Oxford University Press on Demand, 2000.

A Soloviev and R Lukas. *The near-surface layer of the ocean: structure, dynamics and applications*, volume 48. Springer Science & Business Media, 2013.

P A Stewart and F T Smith. Three-dimensional nonlinear blow-up from a nearly planar initial disturbance, in boundary-layer transition: theory and experimental comparisons. *Journal of Fluid Mechanics*, 244:79–100, 1992.

K Stewartson. On the flow near the trailing edge of a flat plate ii. *Mathematika*, 16 (1):106–121, 1969.

Bruce R Sutherland. *Internal gravity waves*. Cambridge university press, 2010.

D R S Ko T. Kubota and L D Dobbs. Weakly-nonlinear, long internal gravity waves in stratified fluids of finite depth. *Journal of Hydronautics*, 12(4):157–165, 1978.

A S W Thomas and W S Saric. Harmonic and subharmonic waves during boundary-layer transition. *Bull. Am. Phys. Soc*, 26:1252, 1981.

S N Timoshin. Multiple deck theory. In *Fluid and Solid Mechanics*, pages 35–69. World Scientific, 2016.

S Toh, H Iwasaki, and T Kawahara. Two-dimensionally localized pulses of a nonlinear equation with dissipation and dispersion. *Physical Review A*, 40(9):5472, 1989.

W Tollmien, D M Miner, et al. The production of turbulence. Technical report, National advisory committee for aeronautics langley field va langley ..., 1931.

J S Turner. *Buoyancy effects in fluids*. Cambridge university press, 1979.

J R Usher, A D D Craik, and F Hendriks. Nonlinear wave interactions in shear flows. part 2. third-order theory. *Journal of Fluid Mechanics*, 70(3):437–461, 1975.

Milton Van Dyke. Perturbation methods in fluid mechanics/annotated edition. *NASA STI/Recon Technical Report A*, 75, 1975.

V V Voronovich, V I Shrira, and Yu A Stepanyants. Two-dimensional models for nonlinear vorticity waves in shear flows. *Studies in Applied Mathematics*, 100(1): 1–32, 1998.

Xuesong Wu. Nonlinear theories for shear flow instabilities: Physical insights and practical implications. *Annual Review of Fluid Mechanics*, 51:451–485, 2019.

V E Zakharov and E A Kuznetsov. On three dimensional solitons. *Zhurnal Eksp. Teoret. Fiz*, 66:594–597, 1974.

V E Zakharov and E A Kuznetsov. Solitons and collapses: two evolution scenarios of nonlinear wave systems. *Physics-Uspekhi*, 55(6):535, 2012.

V E Zakharov et al. Collapse of langmuir waves. *Sov. Phys. JETP*, 35(5):908–914, 1972.

V I Zhuk and O S Ryzhov. Free interaction and stability of the boundary layer in an incompressible fluid. In *Akademiia Nauk SSSR Doklady*, volume 253, pages 1326–1329, 1980.

V I Zhuk and O S Ryzhov. Locally nonviscous perturbations in a boundary layer with self-induced pressure. In *Doklady Akademii Nauk*, volume 263, pages 56–59. Russian Academy of Sciences, 1982.